TP 6470 E

DESIGN, CONSTRUCTION AND TESTING OF A LINEAR INDUCTION MOTOR POWERED BY COMMERCIAL FREQUENCY (60 Hz)

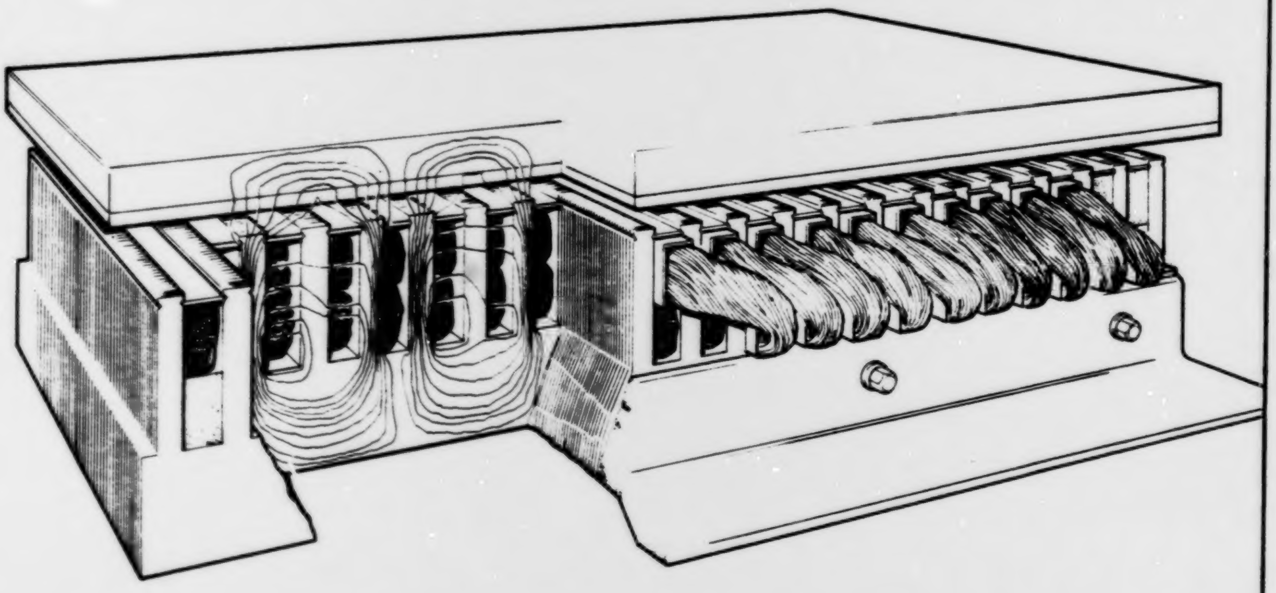

PREPARED FOR:

CA1
DTC 847
85
D21F
c.2

ort Canada
ortation Development Centre

UTDC R&D
UTDC RESEARCH & DEVELOPMENT LTD.

FINAL REPORT

TP TP 6470 E

DESIGN, CONSTRUCTION, AND TESTING
OF A LINEAR INDUCTION MOTOR
POWERED BY COMMERCIAL FREQUENCY (60 Hz)

Library and Information Centre / Centre de Documentation (GSLA)
RECEIVED – REÇU LE
AUG 12 1985
Transport Canada / Transports Canada

PREPARED FOR: Transport Canada
Transportation Development Centre

DSS Contract Serial No: OSD83-00025
UTDC R&D Report No: 453-990-3
Dated: 85.03.31

BY: W.J. Ballantyne
K5-10484

K5-10484

DISCLAIMER

The contents of this report reflect the views of the contractor and not necessarily the official views or policies of the Transport Canada Transportation Development Centre.

PROJECT TEAM

H.H. Baeggli
W.J. Ballantyne
P.D. Moore
R. VanHuuksloot
S. Secher
R. Galster

REPORT DOCUMENTATION FORM

1. Transport Canada Report No.
TP 6470E

2. TDC Project No.
4757

3. Recipient's Catalogue No.

4. Title and Subtitle
Design, Construction and Testing of a Linear Induction Motor powered by Commercial Frequency (60Hz)

5. Report Date
March 1985

6. Performing Organization Report No.
453-990

7. Author(s)
W.J. Ballantyne

8. Transport Canada File No.
D 1465-379-2

9. Performing Organization Name and Address
UTDC Research and Development Ltd.
P.O. Box 160, Station "A"
Kingston, Ontario
K7M 6R1

10. DSS File No.

11. DSS or Transport Canada Contract No.
0SD83-00025

12. Sponsoring Agency Name and Address
Transportation Development Centre (TDC)
1000 Sherbrooke Street West
Suite 2421
Montreal, Quebec (H3A 2R3)

13. Type of Report and Period Covered
Final June 83 - March 85

14. Sponsoring Agency Code

15. Supplementary Notes

16. TDC Project Officer
C.A. Versailles

17. Abstract

Design, construction and testing of linear induction motors (LIMs) powered by commercial frequency (60 Hz) were undertaken by UTDC Research and Development Limited. The technology is characterized by using simple mush wound 2/3, 3/3 or 4/6 linear motors powered by commercial frequency (60 Hz), 600 V, 3-phase supply. The control is achieved by a variable voltage controller. Different types of LIM primaries and secondaries were tested and, in particular, the slip power recovery aspect investigated.

A static test and demonstration system was built at UTDC Kingston test site to investigate the correlation between theoretical model and experimental results.

A 60 m long dynamic test and demonstration system was built at the same facility to verify the dynamic experimental results with the theoretical model modified for the dynamic behaviour of linear induction motors.

The systems were successfully used in the testing of the developed linear motors.

18. Key Words
Linear induction motors,
commercial frequency, 60 Hertz

19. Distribution Statement
Limited number of copies available from sponsoring agency on request.

20. Security Classification (of this report)
Unclassified

21. Security Classification (of this page)
Unclassified

22. No. of Pages
200

23. Price

FORMULE DE DOCUMENTATION POUR RAPPORT

1. Nº du rapport Transports Canada
TP 6470E

2. Nº de l'étude — CDT
4757

3. Nº de catalogue du destinataire

4. Titre et sous-titre
Design, Construction and Testing of a Linear Induction Motor powered by Commercial Frequency (60Hz)

5. Date du rapport
Mars 1985

6. Nº du rapport de l'organisme exécutant
453-990

7. Auteur(s)
W.J. Ballantyne

8. Nº de dossier Transports Canada
D 1465-379-2

9. Nom et adresse de l'organisme exécutant
UTDC Research and Development Ltd.
P.O. Box 160, Station "A"
Kingston, Ontario
K7M 6R1

10. Nº de dossier — ASC

11. Nº de contrat — ASC ou Transports Canada
0SD83-00025

12. Nom et adresse de l'organisme parrain
Centre de développement des transports (CDT)
1000 o., rue Sherbrooke
Suite 2421
Montréal, Québec H3A 2R3

13. Genre de rapport et période visée
Final-Juin 83/Mars 85

14. Code de l'organisme parrain

15. Remarques additionnelles

16. Agent de projet — CDT
C.A. Versailles

17. Résumé

Ce rapport concerne l'étude, la fabrication et l'essai par UTDC Research and Development Limited de moteurs linéaires à induction alimentés en courant alternatif à fréquence industrielle. Il s'agit de moteurs 2/3, 3/3 ou 4/6 à enroulements à fils jetés, alimentés en courant triphasé 600 V à fréquence industrielle (60 Hz), le réglage de la vitesse étant obtenu par variation de la tension d'alimentation. Les essais ont porté sur différents types d'inducteurs et d'induits et, en particulier, sur la récupération des pertes par glissement.

Les variantes proposées ont d'abord été essayées sur banc d'essai statique aménagé dans les installations d'UTDC à Kingston, dans le but de rechercher les corrélations entre le modèle théorique et les résultats expérimentaux.

Par la suite, une ligne expérimentale longue de 60 mètres a été construite au même endroit pour les besoins des essais dynamiques visant à comparer les caractéristiques de marche des moteurs aux résultats de la modélisation utilisant le modèle théorique précité, mais modifié pour figurer le comportement dynamique des moteurs linéaires à induction.

Les deux installations d'essai ont répondu aux attentes formulées à leur égard.

18. Mots-clés
Moteur linéaire à induction,
fréquence industrielle, 60 Hertz

19. Diffusion
Le CDT dispose d'un nombre limité d'exemplaires.

20. Classification de sécurité (de ce rapport)
non classifié

21. Classification de sécurité (de cette page)
non classifiée

22. Nombre de pages
200

23. Prix

CDT TDC 79-005

ACKNOWLEDGEMENT

The work on the Design, Construction, and Testing of a Linear Induction Motor powered by Commercial Frequency (60 Hz) has been carried out under a contract approved by the Department of Supply and Service on behalf of the Transportation Development Centre dated 3 June 1983.

Special thanks go to Tom Mulvenna and staff for their assistance in instrumentation and testing, A.R. Eastham and Queen's University, Kingston, for valuable direction in approaches to modelling and experimentation, and Dorothy Mason and Shari May for their patience and responsiveness in the typing of various manuscripts.

SUMMARY

A review of the Modelling, Experimentation, and Design of Linear Induction Motors is presented. Discussed are some fundamental considerations relating to 60 Hz, low-speed LIMs in particular.

TABLE OF CONTENTS

SECTION		TITLE	PAGE NO.
		TITLE PAGE	i
		DISCLAIMER	ii
		PROJECT TEAM	iii
		REPORT DOCUMENTATION FORM (English)	v
		REPORT DOCUMENTATION FORM (French)	vi
		ACKNOWLEDGEMENT	vii
		SUMMARY	viii
		TABLE OF CONTENTS	ix
		LIST OF FIGURES	xii
		LIST OF TABLES	xiii
		FRONTISPIECE	xiv
1.0		INTRODUCTION	1
2.0		PROGRAM OVERVIEW	3
	2.1	Program Achievements	3
	2.2	Work Summary	4
3.0		GENERAL DISCUSSION	9
	3.1	LIM Weaknesses	9
	3.2	LIM Benefits	11
	3.3	Opportunities for Improvement in Design	14
	3.4	Opportunities for New Designs	16

TABLE OF CONTENTS

SECTION		TITLE	PAGE NO.
4.0		LIM MODELS	19
	4.1	Conceptual Model	20
	4.2	Quantitative Model	40
5.0		LIM EXPERIMENTS	47
	5.1	Static Experiments	48
	5.2	Dynamic Experiments	54
6.0		COMPARISON OF PREDICTED VS EXPERIMENTAL RESULTS	60
	6.1	Circuit Parameter Formulae	60
	6.2	Equivalent Circuit Prediction	63
7.0		LIM DESIGN	68
	7.1	Specifying Performance	71
	7.2	Using the Test Data as a Basis for Design	72
	7.3	Using the Performance Model as a Basis for Design	84
8.0		LIM-BASED MOTION CONTROL	87
	8.1	The LIM as an Actuator	87

TABLE OF CONTENTS

SECTION		TITLE	PAGE NO.
	8.2	The LIM Controller	91
	8.3	The Nature of the Load	92
	8.4	Sensing and Feedback	93
9.0		CONCLUSIONS	94
	9.1	Modelling and Experimentation	94
	9.2	Design	95
	9.3	Present Applications	97
	9.4	Future Applications	97
	9.5	Recommendation	98
		References	99

Appendices

1. Derivation of the Equivalent Circuit Parameters from Theory
2. Derivation of the Equivalent Circuit Parameters from Experiment
3. Static Performance Summary-Base Configurations
4. LIM-Based Control System Model
5. LIM Thermal Model

LIST OF FIGURES

FIGURE NO.	DESCRIPTION	PAGE NO.
3-1	Mechanical Linear Drive Approaches	12
4-1	Principles of Three-Phase Windings	23
4-2	LIM Windings	26
4-3	Principles of the LIM Magnetic Circuit	29
4-4	"Wheel Slip" Analogy of LIM Forces	34
4-5	LIM Energy Model	36
4-6	Principles of the "Equivalent Circuit" Modelling Approach	42
5-1	Static Test Stand	49
5-2	Test System Block Diagram	50
5-3	Flux Density Wave	53
5-4	LIM Dynamic Test Facility	56
5-5	Data Measurement and Reduction System	57
5-6	60 Hz Dynamic Test Results Sample	58
5-7	60 Hz Dynamic Test Results Sample	59
6-1	Curve-Matching Procedure	64
6-2	Test Results - Measured vs Theoretical	66
6-3	Test Results - Measured vs Theoretical	67
7-1	Alternative Design Technique - Design vs Performance Models	69
8-1	Generalized Motion Control System	88

LIST OF TABLES

TABLE NO.	DESCRIPTION	PAGE NO.
4-1	Fundamental Relationships	44
7-1	Reasons for, and Effects of, Design Parameter Manipulation	86

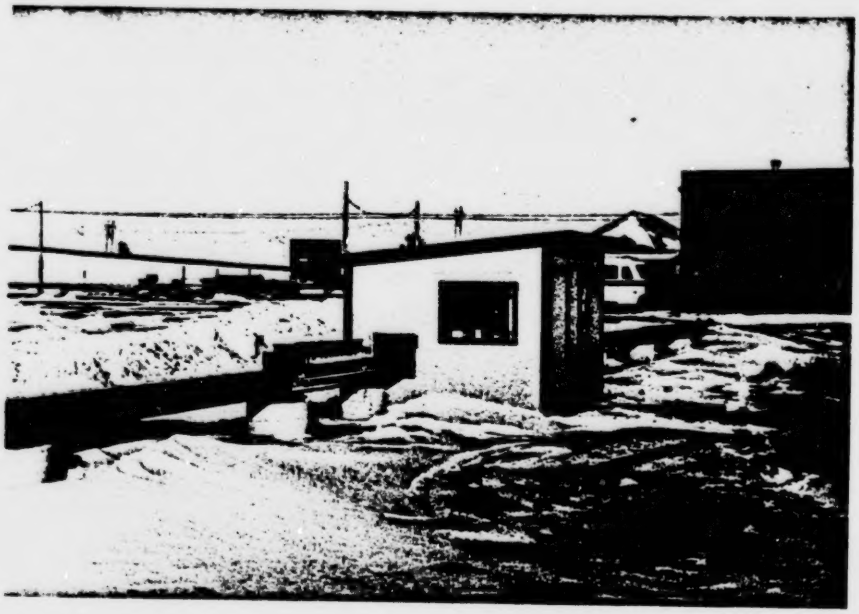

VIEW OF 60 Hz LINEAR MOTOR DYNAMIC TEST TRACK

1.0 INTRODUCTION

The body of literature relating to Linear Electric Motors is large, representing the work of investigators in many countries over two decades. The greatest proportion of effort by far involves LIMs for medium- and high-speed guided transportation applications. Most of these systems use LIM Primaries carried on the vehicle, with ratings anywhere from 100 to 1000 kVA.

An almost-neglected area of serious investigation concerns the low-speed, low-power, LIM-in-track configuration. Such systems have many applications which can be shown to provide several benefits over competing approaches.

The 60 Hz Linear Induction Motor Development Program was undertaken to extend the limits of performance and applicability of low-speed, LIM-in-track technology. This objective was pursued on various levels, drawing from the existing knowledge base as well as contributing new knowledge. Since UTDC R&D began the program, the range of potential applications of LIM technology has grown dramatically, partly because of an increasing understanding within the organization about the nature of the small transportation systems market, and partly because of the introduction of design concepts which promise new benefits.

The development of viable LIM-in-track propulsion has its technical challenges. Small LIMs tend to be inefficient, and their presence in the guideway makes them a major cost-component of the system. However, the potential for gain through performance improvement and better materials utilization justifies an agressive R&D.

The 60 Hz LIM Development Program addressed many of the fundamental issues of LIM technology, and created various analytical and experimental means to deal with the questions which arose.

This report provides an overview of what was learned, and concludes with some recommendations on the future directions of LIM development and applications.

2.0 PROGRAM OVERVIEW

2.1 PROGRAM ACHIEVEMENTS

The following list summarizes the specific achievements of the program:

1. The creation of a Mathematical Model which can generate performance predictions based on LIM physical and operating parameters.

2. The establishment of a Static Test Procedure (and associated hardware and software) which estimates the equivalent circuit parameters for a given LIM based on static measurements.

3. The establishment of a Dynamic Test Facility for testing LIMs at speeds up to 10 metres/second.

4. The introduction of cage and wound secondaries, and the application of the latter in demonstrating the feasibility of LIM Slip Power Recovery.

5. The creation of a LIM Control System Simulation for studying the dynamic behaviour of LIM-based motion control systems.

2.2 WORK SUMMARY

This Program was divided into work tasks with identified milestone points. The following is a review of those tasks.

2.2.1 Modelling, Experimentation, and Design: Problems and Approaches

This work activity included:

- o Comprehensive review of the literature
- o Development of conceptual models
- o Development of analytical models
- o Development of experimental approaches including conceptual design of the Static and Dynamic Test Facilities
- o Conceptual design of prototype test articles
    - LIM Primaries
    - Wound Secondary
    - Cage Secondary

2.2.2 Static Measurement and Analysis Techniques

Included were:

- o Development of measurement techniques
    - flux mapping

  - voltage and current measurement
  - thrust measurement

- Development of data analysis techniques

  - signal conditioning and analysis
  - equivalent circuit parameter determination

2.2.3 Measurement System Specification/Test Stand Specification

Included were:

- Designs of apparatus

  - flux transport mechanism
  - current amplifiers
  - voltage amplifiers

- Specification of Instrumentation

  - shunts
  - loadcells
  - conditioning amplifiers
  - data sampling and storage system

- Design of test frame and power circuit

2.2.4 Experimental Prototype Specification

- Design of 2/3, 3/3 and 4/6 LIM windings

- Design of wound and cage secondaries
- Design of sheet secondaries

2.2.5 LIM Model Computer Program

- Implementation of first LIM Equivalent Circuit Model in FORTRAN

2.2.6 Data Analysis Computer Program

- Implementation of static analysis algorithms in FORTRAN
- Development of sampling, storage, and retrieval software

2.2.7 Milestone: Static Test Facility Installed and Commissioned

2.2.8 Static Experiments

- Approaches and results relating to static tests on three LIM primaries with various secondary configurations and airgap settings

2.2.9 Dynamic Measurement and Analysis Techniques

- Extension of static measurement techniques
- Development of new techniques
  - speed measurement
  - airgap measurement
  - vertical force measurement

2.2.10 Test Track/Measurement System Specification

- Specification of Test Track layout
- Design of control system
- Design of measurement systems

2.2.11 Data Analysis Computer Program (Dynamic)

- Implementation of dynamic analysis methods in FORTRAN

2.2.12 Test Track Construction/Commissioning

- Construction of
    - track and shed
    - carriage
    - LIM, sensing and control systems
    - test stand
- Commissioning of
    - measurement systems
    - speed control system

2.2.13 Dynamic Experiments

- Approaches to, and results of, testing two LIM primaries with various secondary configurations and airgap settings

2.2.14 System Control Problems and Approaches

- Development and computer implementation of a time-step simulation of a generic LIM motion control system

3.0 GENERAL DISCUSSION

The 60 Hz LIM Development Program has generated a great deal of technical information about small Linear Induction Motors. The information facilitates "design-to-specification" as well the performance of design trade-off assessments. Before entering into detailed descriptions of the program findings, we will take a broader view of the subject of 60 Hz LIM propulsion and attempt to extract some general reactions to the knowledge gained.

3.1 LIM WEAKNESSES

Those familiar with conventional electric motors are often surprised at the performance characteristics of small LIMs, particularly in terms of their smaller efficiency, power factor, and power per unit mass.

If the benefits of linear propulsion are easily recognized, it is not so obvious why LIMs are inefficient and large compared to conventional machines. To focus on the relatively large airgap as the cause of deficiency is not at all accurate. Nor is it correct to attribute the low efficiency to the inherently high slip at which 60 Hz LIMs operate. These points represent only part of the cause.

The major reason for low performance in small LIMs is the relatively short pole pitch required for low speed. Short pole pitches result in a variety of problems, the most notable ones being the poor ratio of magnetic circuit permeance to electric circuit resistance, and the increased tendency toward magnetic leakage.

There is a second difficulty associated with low-speed LIMs which is quite fundamental but often overlooked. That is, because the speeds are low, the amount of power developed per unit mass of LIM is low. Rotary machines develop considerably more power for a given amount of copper and steel because they operate at high peripheral speeds. (Recall that power equals force x speed). This speed is usually converted to a lower "working" speed via some sort of mechanical transmission. With the LIM, of course, there is no analogue to a transmission, and this is often thought of as one of the LIM's benefits, i.e., that it is a direct-drive device. The "cost" of this benefit is a machine which has a power-to-mass ratio many times inferior to the rotary machine.

We therefore acknowledge two reasons why the 60 Hz, low-speed LIMs tend to be relatively large and inefficient:

1) They have small pole-pitch.
2) They operate at low speed.

The first of these is related to the use of 60 Hz as a supply frequency. A lower frequency would allow a longer pole pitch and an improved LIM.

The second reason is fundamental, and is universal to all electric machines. LIMs cannot have power-to-mass ratios comparable to rotary motors. However, as Prof. Laithwaite, a pioneer in the field points out, this does not mean the machine is useless. Some applications require a LIM to produce static thrust. If this implies a power-to-weight ratio of zero, the machine still performs a useful function.

3.2 LIM BENEFITS

In terms of traditional electrical motor specifications such as efficiency, power factor, and power-per-unit mass, small 60 Hz LIMs do not compare favourably with conventional motors. By their unique topology, however, they do open up a large range of applications in which conventional motors are not as well suited. Clearly, the utility of the LIM cannot be measured by standard specifications; rather, it must be compared with other options within the context of the system in which it will be applied. Does its use improve reliability? Enhance safety? Reduce maintenance? These and other considerations often make the LIM a favoured option as a drive-system element. The following sections discuss some typical situations in which LIMs offer benefit.

3.2.1 Simpler Mechanical Design

Various mechanical means exist for converting rotary motion to linear motion. Figure 3-1 illustrates some of these. Common to all mechanical approaches is the fact that force is transferred through one or more mechanical interfaces. The requirement to transfer force brings with it the need for mechanical components: shafts, gears, cables, couplings,

1) DRUM & CABLE

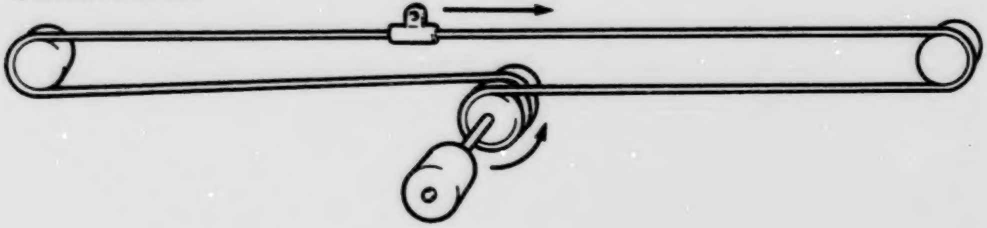

2) RACK & PINION

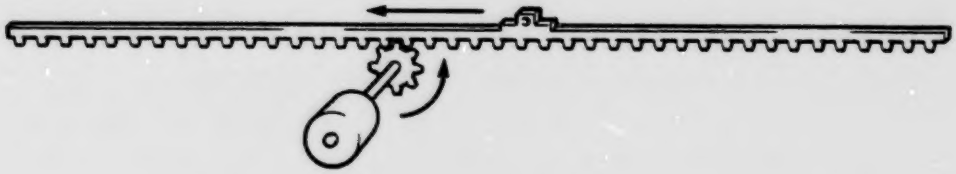

3) SCOTCH YOKE

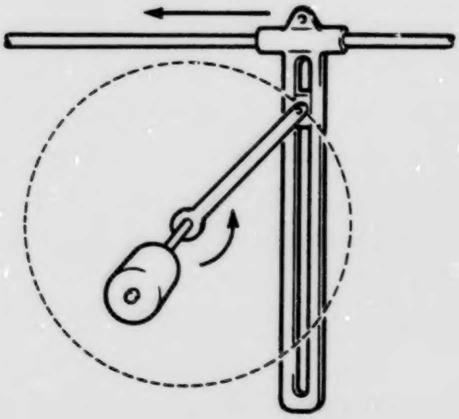

4) LEAD SCREW

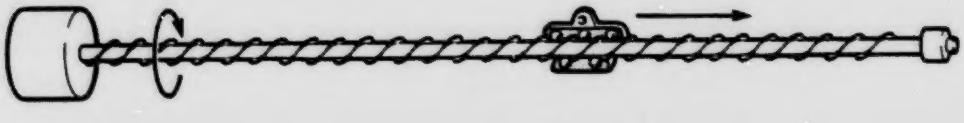

FIG. 3-1: MECHANICAL LINEAR DRIVE APPROACHES

sheaves, and so on. These elements are eliminated in a LIM-based drive, since force in the LIM is transferred at an electromagnetic interface, directly, with no intermediate mechanical linkage.

3.2.2 Reduced Noise/Wear

Wherever force is transferred mechanically, there will be noise and wear. As the speeds associated with the transfer increase, noise and wear also increase, so much so that many types of rotary-to-linear drive mechanisms are simply not practical beyond certain limiting speeds.

LIMs, because they do not depend on a mechanical interface for force transfer, are free of wear, and have comparatively low noise.

3.2.3 Responsive Control

A key design focus in motion control systems is the characteristic of the drive as an actuator: its linearity of response, speed of response, and repeatability of response. Many mechanical drive approaches suffer inherently from non-linearity, poor transient response, and poor repeatibility due to such factors as "gear backlash," cable-stretching, variable friction, variable geometry, and mechanical inertia. All of these sources of difficulty are eliminated in the LIM, making it a near-ideal control element.

3.2.4 Inherent Safety Features

- 60 Hz LIMs are inherently speed-limited, eliminating the need for mechanical overspeed protection found in DC rotary drives.
- LIM primaries may be placed in the floor or track structure eliminating need for exposed power rail.
- The absence of mechanical linkages means the elimination of components that can pinch, scrape, or strike.

3.2.5 Rugged, Reliable

- LIM primaries may be totally encapsulated, making them impervious to many damaging environmental factors.
- The simple design of both primary and secondary structures, and the elimination of such components as brushes, commutators, slip rings, and bearings, ensures high reliability.

3.3 OPPORTUNITIES FOR IMPROVEMENT IN DESIGN

To a certain extent, it is possible to make improvements over existing commercial designs for 60 HZ LIMs. LIM suppliers tend to use a very few standard designs on which they base all variant designs. This minimizes their re-tooling and set-up requirements and at the same time simplifies their design task. For the type of market these suppliers have targeted, it simply does not pay to use a more sophisticated design approach. When unusual requirements come along and a truly new design is required, the client must be convinced to pay for an expensive development and test effort. It is not difficult to see why LIMs do not proliferate in industrial applications despite their generic benefits: there is limited scope in the "standard" commercial design.

If a LIM were being designed for a specific application which was going to use a large quantity (e.g.,1,000 or more), there would be ample reason to abandon the standard design and "start from scratch." The benefits would include improved efficiency and power factor, smaller size and weight, and reduced cost. The design procedure would involve the use of:

1) A model or system simulation of the in-situ operation, so as to determine the thrust-versus-time and speed-versus-time requirements.

2) The LIM performance model, which would be used in an iterative procedure to arrive at a design configuration.

3) A finite-element magnetic model, which would be used to check flux densities in the magnetic circuit.

These design tools have been developed by, or are available to, UTDC R&D. They represent an important asset and will have a great impact on LIM designs in future applications.

3.4 OPPORTUNITIES FOR NEW DESIGNS

In the course of studying existing LIM designs, a number of "new" design concepts have emerged. Some of these simply extend the applicability of the present LIM; however, others may someday replace the present design concept. These opportunities are briefly discussed in the following subsections.

3.4.1 Wound Secondary

A wound secondary was designed, constructed, and demonstrated under the 60 Hz Development Program. Further analysis and design will be required, but the prototype does demonstrate that thrust and power recovery can be achieved concurrently and at reasonable levels. Possible applications for the wound secondary include:

1) Vehicle battery-charging, when combined with a Slip Power Recovery Unit (SPRU).

2) Supply of power to vehicle loads, by direct connection to the winding (e.g., fans, compressors).

3) Power factor improvement, by connecting capacitors to the winding.

4) Thrust control, through manipulation of winding resistance.

3.4.2 "Gramme-Slab" Primary

The approach which was taken in the design of the wound secondary was to wind the coils completely around the core rather than into one face. This type of winding (Gramme) is a very early form and was replaced in rotary AC motors by the standard double-layer winding.

It is possible to imagine a LIM primary being Gramme-wound. This, in fact, was attempted in the early stages of ICTS LIM development but was found unsuitable for that application. There is reason to believe that Gramme winding combined with a slotless core (slab) could be practical for small, in-track LIM primaries.

The configuration appears to be low cost and highly suited to automated manufacturing. In addition, it can have a very shallow profile, thus allowing for relative ease of installation in many applications.

3.4.3 LIM Steering

One of the seldom-used forces generated by the LIM is the lateral "centering" force. The force-displacement characteristic was measured statically for small 60 Hz LIMs and found to be approximately linear, like a spring. Others have considered the possibilities of using this force (as well as the vertical attractive force) in an integrated suspension/guidance/propulsion configuration. Rohr Corporation actually built a small prototype system to demonstrate the concept.

The lateral forces generated by small LIMs are only 10 to 30 percent of the thrust force and are likely too small to be used in vehicle guidance. A more practical approach is to use the forces to drive a steering mechanism on a wheeled vehicle. This system provides the opportunity to let the in-floor LIMs define the guide-path, therefore eliminating tracks and switches.

4.0 LIM MODELS

Understanding begins with investigation, which inevitably involves the use of conceptual and mathematical models. The power of models is not always in their predictive capability: Often they serve to focus our thinking on aspects of the problem in which we lack sufficient understanding. (Sometimes a model can teach us a great deal by its failure to predict).

The art of modelling engineered systems is becoming increasingly sophisticated due to the proliferation of computers (and people who use them) in the engineering workplace. Still, when choosing a basis for modelling it is a good principle to begin simply. Eventually, the simple models are replaced by more sophisticated ones, but at no time should the fundamental relationships be obscured to the investigator because of the model.

One of the principles maintained through the course of the 60 Hz LIM development program was to adopt models which could be easily related to physical experiments. A survey of LIM-related literature indicated that in many cases, investigators neglected to couple their theoretically-based conclusions with anything but the most superficial of experimental comparisons. This unfortunate situation is often attributable to the fact that many researchers lack their own experimental facilities, and cannot generate the type of experimental data needed to truly validate their theories.

In other cases the theories themselves are difficult, if not impossible to experimentally test, even if considerable resources were available.

The models which were developed and used in this program are by comparison to those found in much of the literature, simple, if limited. It was felt important, however, that the theoretical framework should be kept understandable to anyone familiar with classical induction motor theory. It is believed that what limitations there are have not impeded progress towards achieving the program goals.

4.1 CONCEPTUAL MODEL

How does a LIM work?

A verbal answer to this question may be considered a "conceptual model" of the LIM, and while never complete, can still be correct, in the sense that it does not make false assertions about the physical principles involved.

A LIM "works" by converting some of the electrical energy supplied to the primary into mechanical (kinetic) energy. In order to accomplish this, a number of fundamental things take place:

1) Current supplied to the primary is fed to individual motor coils in such a way as to cause a longitudinally travelling, laterally directed, current wave on the primary face.

2. This current wave establishes a longitudinally travelling, perpendicularly directed, magnetic field wave which "pierces" a conducting sheet placed adjacent to, but spaced marginally from, the primary face.

3. The magnetic field wave travels with respect to the conducting sheet, inducing in it a travelling, laterally directed, current wave.

4. The magnetic field wave and secondary current wave interact to provide force in a longitudinal direction.

The above description attempts to outline the fundamental interactions, but is still a long way from a satisfactory explanation of LIM operation. Some questions which follow from this description are:

- How is the current supplied at the motor terminals made to follow a "wave pattern" on the primary face? How does the pattern "travel"?

- What material and geometrical parameters affect the size and shape of the magnetic field resulting from the primary current wave?

- Does the direction of relative travel between the primary wave and the secondary sheet matter?

- How do the concepts of electric current and magnetic field relate to the flow of energy in the LIM?

Each of these questions are important in the design and application of LIM's. Other questions will arise as we attempt to answer these few, and eventually our conceptual model will have grown quite sophisticated, albeit qualitative.

We begin to subdivide the model into parts:

1. Winding Model
2. Magnetic Circuit Model
3. Force Production Model
4. Energy Model

4.1.1 Winding Model

Most books written about the theory of motor windings develop an analysis of a general poly-phase winding of "n" phases. Here we restrict the discussion to three-phase windings because they are by far the most common. (Some small LIM's are manufactured with two-phase windings, but the subject of two-phase operation would complicate the discussion unnecessarily).

Figure 4.1 illustrates a fundamental rule for three-phase motor windings: Three time-alternating currents, symmetrically arranged in their time-phase, feed three "distance-alternating" windings, symmetrically arranged in their "distance-phase".

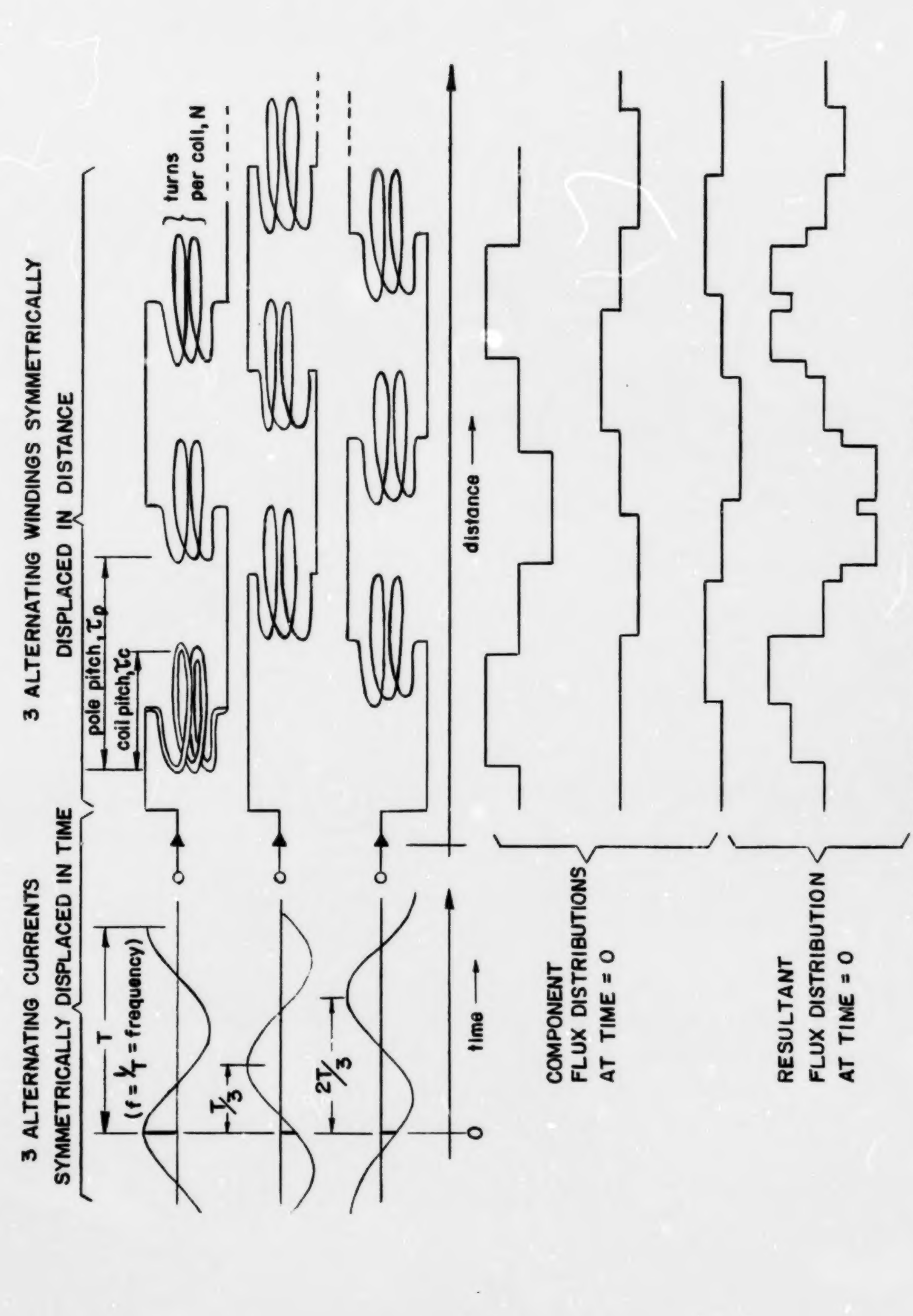
3 ALTERNATING CURRENTS
SYMMETRICALLY DISPLACED IN TIME
T
(f = 1/T = frequency)
T/3
2T/3
time →
0
3 ALTERNATING WINDINGS SYMMETRICALLY
DISPLACED IN DISTANCE
pole pitch, τp
coil pitch, τc
turns per coil, N
distance →
COMPONENT
FLUX DISTRIBUTIONS
AT TIME = 0
RESULTANT
FLUX DISTRIBUTION
AT TIME = 0

FIG. 4-1: PRINCIPLES OF THREE-PHASE WINDINGS

The terminology employed illustrates the point that the currents and the windings can be thought of as "waves" in time and distance respectively. The combination of the three current waves and the three winding waves results in what is effectively a single, travelling, current-density wave, which may be characterized by its wavelength, amplitude, and speed of travel.

Figure 4-1 is only a schematic representation of a winding, but serves to indicate the major parameters which affect the wavelength, amplitude, and speed of the current density wave. They are:

- Supply Current, I
- Supply Frequency, f
- Pole Pitch, τ_p
- Coil Pitch, τ_c
- Turns per Coil, N

It can be shown that the following relationships between the current-density wave and the winding parameters hold:

$$\text{Amplitude} = N \times I \times \sin \frac{\pi}{2} \frac{\tau_c}{\tau_p} \qquad (4.1\text{-}1)$$

$$\text{Wavelength} = 2 \times \tau_p \qquad (4.1\text{-}2)$$

$$\text{Wave Speed} = f \times 2 \times \tau_p \qquad (4.1\text{-}3)$$

There are various types of windings which can be configured for LIMs (for example, see Figure 4-2), but every type develops a current density wave from the same basic principles outlined here.

The most prevalent form of winding is the double-layer type shown in Part 1 of the figure. Note that in this winding there is opportunity to make the coil-pitch-to-pole-pitch ratio as high as unity. This is an important quality, since as can be seen from the relationship 4.1-1 above, this ratio is related to the wave amplitude and is therefore a measure of the "effectiveness" of the winding at developing a current density wave from a given current.

a) DOUBLE LAYER WINDING:

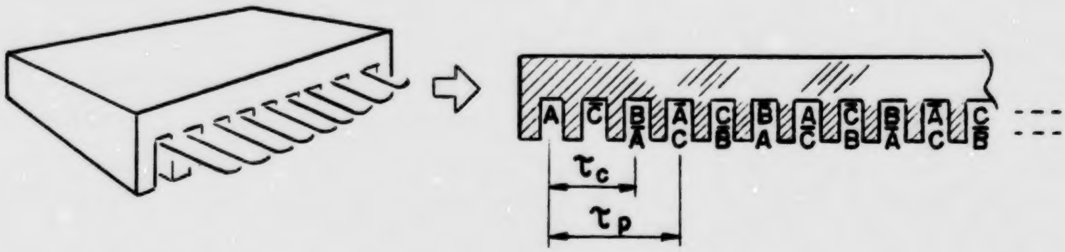
A
C̄
B Ā
Ā C
C B̄
B̄ A
A C̄
C̄ B
B Ā
Ā C
C B̄
τ_c
τ_p

b) GRAMME WINDING:

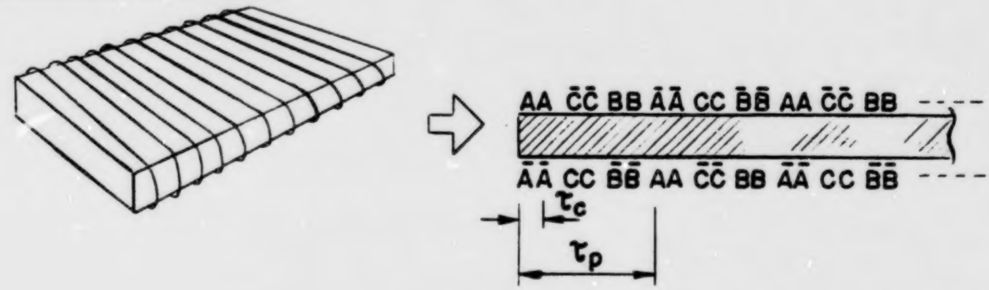
AA C̄C̄ BB ĀĀ CC B̄B̄ AA C̄C̄ BB
ĀĀ CC B̄B̄ AA C̄C̄ BB ĀĀ CC B̄B̄
τ_c
τ_p

c) DISCRETE POLE WINDING:

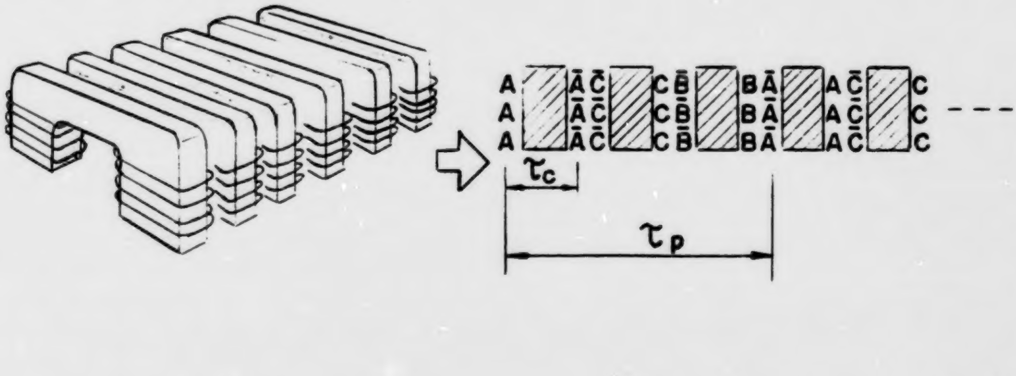
A ĀC̄ CB̄ BĀ AC̄ C
A ĀC̄ CB̄ BĀ AC̄ C
A ĀC̄ CB̄ BĀ AC̄ C
τ_c
τ_p

FIG.4-2: LIM WINDINGS

4.1.2 Magnetic Circuit Model

The so-called "magnetic circuit" is a very useful conceptual tool in understanding LIM operation. In its simplest form, the magnetic circuit is analogous to the dc electrical circuit. The quantities voltage, current, and resistance are replaced with the quantities magnetomotive force (mmf), flux, and reluctance. The mmf is considered to "drive" flux through a reluctance according to the following relation:

$$\mathcal{F} = \Phi \mathcal{R} \qquad (4.1\text{-}4)$$

Where:

$\mathcal{F}$ = mmf
Φ = flux
$\mathcal{R}$ = reluctance

Like the electrical analog, this relation applies to a completed circuit or closed path. Also, just as an electrical source has a "positive" and "negative" pole, an mmf source always has a "north" and "south" pole. Flux is considered to "flow" from north to south.

The mmf of a LIM magnetic circuit is directly related to the current density wave described in Section 4.1.1. In fact, for the purposes of quantitative modelling we will later define an "mmf wave" and relate it to the current density wave by a specific formula.

The reluctances which play a part in the LIM magnetic circuit are predominantly due to the non-ferrous portions of the LIM configuration. Air, copper and aluminum are many hundreds of times more reluctive to magnetic flux than is steel, and so for the purposes of our conceptual model we may consider the steel to have zero reluctance.

Figure 4-3 illustrates, in a pair of diagrams, the principle of the magnetic circuit. Shown are two coils only. This is done for clarity. The ommission of the other coils does not affect the argument.

In the first part of the figure we view the current-carrying coils as sources of mmf. The mmf is in a direction perpendicular to the coil face, i.e., so as to drive flux into the airgap region of the motor. Two circuit paths are indicated: one which links the primary and secondary magnetic structures and one which does not. These two paths are termed the "magnetizing" and "gap leakage" components respectively.

In the second part of the figure we note that the coils, because of the way they are oriented in a double-layer winding, also have a vertical face, which is associated with a longitudinally directed mmf component. This mmf acts to drive flux across the slot regions, and is termed the "slot leakage" component.

The utility of the magnetic circuit model becomes apparent when one recognizes the relationship of the circuit to the physical geometry of the LIM.

a) CIRCUIT FOR AIRGAP FLUX:

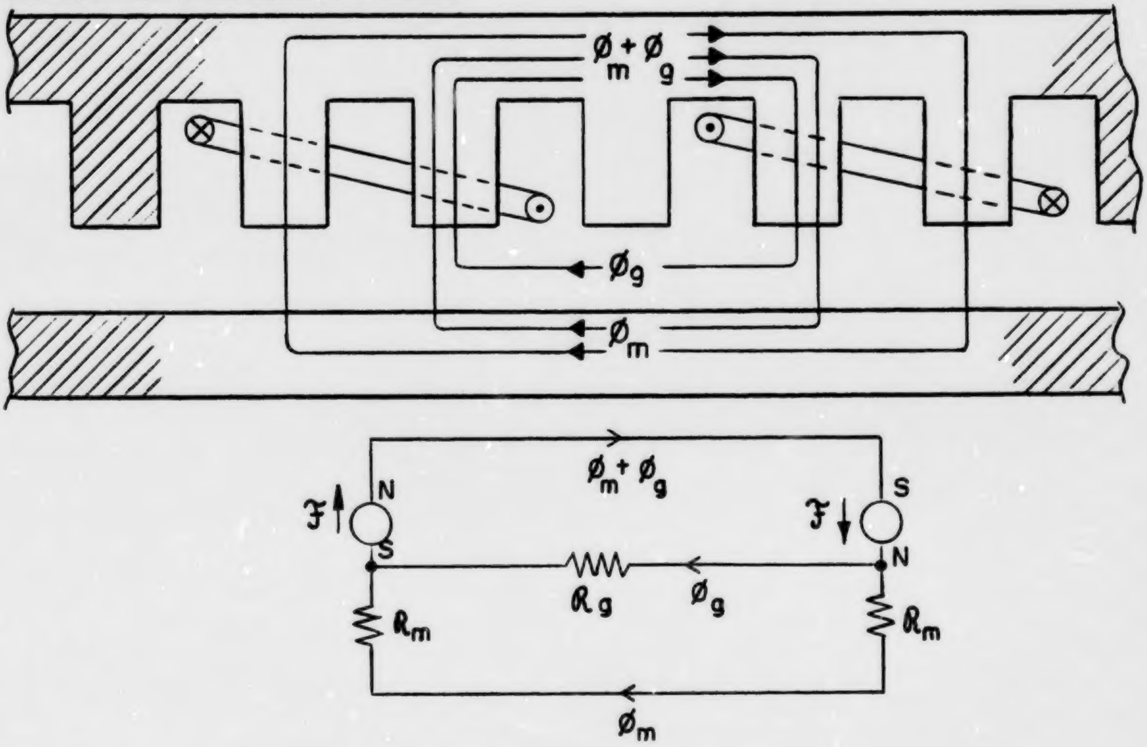
Ø_m + Ø_g
Ø_g
Ø_m
Ø_m + Ø_g
N
S
F
F
S
N
R_g
Ø_g
R_m
R_m
Ø_m

b) CIRCUIT FOR SLOT FLUX:

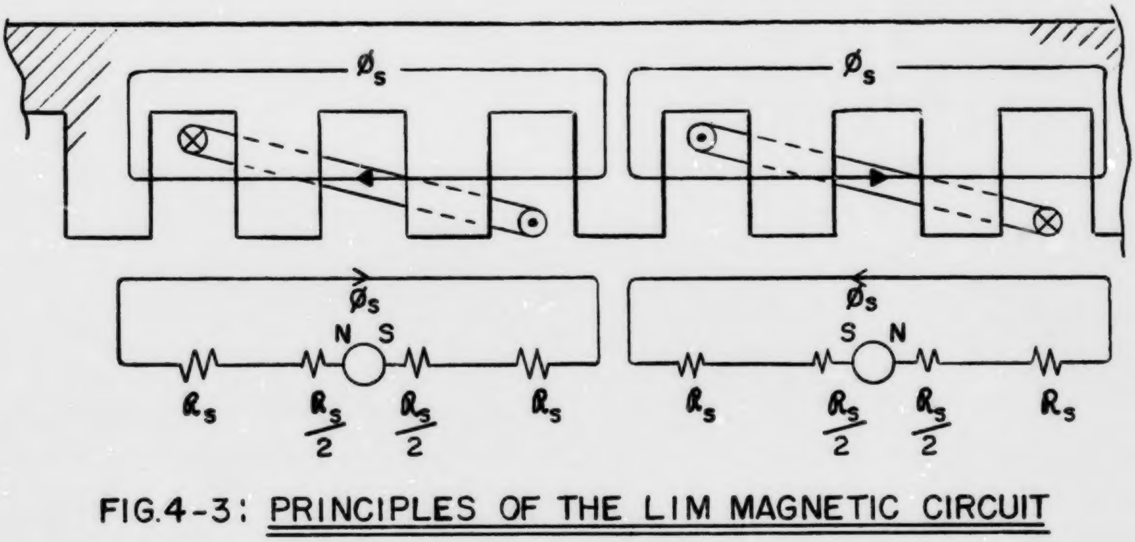
Ø_s
Ø_s
Ø_s
Ø_s
N S
S N
R_s
R_s/2
R_s/2
R_s
R_s
R_s/2
R_s/2
R_s

FIG.4-3: PRINCIPLES OF THE LIM MAGNETIC CIRCUIT

The reluctance of a magnetic path is proportional to its length, and inversely proportional to its cross-sectional area. That is, where we desire the flux to be low, we design for long, narrow magnetic gaps (a magnetic gap is simply a non-ferrous space which the flux must traverse to complete the circuit); where we desire flux to be high, the gap must be short, and large in cross-section.

From the figures we can identify the geometrical parameters that allow us to alter the lengths and cross sections of the magnetic gaps. The following table summarizes the effects of parameter changes on the three flux components identified.

If we increase...	The result is...		
	Magnetizing	Gap Leakage	Slot Leakage
o Pole Pitch	↑	↓	↓
o Airgap	↓	↑	-
o Slot Width	-	-	↓
o Slot Depth	-	-	↑
o Core Width	↑	↑	↑

The table is helpful in showing how we can increase the magnetizing flux relative to the two leakage fluxes. If this were our only model, we would design a motor with a very long pole-pitch, short airgap, and wide, shallow slots. As we shall see, however, there are other things which must be considered in a practical design.

4.1.3 Force Production Model

There are two types of forces produced in induction motors. One is related only to the magnetic field which links the two ferrous masses of the primary and secondary structures. It is termed the magnetic force, and always acts so as to attract the primary to the secondary. (This is the same type of force exerted by a permanent magnet on a piece of iron.)

The other force produced in the induction motor is due to the interaction of current density with magnetic flux density, and is termed the electro-magnetic force. Flux density and current density are vector quantities (meaning they have both magnitude, and a direction in space). When flux density and current density are present within some space, the resulting force will be in a direction which is perpendicular to both quantities. The specific vector relationship is:

$$\underline{F} = \underline{J} \times \underline{B}$$

$\underline{F}$ = force vector
$\underline{J}$ = current density vector
$\underline{B}$ = flux density vector

Electromagnetic force production may be considered to occur in the secondary conducting sheet, or top cap. The current density within the top cap is laterally directed, but the flux density generally has both vertical and longitudinal components. These combine with the current density to generate longitudinal and vertical forces, respectively. (The longitudinal force is, of course, the LIM thrust.) The vertical force is always repulsive, and acts against the attractive magnetic force described earlier. In practice, the combined vertical force generated in a LIM may be attractive, repulsive, or zero, depending on the relative strengths of the magnetic and electromagnetic influences.

4.1.3.1 Examination of the Thrust Force

Current density in the secondary top cap is generated as a result of the relative movement of the travelling magnetic field wave with respect to the top cap material. We can imagine three conditions under which a relative movement can exist:

1) The field is travelling in the same direction as the top cap but at a higher speed.

2) The field is travelling in the same direction as the top cap but at a lower speed.

3) The field is travelling in the opposite direction to the top cap.

We speak of conditions of "slip" to describe the difference in "field" and "mechanical" speed, and later we will quantify slip more precisely. The point to be made here is that the first condition described above results in an induced current which, combined with the flux density vector, generates a force which tends to increase the speed of the secondary relative to the primary. The other two conditions result in forces which tend to decrease the speed.

An analogy which reflects the principle of induction motor slip very well is that of a wheel on a road surface (see Figure 4-4). If we cause the wheel to rotate such that the peripheral speed exceeds the speed of forward travel there will be slippage, and a tractive force will develop at the tread/road contact patch. If the rotational speed of the wheel is reduced so that the peripheral speed is smaller than the speed of forward travel, the force developed will be in a direction so as to retard the forward motion. Lastly, suppose the wheel rotation were opposite to the direction of travel. The slippage is more pronounced than in the previous case, but, again, retarding forces are developed.

It is interesting to note that, in the case of a wheel on a road surface, force at the tread/road interface can only exist if there is some finite slip. This principle of wheel behaviour has an exact dual in the induction motor. Under conditions of zero slip, currents cannot be induced in the secondary conduction sheet, and electromagnetic forces do not develop.

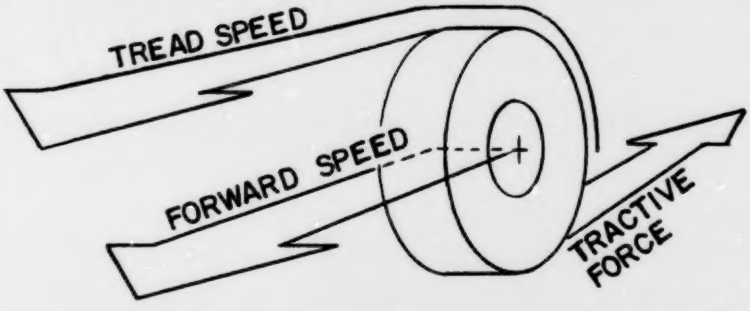
TREAD SPEED
FORWARD SPEED
TRACTIVE FORCE

1) TREAD SPEED EXCEEDS SPEED OF FORWARD TRAVEL: TRACTIVE FORCE DEVELOPS

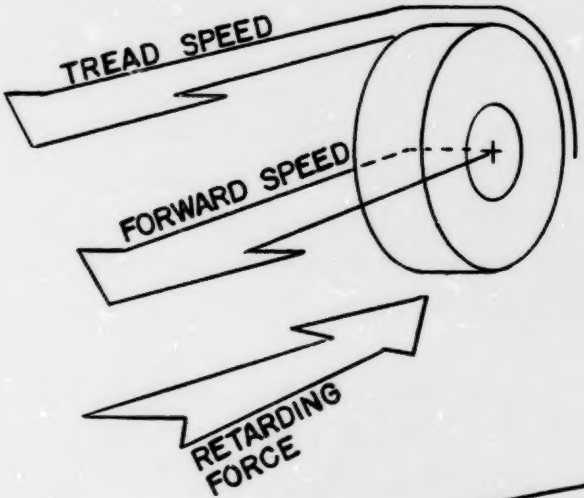
TREAD SPEED
FORWARD SPEED
RETARDING FORCE

2) SPEED OF FORWARD TRAVEL EXCEEDS TREAD SPEED: RETARDING FORCE DEVELOPS

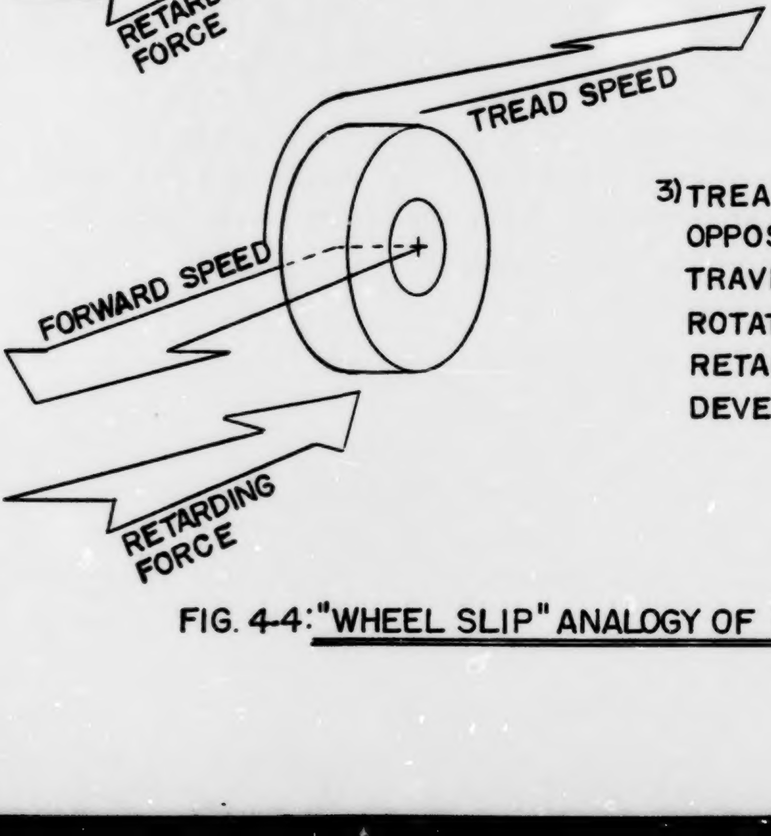
TREAD SPEED
FORWARD SPEED
RETARDING FORCE

3) TREAD SPEED IS OPPOSITE TO FORWARD TRAVEL (WHEEL ROTATION IS REVERSED): RETARDING FORCE DEVELOPS

FIG. 4-4: "WHEEL SLIP" ANALOGY OF LIM FORCES

4.1.4 Energy Model

Where does the energy supplied to the LIM input terminals end up? To answer this question is to take the first step in producing a more energy-effective LIM design.

Figure 4-5 is a power-flow graph of the LIM. From the graph we note that besides being converted to mechanical energy, some of the energy supplied is dissipated in heat; and some is stored. The following sub-sections analyze the nature of each branch in the power-flow graph.

4.1.4.1 Reactive Power Flow

Reactive power is sometimes termed "imaginary power," because it cannot be associated with mechanical work or energy dissipation. It results in ac-supplied systems which contain energy-storage elements. Energy is actually exchanged between the system and its supply in a cyclical manner.

The energy storage in a LIM is due to the magnetic fields established when current flows. We know from our magnetic circuit model of Section 4.1.2 that some of the stored energy will be associated with the magnetic circuit which links the primary and secondary structure and that some of the stored energy will be associated with the so-called "leakage" paths.

If we want to minimize the tendency of the LIM to draw reactive power, we must minimize the energy

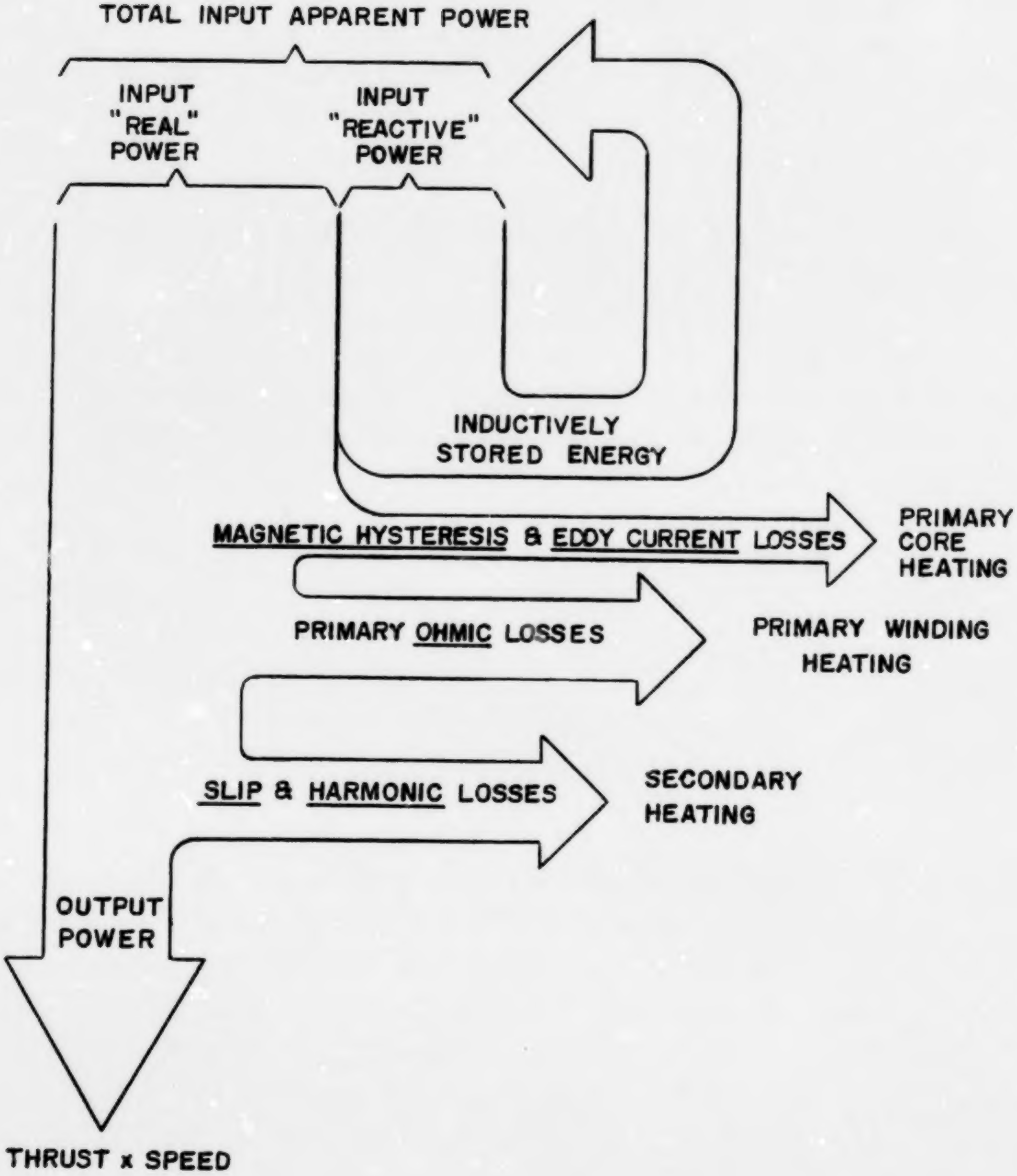
TOTAL INPUT APPARENT POWER
INPUT "REAL" POWER
INPUT "REACTIVE" POWER
INDUCTIVELY STORED ENERGY
MAGNETIC HYSTERESIS & EDDY CURRENT LOSSES
PRIMARY CORE HEATING
PRIMARY OHMIC LOSSES
PRIMARY WINDING HEATING
SLIP & HARMONIC LOSSES
SECONDARY HEATING
OUTPUT POWER
THRUST x SPEED

FIG.4-5: LIM ENERGY MODEL

storage in the various magnetic circuits. The energy in a magnetic circuit is:

$$E = \frac{1}{2}\Phi^2 \mathcal{R}$$

Where:

E = energy
Φ = flux
$\mathcal{R}$ = reluctance

We see that stored energy will be reduced if flux is reduced. This is done in the leakage paths by designing to keep the path reluctance high. We cannot design the magnetizing path this way, however, or we will not achieve the magnetic linkage between the primary and secondary that we require for good energy coupling. We will later see that the best way to minimize stored energy in the magnetizing circuit is to minimize the path reluctance. This seems counter-intuitive until we realize that the flux in the magnetizing circuit is not dependent exclusively on the primary mmf, but also on the "back-mmf" resulting from induced currents in the secondary sheet.

4.1.4.2 Primary Losses

Three types of energy losses occur in the LIM primary:

Winding ohmic losses are a result of the current flowing through the resistance of the LIM winding.

Eddy-current losses develop when the alternating magnetic fields induce currents in the conductive material of the primary core. (Cores are constructed of thin laminations of silicon-steel, oriented spatially so as to greatly reduce the "bulk" conductivity of the core. This approach greatly reduces eddy-currents and their associated ohmic loss.)

Magnetic hysteresis losses occur when the core material is subject to cyclical magnetization. Hysteresis loss, like eddy-current loss, depends on flux density and supply frequency. Electrical lamination material generally carries some sort of specification which incorporates both types of losses.

4.1.4.3 Secondary Losses and Output Power

The force production model of Section 4.1.3 explained that an electromagnetic force develops in the secondary top cap when laterally directed current density and vertically directed flux density co-exist. To further conceptualize the nature of this force, we introduce the idea of "travelling force." If we consider this force to be travelling longitudinally at the speed of the primary current density wave, we can associate the force and the speed with power delivered to the secondary:

$$P_2 = F \times v_{field}$$

Where:

P_2 = total secondary power
F = longitudinal force (thrust)
v_{field} = speed of travelling wave

Some of this power contributes to the output mechanical power:

$$P_{mech} = F \times v_{mech}$$

The remainder of the power must be absorbed by the secondary as heat.

$$P_{loss} = P_2 - P_{mech}$$

$$= F\ (v_{field} - v_{mech})$$

It is interesting to consider the expression for the ratio of secondary power loss to total secondary power:

$$\frac{P_{loss}}{P_2} = \frac{(v_{field} - v_{mech})}{v_{field}}$$

The right-hand side of the equation is known as the "slip" and determines the proportion of the total secondary power which must be dissipated in the secondary sheet. This relationship is valid for each of the slip conditions highlighted in Section 4.1.3.1, but is undefined for conditions where the travelling wave speed is zero.

Referring again to the power flow graph of Figure 4-5, we note a power loss term labelled "harmonic loss." This loss component is associated with travelling waves which are a result of effects due to the possible non-sinusoidal nature of either the supply current waveform or the winding waveform discussed in Section 4.1.1. Normally these losses are second-order effects, but can be an influence on LIM behaviour.

4.2 QUANTITATIVE MODEL

The concepts introduced in the previous sections help to form an understanding of LIM behaviour. To a certain extent, they allow us to discern important parameters and predict trends, but offer little capability for quantitative analysis.

A framework is neeeded to tie the various aspects of our conceptual model together in such a way as to provide a means of performance calculation. There are various approaches available; for example, see References 1 and 2. The approach taken under this program is the classical "equivalent circuit" model. It is felt that of all the available approaches, the equivalent circuit is the one:

1) Most familiar to non-specialists,
2) Most easily linked with physical measurements,
3) Best suited to modification by empirical factors.

The equivalent circuit is basically an accounting of the power flow in the motor through the use of inductive and resistive circuit elements. The specific material and geometrical parameters which characterize a LIM are reduced by means of formulae to generate these elements. The circuit is then formed, and the "forcing functions" (usually the voltage, frequency, and mechanical speed) are specified. Solving the curcuit equations and applying various other relationships allows us to deduce most aspects of the motor behaviour. A schematic block-diagram of the process appears in Figure 4-6.

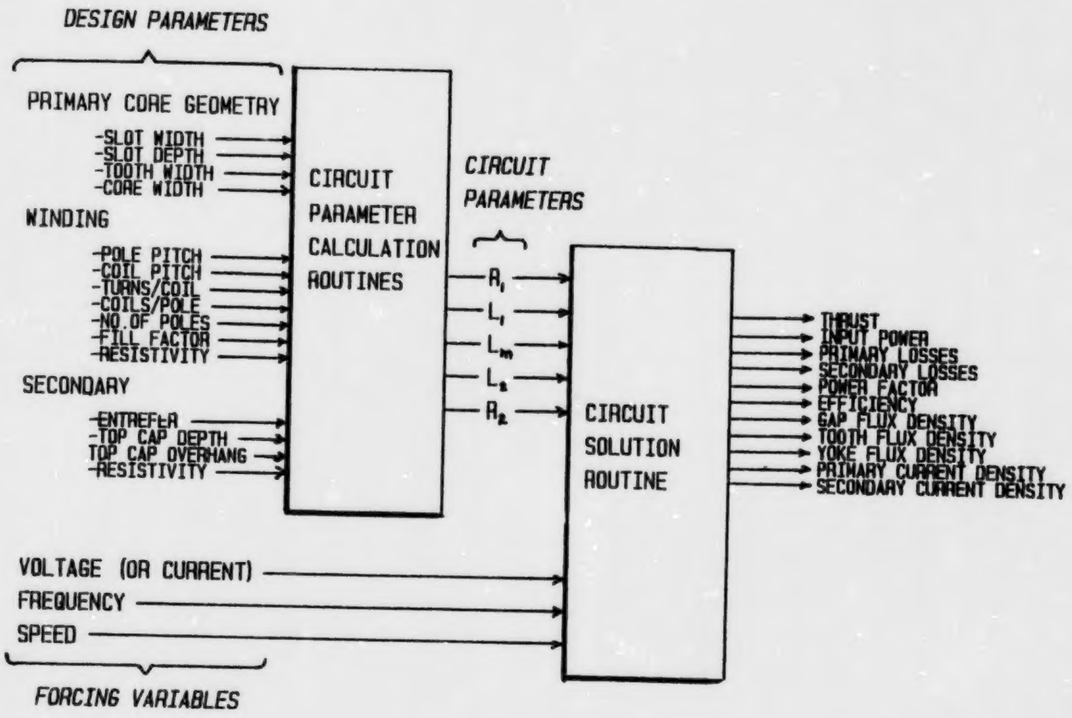
DESIGN PARAMETERS
PRIMARY CORE GEOMETRY
-SLOT WIDTH
-SLOT DEPTH
-TOOTH WIDTH
-CORE WIDTH
WINDING
-POLE PITCH
-COIL PITCH
-TURNS/COIL
-COILS/POLE
-NO. OF POLES
-FILL FACTOR
-RESISTIVITY
SECONDARY
-ENTREFER
-TOP CAP DEPTH
TOP CAP OVERHANG
-RESISTIVITY
CIRCUIT PARAMETER CALCULATION ROUTINES
CIRCUIT PARAMETERS
R1
L1
Lm
L2
R2
CIRCUIT SOLUTION ROUTINE
THRUST
INPUT POWER
PRIMARY LOSSES
SECONDARY LOSSES
POWER FACTOR
EFFICIENCY
GAP FLUX DENSITY
TOOTH FLUX DENSITY
YOKE FLUX DENSITY
PRIMARY CURRENT DENSITY
SECONDARY CURRENT DENSITY
VOLTAGE (OR CURRENT)
FREQUENCY
SPEED
FORCING VARIABLES

FIGURE 4-6 Principles of the "EQUIVALENT CIRCUIT" Modelling Approach

4.2.1 Formulating the Equivalent Circuit Parameters

It is possible to develop analytical formulae for most of the equivalent circuit parameters by adopting a simplified geometrical model. In this model we make the following assumptions:

1. Flux travels in "straight lines" across the magnetic gap (i.e., vertically across the airgap and horizontally across the slots).
2. The "travelling waves" are sinusoidal.
3. Ferrous portions of the magnetic paths contribute zero reluctance (infinite permeability).
4. Current density in the secondary exists only in the conductive "top cap." (Secondary back-iron is non-conducting.)
5. Secondary current density is laterally directed only.

Derivations of the formulae for the equivalent circuit parameters may be found in the Appendix 1. Table 4-1 is a summary of the relationships between the LIM design parameters and the equivalent circuit parameters according to these formulae.

4.2.2 Examination of Formulae

For some types of induction motors, the "standard" formulae generate parameter values which result in

TABLE 4-1: FUNDAMENTAL RELATIONSHIPS

	R_1	L_{ew}	L_s	L_g	L_m	L_2	R_2
g_c				s	i	s	
τ_p	s	s	i	s	d	i	i
τ_c	s	s	s	s	s		s
τ_s			d	s	s		
w_s	i		i	s	s		
h_s	i		d				
W			d	d	d	d	d
P	d	d	d	d	d	d	d
N	d^2	d^2	d^2	d^2	d^2	d^2	d^2
b	d^2	d^2	d^2	d^2	d^2	d^2	d^2
δ						d	i
ρ							i

d: direct relationship i: inverse relationship s: second order effect

Design Parameters:

g_c = equivalent magnetic gap (m)
τ_p = pole pitch (m)
τ_c = coil pitch (m)
τ_s = slot pitch (m)
w_s = slot width (m)
h_s = slot height (m)
W = primary core width (m)
P = number of pole-pairs
N = number of turns/coil
b = number of coils/pole/phase
δ = secondary sheet depth (m)
σ = secondary sheet conductivity (mhos/m)

Equiv. Circuit Parameters:

R_1 = primary resistance
L_{ew} = endwinding leakage
L_s = slot leakage
L_g = gap leakage
L_m = magnetizing inductance
L_2 = secondary leakage
R_2 = secondary resistance

satisfactory predictions of performance. The type of LIMs we consider, however, cannot be adequately modelled using the simplifying assumptions.

The reasons for this are associated with the geometry of low speed, 60 Hz LIMs:

- Pole-pitch is small (i.e., #5-10 centimeters) in order to avoid excessive slip resulting in low efficiency.
- Entrefer is large (i.e.,5-10 millimeters) in order to accommodate the secondary top-cap and still leave space for adequate mechanical clearance.

These two geometrical factors introduce "non-ideal" effects which affect our first two assumptions:

- Flux will not travel in "straight lines," particularly in the entrefer region (i.e., the "gap leakage" path described in Section 4.1.2 cannot be neglected).
- Flux waveforms will not be sinusoidal since the short pitch can accommodate very few slots per pole, resulting in substantial "winding harmonic" content.

The remaining assumptions are often valid for low speed, 60 Hz LIMs. Exceptions are as follows:

- Assumption 3 is invalid if the flux density in any ferrous portion of the LIM approaches the saturation limit (usually between 1.5 and 2.0 Tesla).

- Assumption 4 is invalid when solid, as opposed to laminated, steel is used as secondary back-iron material.

- Assumption 5 is invalid when the width of the secondary is made the same or smaller than the width of the primary core, or when the pole pitch is of similar or greater dimension than the primary core width.

4.2.3 Use of Correction Formulae

The limitations imposed by the simplifying assumptions on the induction motor model have prompted many investigators to derive "correction formulae" for various parameters. For example, the "Carter Coefficient" has long been used to account for some of the error introduced by the assumption that flux travels in straight lines in the entrefer region. The "Russel-Norsworthy" factor accounts for some of the error introduced by the assumption that secondary currents are directed only laterally. Many other correcting formulae exist, but invariably they cover a limited range of geometrical variation. The approach used is our investigations was to seek empirical correction formulae by application of specific experimental techniques.

5.0 LIM EXPERIMENTS

Experimentation, like modelling, is somewhat of an art. While the execution of experiments must be exacting, their design, and the interpretation of the acquired data, often involve intuition. What things do we look for? What are effective ways of finding them? How do we interpret anomalous results?

There are a number of reasons to perform experiments, but most of these may be broadly stated in one or the other of the following:

- To confirm the expected.
- To discover the unexpected.

There is no definitive boundary which says an experiment is "type-A" or "type-B," but it is helpful in the design of an experiment to determine whether the purposes are mostly confirmatory or investigatory. Certainly it is a simpler matter to design and perform an experiment when the purpose is to prove the validity of some form of reasoning. If experimentation were always of this nature, however, little knowledge would be gained. Sometimes in the process of testing one's assertions about how a system behaves, discrepencies develop. Anomalies of this sort provide potential for knowledge gain. It becomes a matter of judgement and intuition to decide which anomalies deserve ongoing investigation.

As was stated earlier, the conceptual and quantitative models adopted at the program outset are, by some standards, simple. Nevertheless they do provide the experimental investigator with sufficient background to proceed. The following subsections provide an overview of the program's experimental activities and their relationship to the modelling efforts.

5.1 STATIC EXPERIMENTS

Static LIM experiments involve measurements made while the LIM is under power but constrained from motion. The purpose of the static experiments is to study those aspects of LIM behaviour which are too difficult and/or costly to study dynamically. Because conditions are more easily controlled in a static situation, the experiments can be made to resolve behaviour that may be too subtle to deduce from less precise means. Figures 5-1 and 5-2 show the static test configuration.

5.1.1 Flux Mapping Tests

The distribution of flux in the LIM entrefer region is of fundamental importance to LIM behaviour. An experimental technique was conceived and implemented whereby a "snapshot" of the travelling flux density wave could be "taken" at any instant in the supply-cycle. The data gathered from these

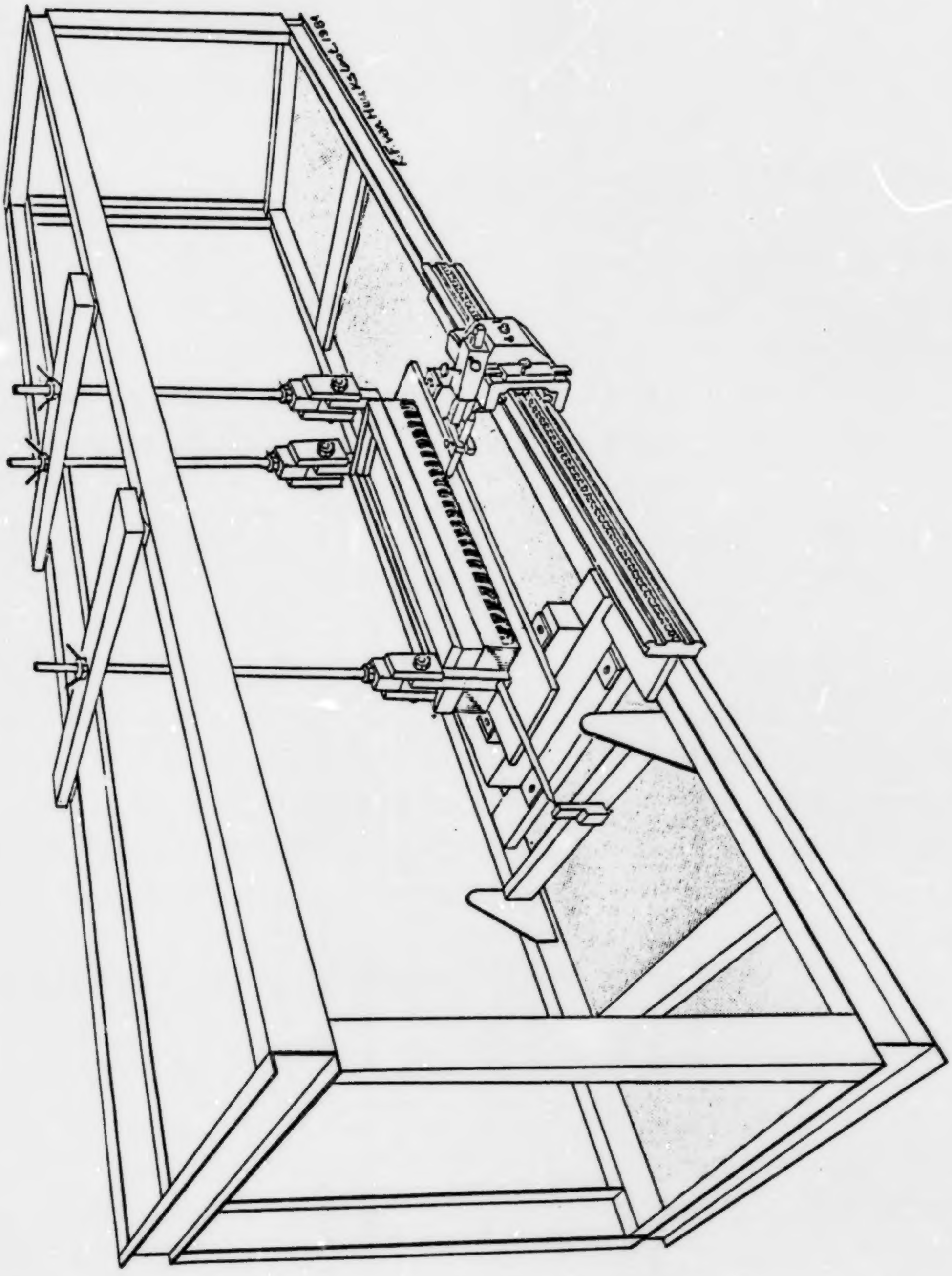

FIG.5-1: STATIC TEST STAND

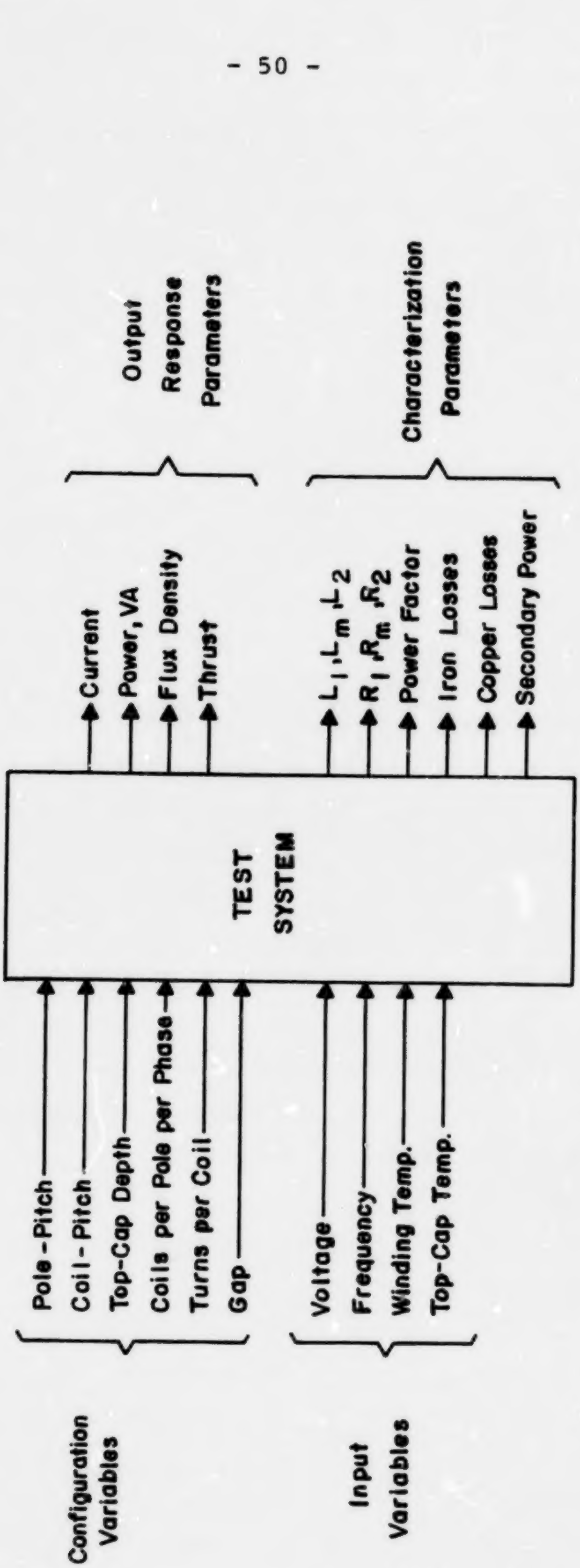
Configuration Variables
Pole-Pitch
Coil-Pitch
Top-Cap Depth
Coils per Pole per Phase
Turns per Coil
Gap
Input Variables
Voltage
Frequency
Winding Temp.
Top-Cap Temp.
TEST SYSTEM
Current
Power, VA
Flux Density
Thrust
L1, Lm, L2
R1, Rm, R2
Power Factor
Iron Losses
Copper Losses
Secondary Power
Output Response Parameters
Characterization Parameters

FIG.5-2: TEST SYSTEM BLOCK DIAGRAM

experiments provides considerable information, including:

1) The shape of the normally directed, longitudinal flux-density waveform:
   - at various instants in the time-cycle,
   - at various distances from the primary face,
   - for various entrefer settings.
2) The shape of the normally directed, lateral flux density distribution.

One of the conclusions that arise from considering the nature of windings for small pole pitch LIMs is that the flux density waveform will be non-sinusoidal, resulting in the appearance of "space-harmonics" of the fundamental flux wave. Figure 5-3 shows typical flux density waves as measured on the static test stand. Also shown are their harmonic spectra as determined by Fourier Analysis.

5.1.2 Equivalent Circuit Determination

It was stated earlier that an equivalent circuit approach was used in LIM quantitative modelling because, among other things, it could be related to physical experiments. The particular tests used to determine the equivalent circuit parameters are described in detail in Appendix 2. The data resulting from the equivalent circuit tests indicates the manner in which various physical design parameters affect each of the circuit elements.

5.1.3 Static Performance Measurement

To a certain extent, measured performance at standstill is relevant information on its own, since many LIM applications involve using the LIM at standstill or very low speeds. (Based on the LIMs available from commercial suppliers, it appears that these designs have been more or less optimized for the static condition.) A fairly complete characterization of static performance for various configurations is available. See for example Appendix 3.

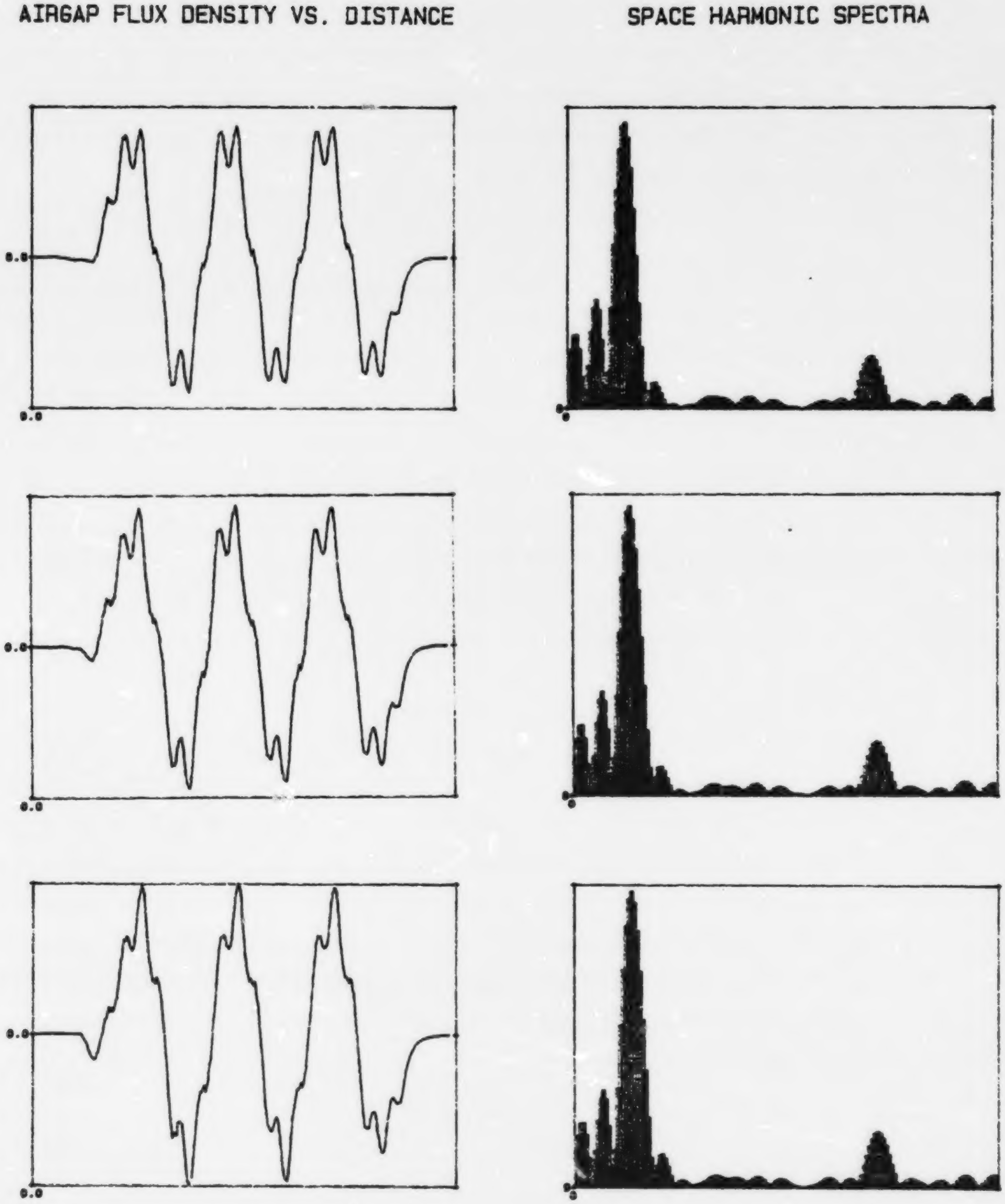

FIG. 5-3 FLUX DENSITY WAVE

It must not be assumed, when using this data, that any particular configuration is generically "better" or "worse" than another just because the static performance indicates so. Performance of one LIM relative to another may be considerably different as speed increases from zero. For this reason, "projected performance graphs" are included in the data. These graphs show the performance with speed based on predictions made with the equivalent circuit parameter test values.

5.2 DYNAMIC EXPERIMENTS

It is difficult in a dynamic testing situation to approach the same level of repeatability, precision, accuracy, and flexibility that are possible in a static situation; hence, it was decided not to attempt to develop a dynamic test technique which would yield a "circuit model" in the sense that the static experiments produced such a model. Rather, the experiments were aimed at collecting the type of data which the static circuit model is supposed to predict. In addition to this, they would generate data which is beyond the predictive capability of the static model, that is, transient effects, vertical forces, and performance of non-laminated secondary back iron. The study of this data has made apparent the means of refining the basic equivalent circuit model.

5.2.1 Test System Description

Schematic representations of the test and measurement systems are shown in Figures 5-4 and 5-5. Featured are:

1. Stationary Test LIM Primary: instrumented for voltage, current, vertical force, thrust, and mechanical gap.
2. Adjustable test stand frame and support links to accommodate a variety of test LIM Primaries.
3. Test LIM Secondary supporting carriage including: wheels for suspension, guidance, and anti-lift; drive LIM; power collector assembly; target rail for speed sensing system.
4. Silicon-Controlled Rectifier (SCR) LIM-drive system for regulation of carriage speed.
5. "I-beam" integral track/drive LIM secondary.
6. Fourteen-channel analog data recorder.
7. Digital data acquisition/storage/processing system.

The system was arranged so that all measurements were made on the non-moving side of the LIM under test. This simplified measurement and recording of data, LIM power supply requirements, and set-up procedure. Sample plots of the data collected are shown in Figures 5-6 and 5-7.

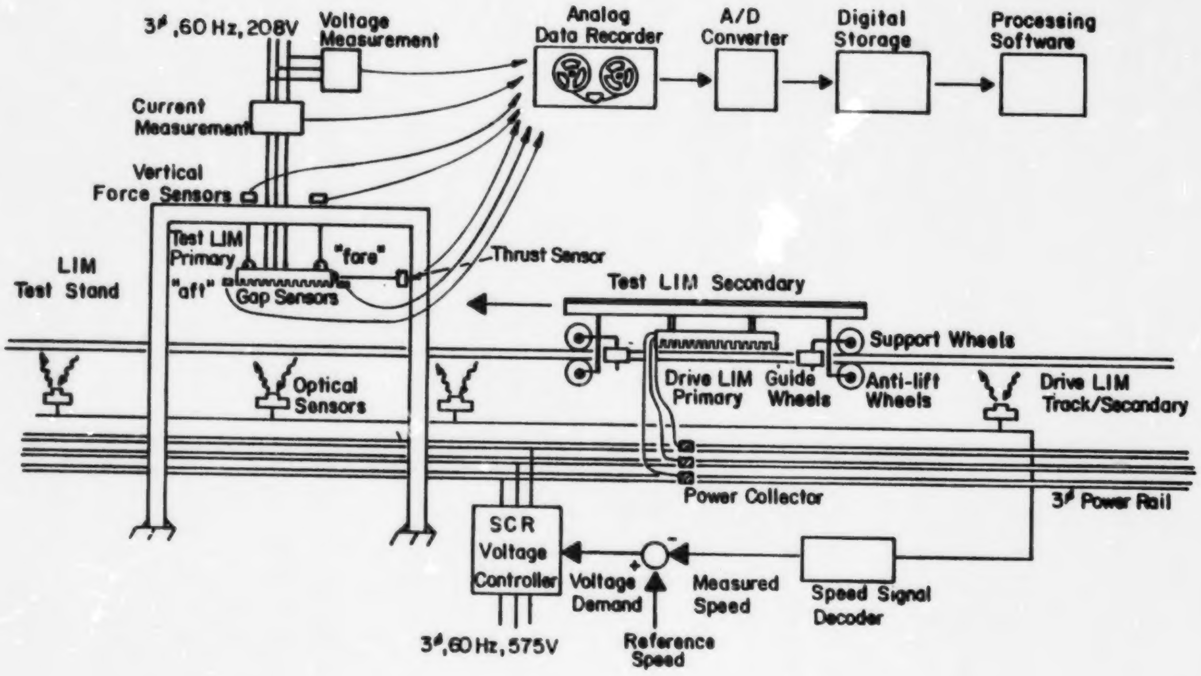
3ϕ,60 Hz,208V
Voltage Measurement
Analog Data Recorder
A/D Converter
Digital Storage
Processing Software
Current Measurement
Vertical Force Sensors
LIM Test Stand
Test LIM Primary
"fore"
"aft"
Gap Sensors
Thrust Sensor
Test LIM Secondary
Support Wheels
Anti-lift Wheels
Guide Wheels
Drive LIM Primary
Optical Sensors
Drive LIM Track/Secondary
Power Collector
3ϕ Power Rail
SCR Voltage Controller
Voltage Demand
Measured Speed
Speed Signal Decoder
Reference Speed
3ϕ,60 Hz,575V

FIG.5-4: LIM DYNAMIC TEST FACILITY

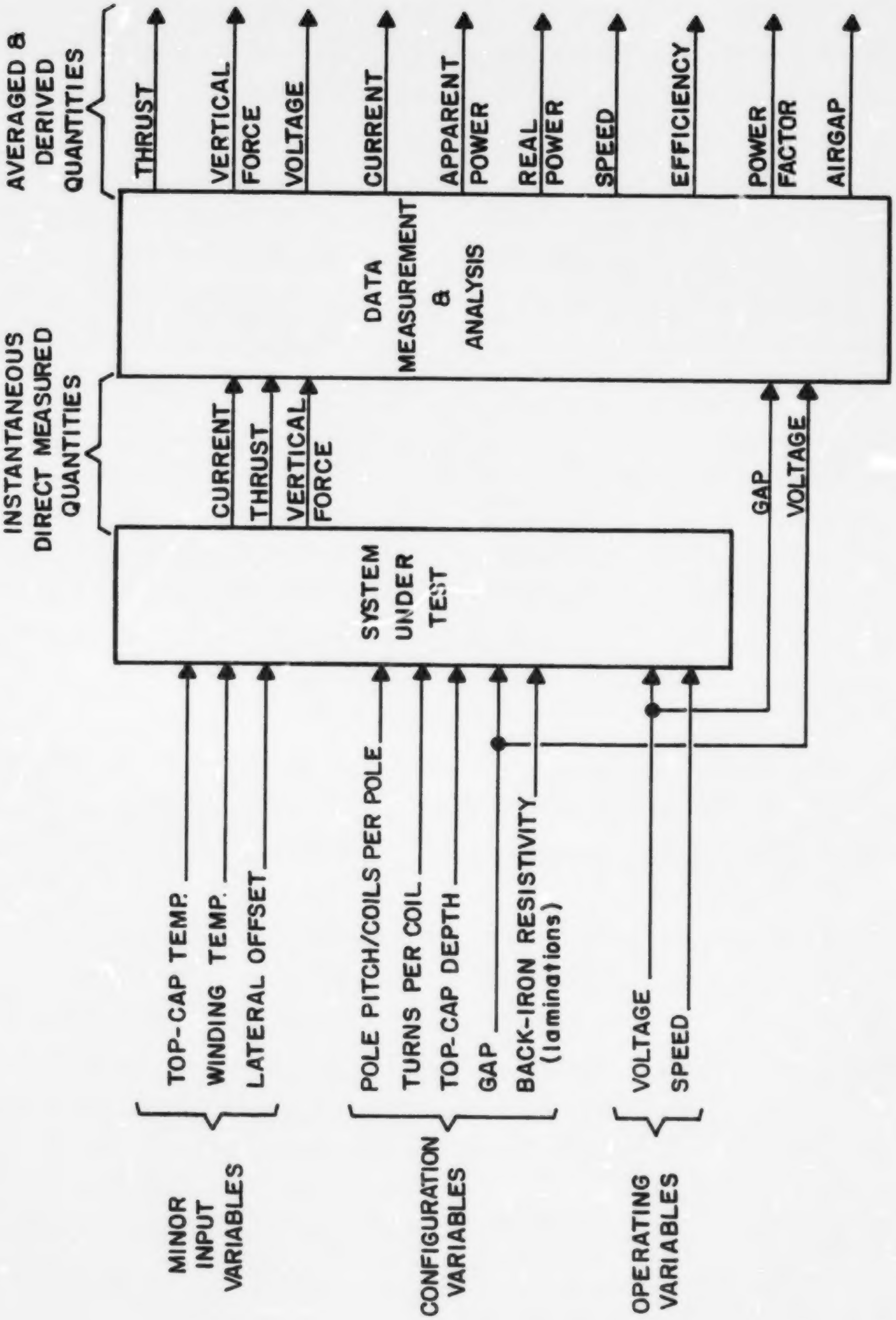
MINOR INPUT VARIABLES
TOP-CAP TEMP.
WINDING TEMP.
LATERAL OFFSET
CONFIGURATION VARIABLES
POLE PITCH/COILS PER POLE
TURNS PER COIL
TOP-CAP DEPTH
GAP
BACK-IRON RESISTIVITY (laminations)
OPERATING VARIABLES
VOLTAGE
SPEED
SYSTEM UNDER TEST
INSTANTANEOUS DIRECT MEASURED QUANTITIES
CURRENT
THRUST
VERTICAL FORCE
GAP
VOLTAGE
DATA MEASUREMENT & ANALYSIS
AVERAGED & DERIVED QUANTITIES
THRUST
VERTICAL FORCE
VOLTAGE
CURRENT
APPARENT POWER
REAL POWER
SPEED
EFFICIENCY
POWER FACTOR
AIRGAP

FIG. 5-5 : DATA MEASUREMENT & REDUCTION SYSTEM

FIG. 5-6:60 Hz. Dynamic Test Results Sample

Nominal Airgap : 4.20 mm
Motor Type : 1 (2/3)
Top-Cap Depth : 3.2 mm

Nominal Voltage (phase to phase) : 208 V.
Back-Iron Type : 38 mm. Laminated
Reference Data File : DR111.OUT

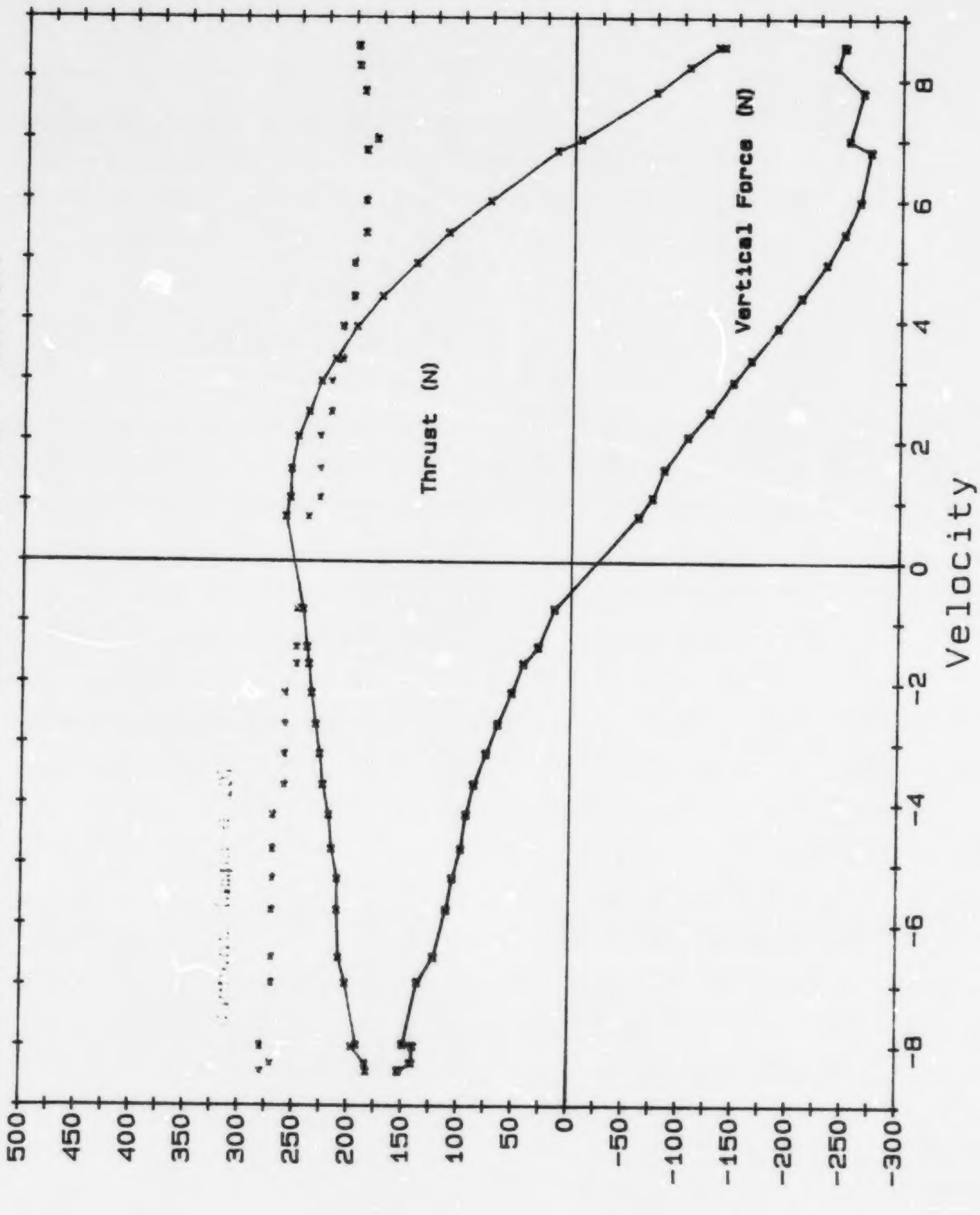

FIG.5-7: 60 Hz. Dynamic Test Results Sample

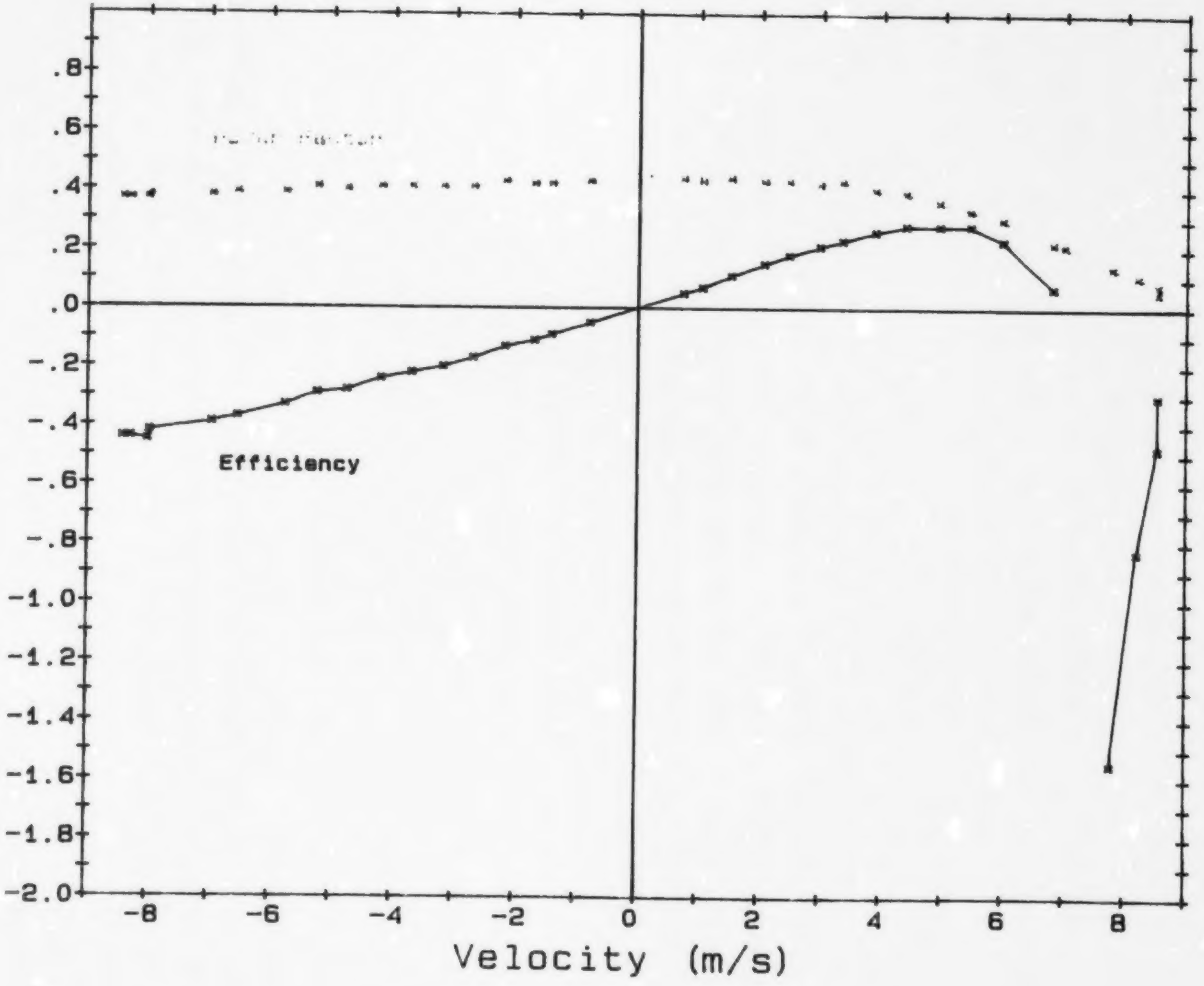

Nominal Airgap : 4.20 mm
Motor Type : 1 (2/3)
Top-Cap Depth : 3.2 mm

Nominal Voltage (phase to phase) : 208 V.
Back-Iron Type : 38 mm. Laminated
Reference Data File : DR111.OUT

6.0 COMPARISON OF PREDICTED VERSUS EXPERIMENTAL RESULTS

The data generated by the static and dynamic LIM experiments serve as a basis against which the LIM models may be compared. The static experiments yielded estimates of the Equivalent Circuit Parameters, while the dynamic experiments gave the LIM performance as a function of speed. It is important to realize that the equivalent circuit representation is itself an imperfect representation. Even if we could calculate the circuit parameters absolutely, we would not expect exact performance predictions. In fact, we are unable to calculate these parameters exactly, due to the number and type of assumptions made in the various formulae (see section 4.2.1). We therefore seek to test our model on two levels;

1. Circuit Parameter Formulae vs.
   Static Test Parameter Estimate

2. Equivalent Circuit Prediction vs.
   Dynamic Performance Experimental Results.

6.1 CIRCUIT PARAMETER FORMULAE

Appendix 1 develops the formulae for some of the equivalent circuit parameters from simple theory. There are, however, parameters which cannot be developed in this way because the simple theory is not adequate. The following subsections summarize the methods used to arrive at each of the equivalent circuit parameters, and how the formulae compared against the Static Test Parameter estimates.

6.1.1 Winding Resistance, R1

The theory behind the "R1" formulae makes few assumptions, and the comparison to test is very good. What error there is is due to the lack of a precise formulae for the length contributed by the end windings.

6.1.2 Primary Leakage Inductance, L1

The Primary Leakage inductance is composed of Slot leakage, Endwinding leakage, and Gap Leakage. Of these, only the Slot Leakage is calculated from simple theory.

Endwinding Leakage is calculated from a "standard" empirical formulae.

A Gap Leakage formulae was derived empirically by observing that in the static test results, L1 was seen to increase with entrefer (see App. 1, figure A1-7). (The only component of L1 which is expected to be related to entrefer is the Gap Leakage.) The formulae also attempts to account for the observation that gap leakage was greatest for shorter pole pitch LIMs.

$$L_G \propto \frac{g}{\tau_p}$$

where

L_G = Gap Leakage Induction
g = entrefer
τ_p = pole-pitch

6.1.3 Core Loss Resistance, RM

The core loss resistance cannot be derived from simple theory. Fortunately, its effect on the calculated performance is quite small. No formulae was available, and the effect was assumed to be negligible.

6.1.4 Magnetizing Inductance, LM

The magnetizing inductance is derived from simple theory in Appendix 1. The theoretical result tended to be consistently higher than the static test result by a small amount. Application of the "Carter Coefficient" which increases the nominal entrefer to an "effective" value, taking into account tooth fringing effects, provided improved correlation. (The Carter coefficient is discussed in Ref. 1, Pg. 38.)

6.1.5 Secondary Leakage Inductions, L2

The secondary leakage term is relatively important and cannot be ignored. However, it cannot be derived from simple theory.

Suitable formulae for L2 are lacking in the literature, though recent attempts have been made by Hesmondhalgh and Tipping (see Ref. 2). It was discovered that the Mesmondhalgh-Tipping factor produced a value for L2 in the order of ten times lower than the static experiment result. Clearly, further work will be required in order to arrive at a satisfactory formula.

6.1.6 Secondary Resistance Formula, R2

The secondary resistance formula is derived from simple theory in Appendix 1. The calculated results appeared to match the static results better for the small pole pitch motors. This is certainly an indication that for longer pole pitch, lateral edge effects become important. The Russel-Norsworthy Factor was adopted to account for these edge effects. (The Russel-Norsworthy formula may be found in Ref. 2.)

6.2 EQUIVALENT CIRCUIT PREDICTION

The utility in comparing theoretical prediction with experimental results is that patterns or trends may emerge which point to specific deficiencies in the model. In an iterative process, various attempts may be made at refining the model to yield improved correlation with test data. At some point, the model is considered to be sufficiently accurate over the range of configurations compared against, and serves as a useful tool in design and analysis.

The procedure involved in model refinement is tedious and lengthy. The actual mechanics of the procedure may be made simpler by the exploitation of computer-based data handling and presentation. Figure 6-1 shows the system used. It gives the investigator the ability to display experimental and theoretical data very quickly. Plots of data may be overlaid for easy comparison.

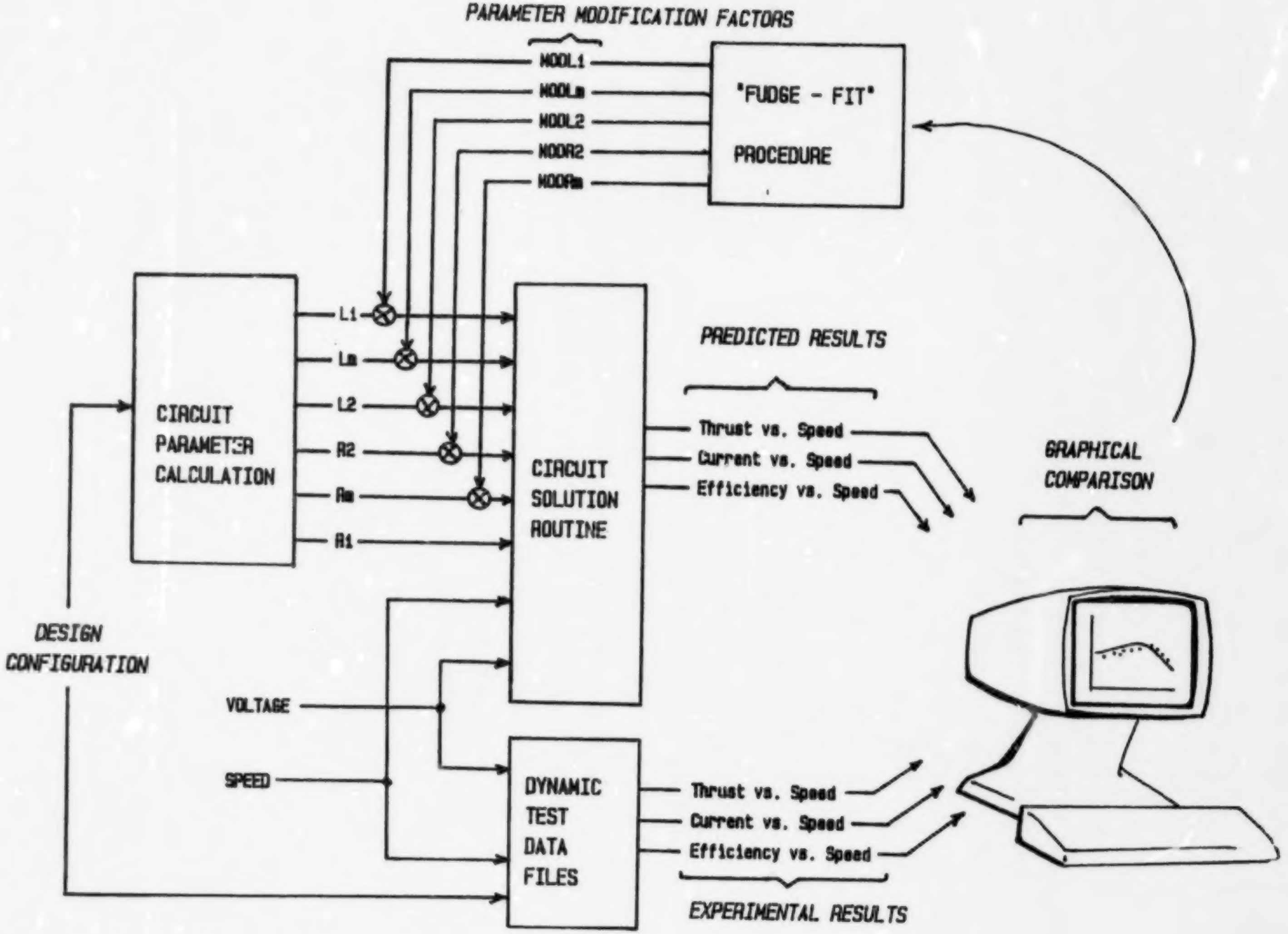
PARAMETER MODIFICATION FACTORS
MODL1
MODLm
MODL2
MODR2
MODRm
"FUDGE - FIT" PROCEDURE
CIRCUIT PARAMETER CALCULATION
L1
Lm
L2
R2
Rm
R1
CIRCUIT SOLUTION ROUTINE
PREDICTED RESULTS
Thrust vs. Speed
Current vs. Speed
Efficiency vs. Speed
GRAPHICAL COMPARISON
DESIGN CONFIGURATION
VOLTAGE
SPEED
DYNAMIC TEST DATA FILES
Thrust vs. Speed
Current vs. Speed
Efficiency vs. Speed
EXPERIMENTAL RESULTS

Figure 6-1 Curve-Matching Procedure

As a means of modifying the model to provide a match to the test data, a set of keyboard-entered variables which scale the various equivalent circuit parameters is available. Eventually, as more and more configurations are compared and the model is adjusted to provide a match, it becomes clear which of the circuit parameters needs to change, and by how much.

Figures 6-2 and 6-3 demonstrate the approach by using two particular cases as an example. The only parameter varied between these cases is top cap depth. Notice, furthermore, that the amount of increase is smaller for the deeper top cap. (This trend was also observed in the Static Test Results.)

Further investigation would attempt to discern trends between, say, L2 and entrefer, or pole-pitch. The procedure is by no means direct, and requires a sound qualitative understanding of LIM behaviour on the part of the investigator.

Empirical approaches to model refinement are never complete so long as there are configurations which remain untested. Hence the method outlined here should be regarded as part of an ongoing process. As new designs are built and tested, the model should be checked accordingly, and updated when possible.

Figure 6-2 60 Hz. Test Results - Measured vs. Theoretical

Entrefer : 7.70 mm
Motor Type : 1 (2/3)
Top-Cap Depth : 3.2 mm

Nominal Voltage (phase to phase) : 208 V.
Back-Iron Type : 38 mm. Laminated
Reference Data File : DR111.OUT

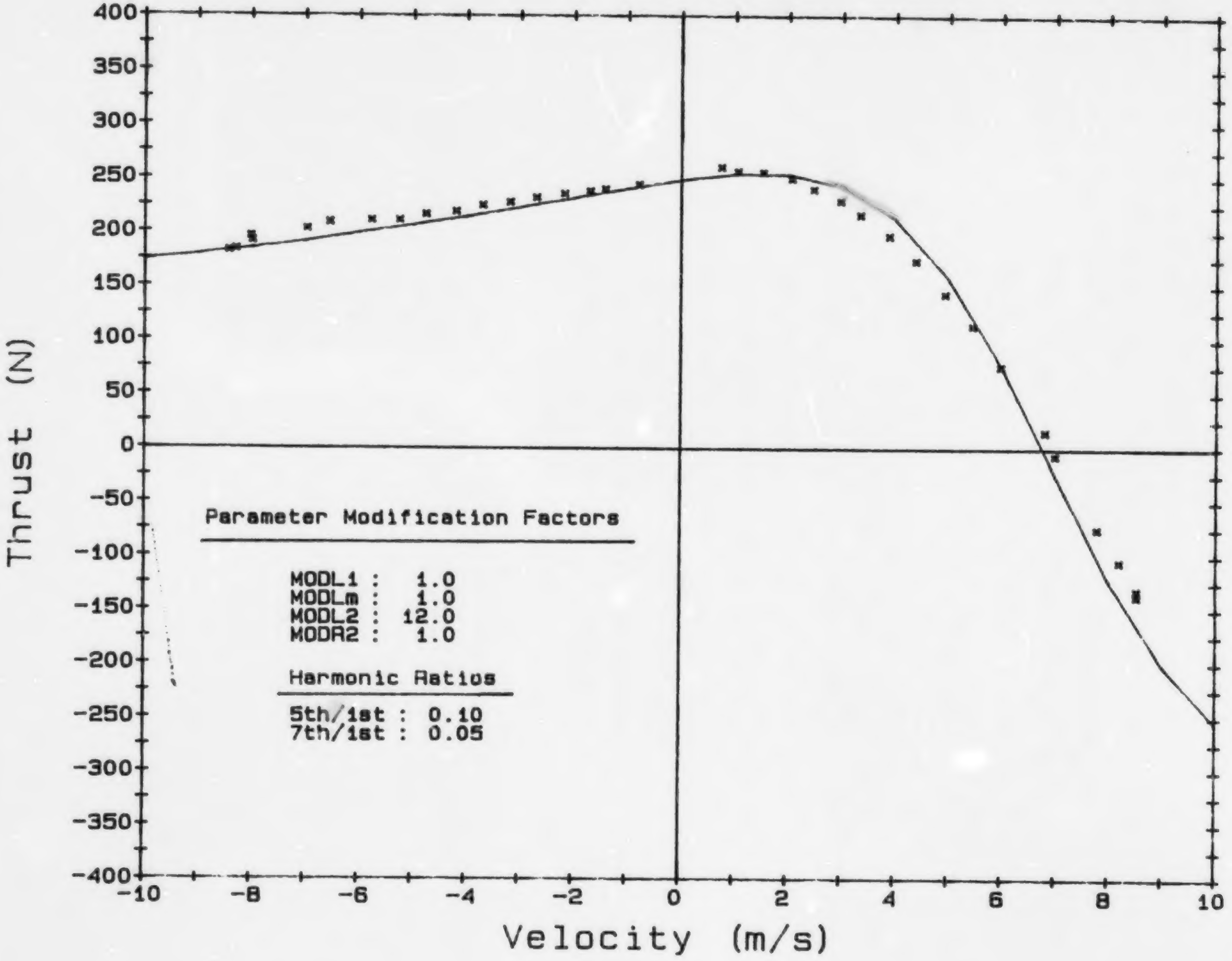

Figure 6-3 60 Hz. Test Results - Measured vs. Theoretical

Entrefer : 7.70 mm
Motor Type : 1 (2/3)
Top-Cap Depth : 4.8 mm

Nominal Voltage (phase to phase) : 208 V.
Back-Iron Type : 38 mm. Laminated
Reference Data File : DR112.OUT

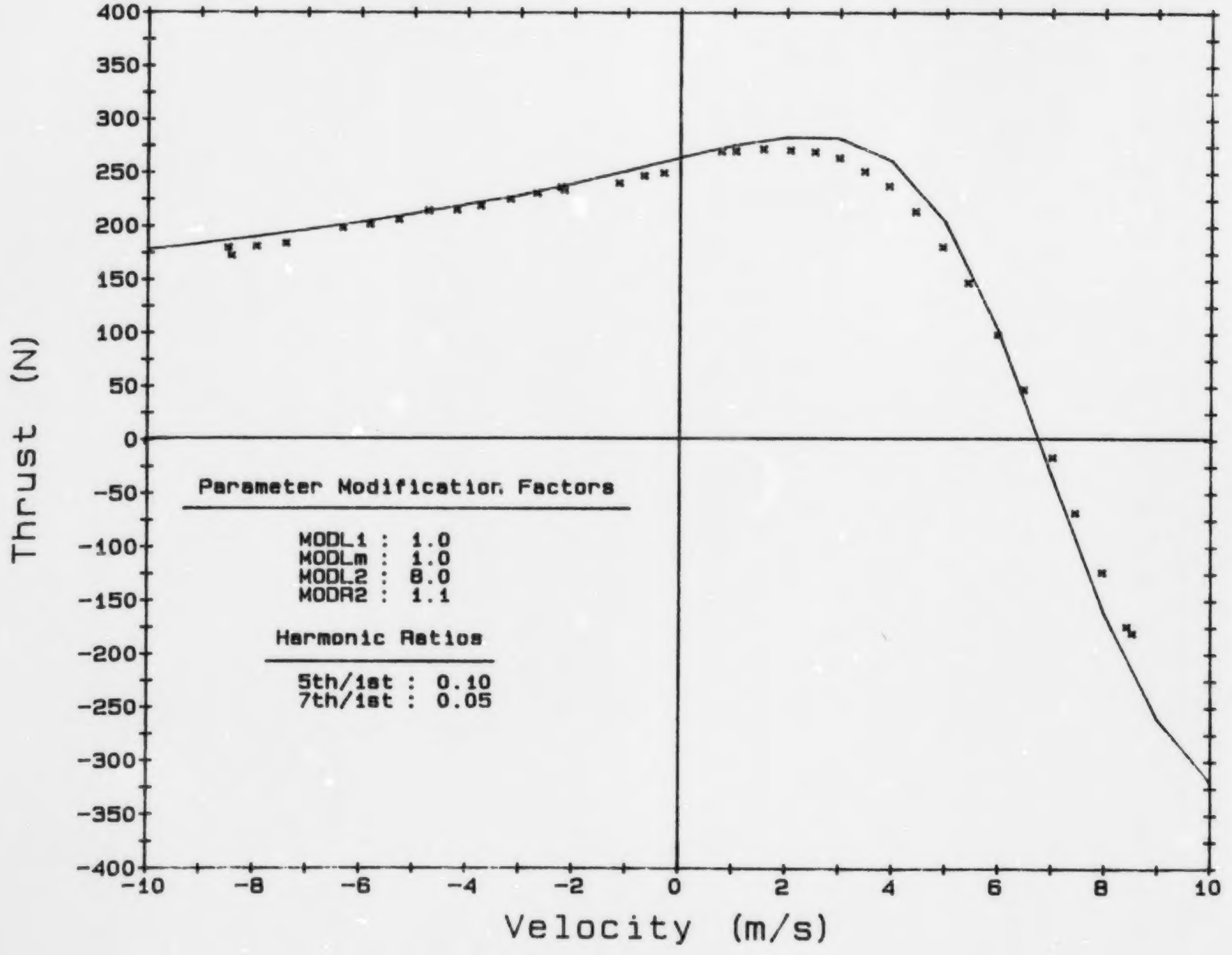

7.0 LIM DESIGN

There are at least two ways one could conceive of producing a LIM design to specification: Use of a Design Model or use of a Performance Model.

A Design Model is a procedure which converts a set of performance requirements into a design by essentially "searching" for the closest suitable design from a catalogue of known designs. Small modifications can then be made based on predetermined rules. Over time, the design model evolves into an increasingly useful tool as new designs are added to the catalogue. One manufacturer of small LIMs has a computerized design model which has been "growing" for more than a decade.

A Performance Model is a mathematical means of predicting the performance of a LIM based on its physical design parameters. To design to specification is an iterative process beginning with an initial estimate and ending with a design which has predicted performance at least equal to the specified performance.

Figure 7-1 uses flowcharts to compare the two design approaches. Note that neither approach will necessarily produce the "best" design, as it is always possible, even likely, that some other design configuration could meet the specification but have higher efficiency, or lower cost, or some other attribute.

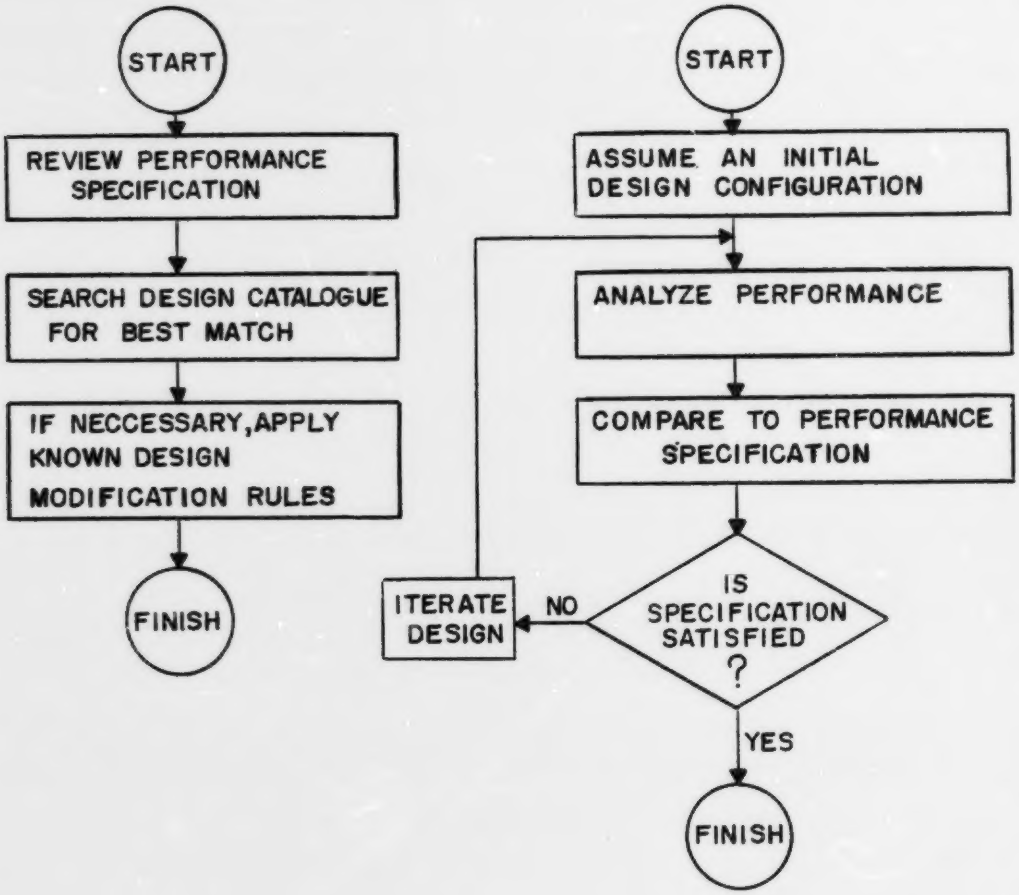
START
REVIEW PERFORMANCE SPECIFICATION
SEARCH DESIGN CATALOGUE FOR BEST MATCH
IF NECCESSARY, APPLY KNOWN DESIGN MODIFICATION RULES
FINISH
START
ASSUME AN INITIAL DESIGN CONFIGURATION
ANALYZE PERFORMANCE
COMPARE TO PERFORMANCE SPECIFICATION
IS SPECIFICATION SATISFIED ?
NO
ITERATE DESIGN
YES
FINISH

FIG.7-1 : ALTERNATIVE DESIGN TECHNIQUE - DESIGN VERSUS PERFORMANCE MODELS

The following sections explain in greater detail how the modelling and experimental work which has been produced in this development program may be used for the purposes of LIM design.

7.1 SPECIFYING PERFORMANCE

Specifying LIM performance can be as simple as stating the required minimum static thrust, but considerably more information is usually needed. For example:

- The peak thrust versus speed characteristic (motoring and braking)
- The thrust-versus-time and speed-versus-time profiles
- Limits on vertical force (repulsive and attractive)
- Limits on secondary heating
- Limits on the power supply (voltage and current)
- Tolerances on the airgap dimension
- Limits on physical dimensions and weight

In practice it is seldom that all of the above items would be specified. Often condensed descriptions are used. For instance, "duty cycle" replaces the thrust-versus-time specification with a single figure. "Static thrust" and "synchronous speed" usually are the only parameters used to specify the thrust-versus-speed characteristic.

7.1.1 Optimization

Besides specifying what a LIM must do, it may also be necessary to introduce criteria for selecting the better of two or more satisfactory designs. For example, consider the following:

- Thrust per unit weight
- Efficiency
- Power Factor

Because the cost of re-tooling to construct a new LIM design is prohibitively high, commercial LIM suppliers seldom are concerned with whether or not a design has the best possible efficiency, power factor, etc., so long as the basic performance specification is met. However, in applications requiring a large quantity of LIMs, a serious optimization effort would seem to have merit.

7.2 USING THE TEST DATA AS A BASIS FOR DESIGN

The test results may be used along with appropriate rules of scaling to generate variant designs. The technique uses assumptions which limit its range of applicability; nevertheless, it may be successfully applied in a great number of cases with good results. Rules for checking whether the assumptions are valid for a given design also exist, and are simple to apply.

7.2.1 Basic Rules of Scaling

Consider a LIM of given geometry (pole pitch, gap, core width, etc.) and supply voltage to be the "base" configuration. If the thrust available from the base configuration is larger or smaller than the requirement, it is possible to scale up or down by varying one or more parameters. There are a number of basic criteria which one may want to work to, but two are the most important: i) that the thrust is sufficiently high, and ii) that the root-mean-square current density (over the operating cycle) is sufficiently low. To satisfy these two criteria is to have a motor which will supply the required thrust without overheating. It is not necessarily the case, however, that the resultant design provides best thrust per unit of power, apparent power, or mass. It should be understood at the outset that the scaling method provided here is not appropriate for optimizing a design to multiple constraints. It is possible, however, to generate a number of designs which satisfy the thrust and thermal criteria, and then to compare them against each other on the basis of real and apparent power consumption, mass, etc.

The first rule of scaling relates the change in thrust from the base value to changes in voltage, turns per coil, core width, and number of poles from their base values.

$$F_{new} = F_{base} \times \frac{V^2_{new}}{V^2_{base}} \times \frac{N^2_{base}}{N^2_{new}} \times \frac{W_{base}}{W_{new}} \times \frac{P_{base}}{P_{new}} \quad (7\text{-}1)$$

Where:

F = Thrust
V = Voltage
N = turns per coil
W = core width
P = number of poles

The above formula makes it is quite simple to calculate the "new" thrust due to a change in one or all of the parameters V, N, W or P. It may at first seem suprising to learn that a reduction in core width or number of poles results in an increase in thrust, but this is actually true. The hidden fact is that the motor current increases when W or P are reduced and that the motor must therefore run "hotter." This situation leads us to the second rule of scaling, which relates the changes of V, N, W, and P to the change in motor current density, J.

$$J_{new} = J_{base} \times \frac{N_{base}}{N_{new}} \times \frac{V_{new}}{V_{base}} \times \frac{W_{base}}{W_{new}} \times \frac{P_{base}}{P_{new}} \qquad (7\text{-}2)$$

where:

$$J_{base} = \frac{2NI_{base}}{A_{base}}, \qquad A_{base} = \text{slot area of base design} \qquad (7\text{-}2a)$$

With aid of the above formula, it can be seen that to reduce W or P increases the motor current density. Motor temperature rise is related to current density, but one more relationship is needed before the above formula is useful. This last formula relates the temperature rise to the current density and the operating duty cycle:

$$T \propto J^2 D \qquad (7\text{-}3)$$

where:

T = temperature above ambient

$$D = \text{duty cycle} = \frac{\text{time on}}{\text{cycle time}} \qquad (7\text{-}4)$$

The relationship is expressed as a proportionality rather than an equation because the actual temperature rise will depend on other things such as cooling means, insulation type, etc. However, if we consider these things as fixed parameters, we can specify a maximum J^2D corresponding to a maximum permissible temperature rise. For LIMs of the type tested, the recommended maximum for J^2D is 3.9, where J is in Amps per square millimeter and D is a dimensionless quantity between zero and one. (This figure is arrived at by working back from data supplied by Telectric Ltd.)

7.2.2 Limitations on Scaling

There are at least two effects which can complicate the simple rules of scaling outlined in the previous section: i) magnetic saturation effects, and ii) lateral edge effects.

The first becomes significant when flux densities in any part of the magnetic configuration (primary teeth, primary back-iron, secondary back-iron) are higher than about 1.8 Tesla. The second is a concern when core width is reduced to the extent that resistive and inductive losses in the primary coil-ends and the secondary lateral edges become pronounced.

The LIMs tested always operated at flux densities well below saturation levels. The airgap flux density under "no top-cap conditions" was measured for every configuration tested and appears in the test data. This data may be scaled in proportion to current density to determine the gap flux-density of the variant design.

7.2.3 Examples

Let us consider the use of the scaling method provided in the previous section to produce LIM designs to a particular specification. Suppose our requirements are as follows:

Thrust: 1,000 N @ 2 m/s
Voltage: 600 V phase to phase
Duty Cycle: 0.5 sec "on" 5 sec "off"
Airgap: no less than 6 mm

We first identify the range of LIM configurations from the static test data which we may consider as "base" configurations.

Case	Motor Type	Top Cap Depth (mm)	Entrefer (mm)	Airgap	Turns per Coil, N_{base}
1	2/3	4.8	10.8	6.3	33
2		3.2	9.2	6.0	
3		1.0	7.7	6.7	
4	3/3	4.8	10.8	6.3	30
5		3.2	9.2	6.0	
6		1.0	7.7	6.7	
7	4/6	4.8	10.8	6.3	16
8		3.2	9.2	6.0	
9		1.0	7.7	6.7	

Now for every configuration we have the same base voltage, core width, number of poles, and slot area.

$V_{base} = 208$ V
$W_{base} = 177$ mm
$P_{base} = 6$
$A_{base} = 451\ mm^2$

We will not consider all nine cases in this example, but a few will demonstrate the principles and indicate some design trade-off areas.

7.2.3.1 Case 1

If we consider equation 7-1, it is clear that we can alter one or more parameters to change thrust from F_{base} to F_{new}. Referring to the predicted thrust vs. speed curve shown in Appendix 3 for case 1, we see that thrust at 2 m/s is very nearly the same as it is at standstill. The measured value of this thrust is:

$$F_{base} = 221 \text{ N}$$

Suppose we choose to change N so as to make F_{new} equal to the specified 1,000 Newtons.

Rewriting equation 5-1 and inserting the known values, we have:

$$N^2_{new} = \frac{221}{1{,}000} \times \frac{600^2}{208^2} \times 33^2 \times \frac{177}{177} \times \frac{6}{6}$$

$$N_{new} = 45 \text{ turns}$$

Next we need to check the current density of the "new" winding. From equation 7-2a and the static experiment results for current, we calculate the base current density:

$$J_{base} = \frac{2 \times 33 \times 27.7}{451}$$

$$= 4.05 \text{ A/mm}^2$$

Now we calculate the "new" current density from equation 7-2:

$$J_{new} = 4.05 \times \frac{33}{45} \times \frac{600}{208} \times \frac{177}{177} \times \frac{6}{6}$$

$$= 8.6 \text{ A/mm}^2$$

Lastly we check to see if the "J^2D" product is smaller than the recommended value of 3.9.

$$J^2_{new} \times D = 8.6^2 \times \frac{0.5}{5.5} = 6.7$$

We have exceeded the thermal criterion and therefore must iterate the design to mutually satisfy thrust and thermal requirements. Alternatively, we can solve two simultaneous equations if we restrict ourselves to only two unknowns, for example N and W. Let us attempt the latter.

Firstly, we make the assertion that:

$$J_{new}{}^2D = 3.9$$

from our specification:

$$D = \frac{0.5}{5.5}$$

hence:

$$J_{new} = 6.54$$

Rewriting equations 7-1 and 7-2 and substituting in the appropriate values, we have:

$$N^2_{new}W_{new} = \frac{221}{1,000} \times \frac{600^2}{208^2} \times 30^2 \times 177 \times \frac{6}{6} = 292,944 \quad (1)$$

$$N_{new}W_{new} = \frac{4.05}{6.54} \times 30 \times \frac{600}{208} \times 177 \times \frac{6}{6} = 9,485 \quad (2)$$

Dividing (2) into (1)

$$N_{new} = \frac{292,944}{9,485} = 31 \text{ turns} \quad (3)$$

Substituting (3) into (2)

$$W_{new} = \frac{9,485}{31} = 306 \text{ mm}$$

Hence, we have designed a LIM which differs from the base LIM in that it has:

V = 600 V
N = 31 turns
W = 306 mm

We can deduce the current by application of equation 7-2a since we specified J.

$$I = \frac{JA}{2N}$$

$$= \frac{6.54 \times 451}{2 \times 31}$$

$$= 47.6 \text{ A}$$

To ensure that calculation errors have not been committed, we test against the rule that the increase in the (voltage x current) product must be proportional to the increase in thrust. Small differences may be attributed to round-off errors made by converting calculated values of N_{new} to integers.

$$\frac{V_{new}I_{new}}{F_{new}} \propto \frac{V_{base}I_{base}}{F_{base}}$$

Left hand side:

$$\frac{600 \times 47.6}{1,000} = 28.6$$

Right hand side:

$$\frac{208 \times 27.7}{221} = 26.1$$

And we have reasonable correspondence.

7.2.3.2 Case 2

Referring to the Thrust-Speed projection corresponding to the second case, we note that thrust at 2 meters/sec is down to 91% of the static value. We must therefore design a LIM to give about 1,100 Newtons statically if it is to satisfy the design criteria. Again we choose core width and number of turns as our design variables. From the static test measurements we know that:

$$F_{base} = 253 \text{ N}$$

$$I_{base} = 25.6 \text{ A}$$

$$J_{base} = \frac{2 \times N_{base} \times I_{base}}{A_{base}} = 3.75 \text{ A/mm}^2$$

Again we set J_{new} to correspond to the thermal limit for the specified duty cycle:

$$J_{new} = 6.54$$

We now write two equations in terms of the unknowns N_{new} and W_{new}.

$$N^2_{new}W_{new} = \frac{253}{1{,}000} \times \frac{600^2}{208^2} \times 30^2 \times 177 = 304{,}873 \qquad (3)$$

$$N_{new}W_{new} = \frac{3.75}{6.54} \times 30 \times \frac{600}{208} \times 177 = 8{,}783 \qquad (4)$$

Solving for N_{new} and W_{new}

N_{new} = 35 turns

W_{new} = 251 mm

7.2.3.3 Case 9

We again refer to Appendix 3 for the configuration of case 9. At 2 metres/sec, thrust has dropped to 92% of the static value. We therefore require 1,090 Newtons of static thrust to satisfy the design criterion. From the static measurements we know:

F_{base} = 314 N

I_{base} = 27.3 A

$$J_{base} = \frac{2NI_{base}}{A_{base}} = \frac{2 \times 16 \times 27.3}{451} = 1.94 \text{ A/mm}^2$$

We write two equations (7-1 and 7-2) in terms of N_{new} and W_{new}

$$N^2_{new}W_{new} = \frac{314}{1,090} \times \frac{600^2}{208^2} \times 16^2 \times 177 = 108,616$$

$$N_{new}W_{new} = \frac{1.94}{6.54} \times 16 \times \frac{600}{208} \times 177 = 2,423$$

N_{new} = 45 turns

W_{new} = 53.8 mm

7.3 USING THE PERFORMANCE MODEL AS A BASIS FOR DESIGN

The LIM performance model as described in section 4.2 allows the designer to input a given set of physical design parameters and generate performance predictions. From an arbitrary starting point, the designer can use particular pieces of information from these predictions to help him decide what changes are required to bring the design closer to his objective. This process is analogous to a control system with multiple inputs, outputs, and feedback loops. In such systems, the algorithms which determine the direction and degree of corrective action are of great importance. Likewise, the algorithms required to generate changes to the design data driving the performance model are also important.

7.3.1 Physical Design Limits

The performance model which was developed assumes magnetic linearity. This means that regardless of the design configuration, required thrust levels will be met (at least in prediction, if not fact) by simply choosing a high enough current/voltage. Of course, an actual motor cannot accept current of an arbitrarily high amount without eventually reaching magnetic saturation, insulation breakdown, or both.

Though the model does not have a built-in capability to simulate the magnetic and thermal conditions resulting from excessive current, it does provide information which the designer can evaluate in order to determine whether magnetic and thermal limits have been exceeded. This information is available from the model as:

1) Airgap Flux Density
2) Volume Current Density

The airgap flux density, coupled with a knowledge of the slot/tooth geometry of the primary, can give an estimate of the tooth flux density, which normally is enough to indicate conditions of magnetic saturation.

The volume current density, on its own, does not serve as an indicator of the LIM thermal condition. In addition to this, the designer must specify the duty cycle. In its simplest form, duty cycle is defined as the time the LIM is "on" divided by the total duration of the "on/off" cycle. A more sophisticated approach to determining the thermal condition is outlined in Appendix 5, "LIM Thermal Model."

If, after considering the magnetic and thermal response corresponding to the model output, the designer finds that his initial design has exceeded prescribed magnetic and thermal limits, he is forced to make some change to the LIM geometry. The possibilities are numerous, but the following list describes certain kinds of design modification, the reasoning behind each, and the "side effects."

DESIGN CHANGE	REASONS	SIDE EFFECTS
- Increase slot width (constant slot pitch).	- Reduce current density to avoid exceeding thermal limits.	- Increase tooth flux density toward magnetic limits .
- Increase slot depth.	- Same as above.	- Increases slot leakage inductance.
- Increase tooth width (constant slot pitch).	- Reduce flux density in tooth to avoid exceeding magnetic limits.	- Increases current density toward thermal limits.
- Increase LIM core width.	- Cannot provide required thrust with existing design.	- Reaction plate must also be wider, heavier.
- Increase pole pitch.	- Cannot achieve required speeds with existing design. - Want to improve LIM power factor.	- Increases LIM length. - Primary and secondary back-iron must be made proportionally deeper.
- Increase number of poles.	- Cannot provide required thrust with existing design.	- Increases LIM length.
- Increase secondary top-cap depth.	- Reduce secondary heating. - Change shape of thrust/speed curve.	- Increases entrefer possibly reducing power factor.

TABLE 7-1: REASONS FOR, AND EFFECTS OF, DESIGN PARAMETER MANIPULATION

8.0 LIM-BASED MOTION CONTROL

Linear Induction Motors are used in a variety of control systems where non-contact linear thrust is required. Sometimes it may be required of the LIM to provide static thrust only, but more usually the LIM will be employed as part of a dynamic system; for example, in the regulation of vehicle speed, or the accurate positioning of a load. Figure 8-1 is a block-diagram representation of a generalized motion control system. Virtually any system will consist of the four elements shown.

1. Actuator
2. Controller
3. Load
4. Sensor(s)

We will consider each of these elements in their typical forms and attempt to highlight those aspects which will have consequence on the design and performance of practical systems.

8.1 THE LIM AS AN ACTUATOR

The simplest description of the LIM recognizes that thrust is provided in response to input electrical power. We may further characterize LIM behaviour by noting the following points:

1. Thrust is also dependent on:
    - speed of the primary relative to the secondary

FIG. 8-1: GENERALIZED MOTION CONTROL SYSTEM

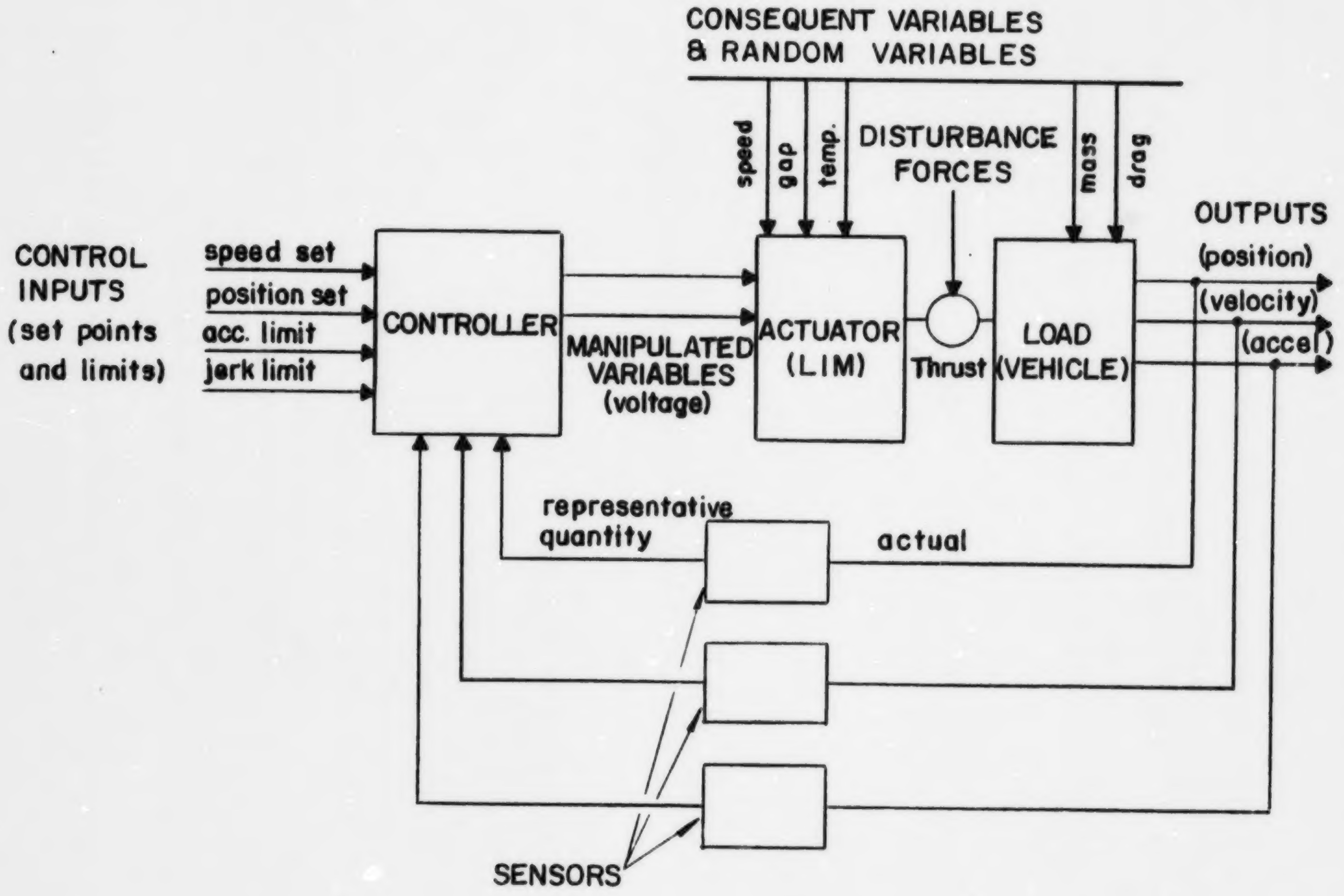
CONSEQUENT VARIABLES
& RANDOM VARIABLES
speed
gap
temp.
DISTURBANCE FORCES
mass
drag
CONTROL INPUTS (set points and limits)
speed set
position set
acc. limit
jerk limit
CONTROLLER
MANIPULATED VARIABLES (voltage)
ACTUATOR (LIM)
Thrust
LOAD (VEHICLE)
OUTPUTS
(position)
(velocity)
(accel)
representative quantity
actual
SENSORS

  - spatial orientation of the primary with respect to the secondary,
  - frequency of the electrical supply,
  - phase sequence of the electrical supply,
  - temperature of the secondary conducting plate (top-cap),
  - magnetic loading of the primary and secondary cores.

2. Transient response is governed by the LIM electrical time-constant.

3. In addition to thrust, vertical force is developed. It may be attractive or repulsive and can exceed the thrust force. The factors which affect vertical force are similar to those governing thrust, but the specific functional relationships are dissimilar.

4. Lateral forces develop as a result of lateral offset of the primary with respect to the secondary.

5. Secondary Power Loss (heating) develops in response to applied thrust and "slip." (Slip is the difference in linear speed of the secondary with respect to the travelling field pattern of the primary.)

Despite the apparent complexity of the LIM characteristic, it is often reasonable for the purposes of Control System analysis and design to consider a simplified representation. We usually have input voltage available as the manipulated variable, and can change both its magnitude and phase sequence. (Recall that we are dealing with a multiphase supply.) We relate output thrust to input voltage by a factor which we make dependent on speed, voltage, and phase sequence. Appendix 4 outlines a LIM model which may be used for control system analysis.

8.1.1 LIM Behaviour as a Function of Supply Frequency

Variable frequency control of LIMs will not be considered in detail in this report; however, a brief discussion will serve to highlight the specific differences between variable frequency (VF) and fixed frequency (FF) control, and the instances in which VF control is preferred.

Suppose that both Input Power and Frequency are considered as the manipulated variables, and Thrust, Vertical Force, and Secondary Power as output variables. If we wish to control one or all of the output variables, we must find suitable algorithms to adjust Power and/or Frequency. It so happens that there are a number of possible algorithms, and the choice of which to use will depend on the nature of the system being controlled. The following list represents some of the possible criteria on which to base the choice. (Note that with FF control it is not possible to satisfy any of the following except at a unique speed.)

1. Maximize Motor Efficiency (minimize energy consumption),

2. Maximize Thrust per Input Apparent Power (minimize power conditioner size),

3. Maximize Thrust per Secondary Power loss (minimize reaction-plate heating),

4. Maximize Thrust per Attractive Force (minimize suspension requirement).

The extra flexibility offered by VF control offers potential gains in LIM performance over FF control. In systems where the impact of the LIM on the power supply is important, or in systems which have particular problems associated with reaction rail heating or the control of vertical force, the benefits of the VF approach can justify the additional complexity.

8.2 THE LIM CONTROLLER

The most rudimentary form of LIM controller simply connects the LIM primary winding to the 3-phase supply. (An "ON-OFF" type control is usually not suitable if speed regulation or stop-positioning is required, though for systems with very low acceleration requirements and high-inertia/low-drag loads, it could be acceptable.)

The common form of LIM controller uses a network of Silicon Controlled Rectifiers (SCRs) to adjust the voltage to the LIM. Various specific forms of this type of controller are possible (for example, see Ref. 3, Chapter 4).

Beyond the basic function of providing voltage control to the LIM, we may wish the LIM controller to have some or all of the following features:

- Phase reversal (for "plug-mode" braking),
- Line Rectification (for eddy-current braking),
- Control-Signal Conditioning (to aid in linearizing the LIM-thrust/voltage relationship),
- Proportional-Integral Compensation (to eliminate steady-state error in feedback control applications),
- Multi-input Difference Amplifier Input (to accommodate multiple control loops, eg. speed, position, acceleration).

Appendix 4 develops a model of a LIM controller for the purposes of control system analysis.

8.3 THE NATURE OF THE LOAD

In general the load the LIM must move will have variable mass and drag. The system must be designed to account for the range of variation. This involves:

1) Sizing the LIM to meet the maximum thrust requirement,

2) Designing the controller for adequate transient response, steady-state error, and stability over the range of variation.

8.4 SENSING AND FEEDBACK

Appendix 4 goes into some detail in the modelling of typical position- and speed-sensing methods for LIM-based control systems. A major difference between LIM-based control and rotary-motor-based control is that we are often dealing with sensors which have much poorer resolution than the typical "shaft-encoders" and "tachometers" used in rotary motors. Low resolution translates into delayed feedback, especially al low speeds. This becomes critical in stop-positioning, where stability margins become increasingly smaller as the speed approaches zero. For many applications it is only necessary to maintain closed-loop control to moderately low speeds before some form of friction braking takes over. Other times it is required to achieve the best low speed control possible from a given sensor. The design of such a system is greatly aided by having available a control system model which simulates the essentially non-linear behaviour of the various system elements.

9.0 CONCLUSIONS

9.1 MODELLING AND EXPERIMENTATION

- Traditional Equivalent Circuit Models are a suitable framework for studying 60 Hz LIM behaviour providing the parameters are determined by experimental means. The standard analytical formulae for generating the circuit parameters do not result in accurate predictions.

- Static test techniques may be used to generate repeatable and reasonably accurate estimates of the equivalent circuit parameters for a given LIM configuration. These techniques save considerable time in assessing LIM designs.

- The parameter most difficult to accurately predict from theory is the secondary leakage inductance, L2. An empirical formula developed from static tests indicates that secondary leakage inductance is dependent on airgap, pole-pitch, and top-cap depth. Further tests, specifically designed for the purposes of generating an improved empirical expression, should be considered in the future.

- Extensions to the basic equivalent circuit model were made to include the effect of "space harmonics" in the airgap flux waveform. The space harmonic components of the flux wave were measured, and their relative amplitudes, speeds, and directions of travel determined. This data, however, only serves to confirm the basis of the theory, i.e., that the harmonic components are present. It was not possible, however, to prove conclusively that space harmonic branches, added to the equivalent circuit, are a correct means of dealing with the presence of the harmonic airgap fields. Future experiments aimed at validating the approach may attempt to measure "harmonic thrusts," perhaps by distributing strain-gauges along the top-cap length. "Snap-shots" of the thrust versus distance distribution may reveal the presence of harmonic thrusts, and serve as a very direct comparison with the model result.

- Extension to the basic equivalent circuit model was made to account for the so-called "entry-end effect" due to the finite length of the LIM primary. (The approach had been used successfully in predicting the behaviour in larger LIMs for speeds in the order of ten to twenty metres per second.) The small LIMs studied under the 60 Hz program appeared to exhibit negligible entry-end effect when analyzed by the model.

  This conclusion was supported by the dynamic test results.

9.2 DESIGN

- Small, 60 Hz LIMs have poor efficiency, power factor, and power-to-mass ratio compared to rotary motors. These are due mostly to fundamental reasons, but modest improvements (e.g., increases in the order of 10 to 20% on power factor x efficiency) may be made through design refinements. "Breakthrough" performance improvements are achieveable at the cost of including a variable-frequency source.

- When systems involving a large number of LIM primaries are considered, it is advised to perform a comprehensive design study prior to selecting a design. Commercially available designs will not necessarily be optimized to the particular speed, thrust, and duty cycle requirements of a proposed system, and to use these designs could imply poor materials utilization and higher than necessary cost. The data and modelling approaches developed in the 60 Hz LIM program are suitable for design studies, and the static and design test facilities provide a ready means of testing prototype designs.

- A number of related design concepts have been identified which may extend the range of applicability and/or reduce the costs of LIMs. These are:

    - Wound secondary applications
    - "Gramme-slab" primary
    - LIM steering

- Compared to conventional motors, the design techniques applied to small LIMs are rather unsophisticated. A continued effort to integrate those aspects of LIM technology learned under this program with those currently practiced, and those anticipated as the LIM is applied to such areas as people-moving and materials-handling, would be desirable. The result of such effort would be improved accessibility of LIM technology to larger groups of engineers, which, in turn, would result in the LIM's technological and commercial growth.

9.3 PRESENT APPLICATIONS

- Until variable-frequency supplies are available at lower cost, 60 Hz variable-voltage control will probably be preferred in most low-power LIM-in-track applications.
- Design tools and facilities created under this program are well suited to developing LIM designs for low speed, 60 Hz applications. A control system model was also developed and may be used to design feedback and compensation schemes for many LIM-based motion control applications.

9.4 FUTURE APPLICATIONS

- Variable frequency control of LIMs adds complexity but results in propulsion systems with greater flexibility and higher efficiency. This is almost certainly the future direction for in-track LIM development.

9.5 RECOMMENDATIONS

It is recommended that work now be undertaken to develop an advanced linear motor power and control package (LPCP), suitable for initial use in a variety of transportation systems.

The Research and Development would build upon UTDC's existing knowledge of linear motor design, and utilize linear motor performance models and test facilities created through this development program. This would produce a thoroughly tested Linear Motor Power Control Package (LPCP) which has lower cost than existing modules, is more compact in size and more efficient in its power translation. The state-of-the-art in LIM power and control technology would be advanced and would have spin-off benefits for transportation vehicle design and could cause the popularization of the LPCP in Original Equipment Manufacturer (OEM) markets.

Fundamental research would also be conducted into revolutionary new design concepts for LIMs, which could lead to very advanced products being offered to the transportation and OEM marketplace.

REFERENCES

1. Say, M.G., Alternating Current Machines, 4th Edition, Pitman Publishing, 1976.

2. Hesmondhalgh, D.E., and Tipping, D., Equivalent Rotor Impedance of Sheet-Rotor Induction Motors, IEE Proc., Vol. 130, Pt. B, No. 5, September 1983.

3. Dewan S.B., Straughen A., Power Semiconductor Circuits, John Wiley & Sons, 1975.

APPENDIX 1

DERIVATION OF THE EQUIVALENT CIRCUIT PARAMETERS FROM THEORY

DERIVATION OF PRIMARY RESISTANCE, R_1

Of all the equivalent circuit parameters the primary resistance, R_1 is the most straightforward to formulate a mathematical expression for. It is determined by the conductor cross-section, material resistivity, and overall length of the primary winding.

1. Conductor Cross Section

The conductor section is written in terms of more general design parameters; turns per coil, slot height and width, and fill factor.

$$CCS = \frac{h_s w_s k_f}{2N}$$

2. Overall Length

For series connected windings the overall length of a single phase can be expressed in terms of the coil-pitch, the terns per coil, the motor width and the number of poles.

$$OL = 4NbP(W + \frac{\pi}{2} \tau_c)$$

This formula assumes semi-circular end-turns.

3. Per-Phase Resistance

$$R_1 = \rho \frac{(OL)}{(CCS)} = \frac{\rho_{AL} 8N^2 bP}{h_s w_s k_f} (W + \frac{\pi}{2} \tau_c)$$

Examples

1. "2/3" LIM

ρ_{AL} = 1.72 E-8, h_s = .041, w_s = .011, P = 3, N = 33, k_f = 0.436, W = .177, τ_c = .038

R_1 = 0.541 (measures $\approx$ 0.57)

2. "3/3" LIM

same but N = 30, τ_c = 0.57

R_1 = 0.503 (measures $\approx$ 0.55)

3. 4/6 LIM

same but N = 16, b = 1, τ_c = .076

R_1 = 0.319 (measures $\approx$ 0.35)

DERIVATION OF SECONDARY RESISTANCE, R_2

The secondary resistance R_2 of a sheet-conductor secondary may be expressed analytically if simplifying assumptions are made about the geometry of the current distribution in the sheet:

1. The longitudinal current density distribution is sinusoidal
2. The vertical current density distribution is uniform (i.e., no "skin effect")
3. The current flows only in the transverse direction when inside the gap region
4. The current flows longitudinally in zero-resistance "end-bars" when outside the gap region

Analysis

The primary mmf may be written

$$F(x) = \sqrt{2}\, I_1 \frac{6}{\pi} k_w N b \sin \frac{2\pi}{\lambda_m} x$$

The primary current density distribution is

$$J(x) = \frac{d\,F(x)}{dx} = \sqrt{2}\, I_1 \frac{6}{\pi} k_w N b \frac{2\pi}{\lambda_m} \cos \frac{2\pi}{\lambda_m} x \text{ (A/M)}$$

The secondary current density is of the same form but scaled down by the factor I_2/I_1:

$$J_2(x) = \sqrt{2}\, I_2 \frac{12\, k_w N b}{\lambda_m} \cos \frac{2\pi}{\lambda_m} X$$

Over the length of the machine, ℓ, the effective, or rms value of J_2 is

$$J_{2_{rms}} = I_2 \frac{12\, k_w N b}{\lambda_m} \quad (A/M)$$

The bulk current is

$$I_{bulk} = J_{2_{rms}} \ell = I_2 \; 12 k_w N b \frac{\ell}{\lambda_m}$$

The bulk resistance is

$$R_{bulk} = \frac{\rho W}{\delta \ell}$$

The power dissipated in the sheet is

$$P_2 = I^2_{bulk} R_{bulk} = I_2^2 \; 144 \; (k_w N b)^2 \frac{\ell}{\lambda_m^2} \frac{\rho W}{\delta}$$

Now in the equivalent circuit representation

$$P_2 = 3 I_2^2 R_2$$

Hence

$$R_2 = \frac{48 (k_w N b)^2}{} \frac{\ell \rho W}{\lambda_m^2 \delta}$$

Examples

1. "2/3" LIM

$k_w = .866$, $Nb = 33$, $P = 3$, $W = .177$, $\lambda_m = 0.114$, $\rho = 2.9 \times 10^{-8}$, $\ell = 0.4$

$$R_2 = \frac{6.19 \times 10^{-3}}{\delta}$$

2. "3/3" LIM

same as "2/3" except

$k_w = 1$, $Nb = 30$

$$R_2 = \frac{6.82 \times 10^{-3}}{\delta}$$

3. "4/6" LIM

same as "2/3" except

$Nb = 32$, $\lambda_m = 0.114$, $\ell = 0.8$

$$R_2 = \frac{2.91 \times 10^{-3}}{\delta}$$

Comparison with Experimental Results

Figure A1 -1 shows the variation of secondary resistance, R_2, with top-cap depth. The theoretical prediction is in very good agreement with both the "2/3" and "3/3" configurations, but is low for the "4/6" LIM. The discrepancy is likely due to the assumption of "zero-resistance end-bars" which becomes a less valid approximation as the pole-pitch of the motors, and hence the length of the longitudinal current component, become comparable to the motor width, or lateral current component. The ratio of the length of longitudinal to lateral paths is about 0.32 for the "2/3" and "3/3" LIM's and 0.64 for the "4/6" LIM. Reference 8 develops a geometry-dependen constant which is used as a modification to the analytical expression for R_2. In addition to the motor width and pole-pitch it is shown that the end-plate overhand and supply frequency also influence R_2.

UTDC

UTDC Research & Development Ltd.

Report No 453-570-001			
Date 85.03.29	**Issue** 1	**Page** 9 of 24	
Project 60 Hz LIM	**Title** 60 Hz LIM Technology Final Report Appendix 1	**By** W.J.B.	**Appd** HHB

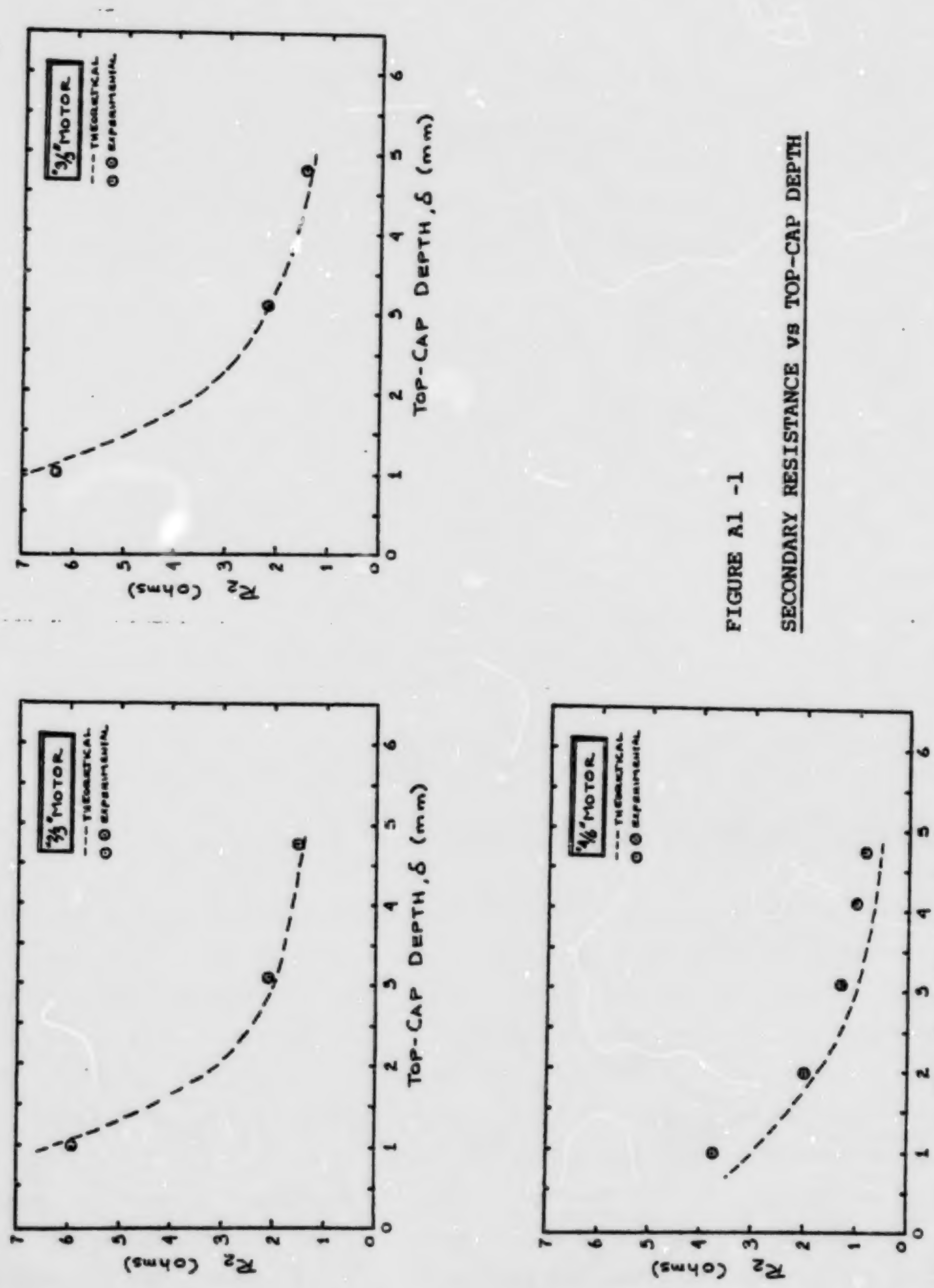

FIGURE A1 -1

SECONDARY RESISTANCE vs TOP-CAP DEPTH

DERIVATION OF MAGNETIZING INDUCTANCE, L_m

Background

The component L_m of the Induction Motor Equivalent Circuit is associated with the magnetic energy coupling the primary and secondary components of the motor. The term "magnetizing inductance" carries the idea that the primary "magnetizes" the secondary, or links it with "lines" of magnetic flux. The formulation of an expression for L_m requires a simplified view of the LIM geometry.

1. The slotted, wound, primary structure is replaced by a smooth surface on which a sinusoidally distributed "current sheet" provides the mmf to drive the magnetic flux across the gap.
2. All flux lines enter and exit the primary and secondary surfaces perpendicularly. There is no fringing at the lateral or longitudinal edges of the gap region.
3. The only magnetic reluctance is provided by the gap. Iron is assumed infinitely permeable and electrically non-conductive.

Analysis

The mmf of a winding may be developed by integrating the "ampere-turns" (at any given instant in time) over the motor length. The following figure illustrates:

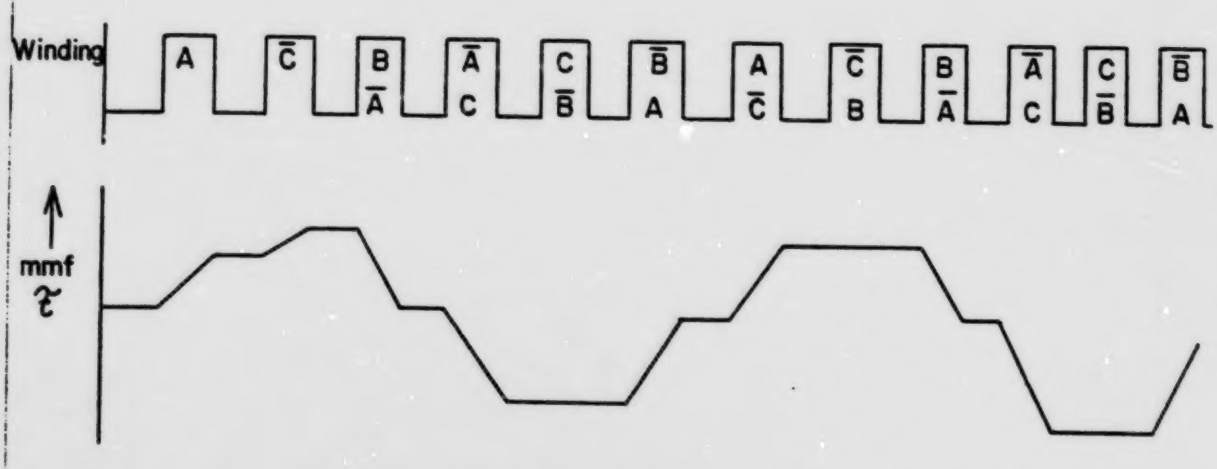

Figure A1 -2: Motor MMF versus Motor Length

It can be shown by Fourier Analysis of a general winding waveform that the fundamental component of mmf is given by

$$F(x) = \frac{6}{\pi} k_w Nbi \sin r_m x$$

Since all the reluctance is provided by the gap, the magnetic field intensity may be calculated as

$$H(x) = \frac{F(x)}{g}$$

The energy associated with the gap field is

$$E = \frac{1}{2} \int_{vol} \mu_o H^2 dv$$

$$= \frac{12W\mu_o (k_w Nbi)^2 P\lambda}{\pi^2 g}$$

The inductance is related to the energy and the current by

$$L_m = \frac{4}{3} \frac{E}{i^2}$$

$$L_m = \frac{12W\mu_o (kNb)^2 P\lambda}{\pi^2 g}$$

Examples

1. **Baseline LIM**

$k_w = .866$, $Nb = 33$, $P = 3$, $\lambda = .114$, $W = .177$

$$L_m = \frac{7.55 \times 10^{-5}}{g} \quad (H)$$

2. "3/3" LIM same but $K_w = 1$, $Nb = 30$

$$L_m = \frac{8.32 \times 10^{-5}}{g} \quad (H)$$

3. "4/6" LIM same as baseline but $Nb = 32$, $\lambda = 0.114$

$$L_m = \frac{1.42 \times 10^{-4}}{g}$$

Comparison with Experimental Results

Figure A1-3 compares the theoretical and experimental results for the three LIM primaries tested. The comparison is quite good, but in each case the theoretical was slightly higher than the experimental result. It is difficult to conjecture just which of the simplifying assumptions play a part in the discrepency. In light of the fact that the experimental result is itself based on a procedure rather than a direct measurement, a refinement of the analytical expression will not be attempted.

UTDC Research & Development Ltd.

Project 60 Hz LIM	**Title** 60 Hz LIM Technology Final Report Appendix 1	**Report No** 453-570-001		
		Date 85.03.29	**Issue** 1	**Page** 14 of 24
		By W.J.B.	**Appd** HHB	

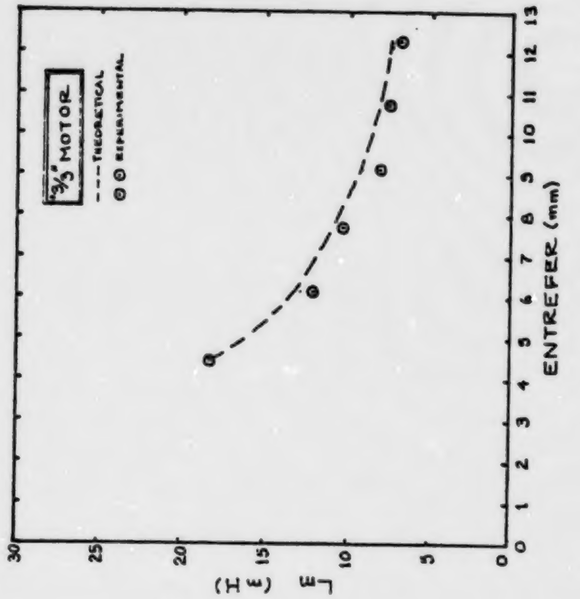

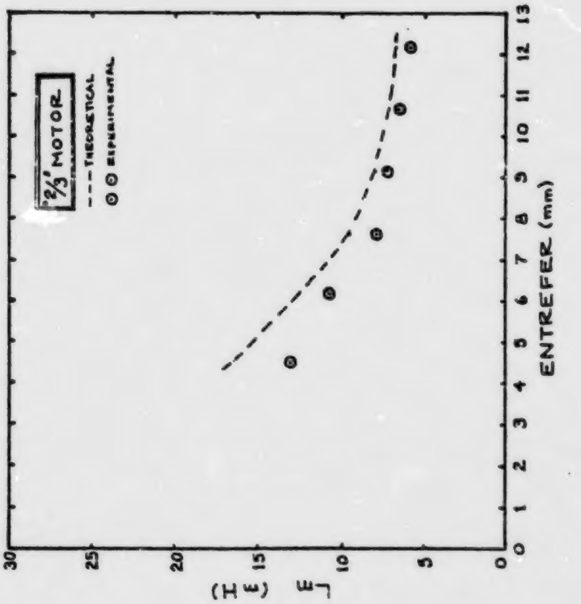

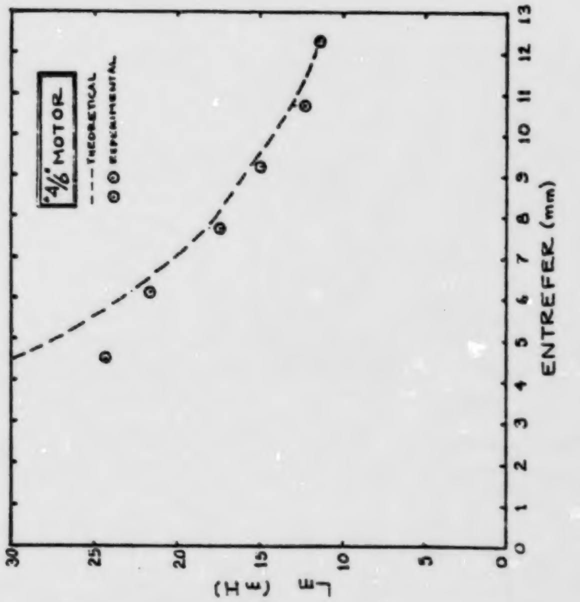

FIGURE A1 -3

MAGNETIZING INDUCTANCE vs ENTREFER

DERIVATION OF PRIMARY LEAKAGE INDUCTANCE, L_1

Background

The component L_1 of the Induction Motor Equivalent Circuit accounts for the energy corresponding to the "lines" of magnetic flux which link only the primary circuit and do not cross the magnetic gap to the secondary. The term "leakage inductance" conveys the notion that part of the magnetic field is not contained by the preferred magnetic path. There are at least three areas of leakage which can be identified, each of which is associated with a particular space within the motor geometry. The divisions are somewhat artificial but greatly simplify the analytical problems. The three components of L_1 are:

1) Slot Leakage

2) Gap Leakage

3) Endwinding Leakage

Figure A1 -4 attempts to illustrate these leakage paths, while Figure A1 -5 relates the slot and gap leakage to a two-dimensional flux map generated by Finite Element analysis of a typical LIM cross-section.

The primary leakage fields are not nearly as amenable to analysis as the main or linking field is. In order to derive a formula for L_1 certain simplifying assumptions are made:

1. Endwinding fields are small compared to Slot Leakage fields and may be neglected.

2. Slot leakage fields are uniform over the slot depth and do not "fringe" at the tooth tip.

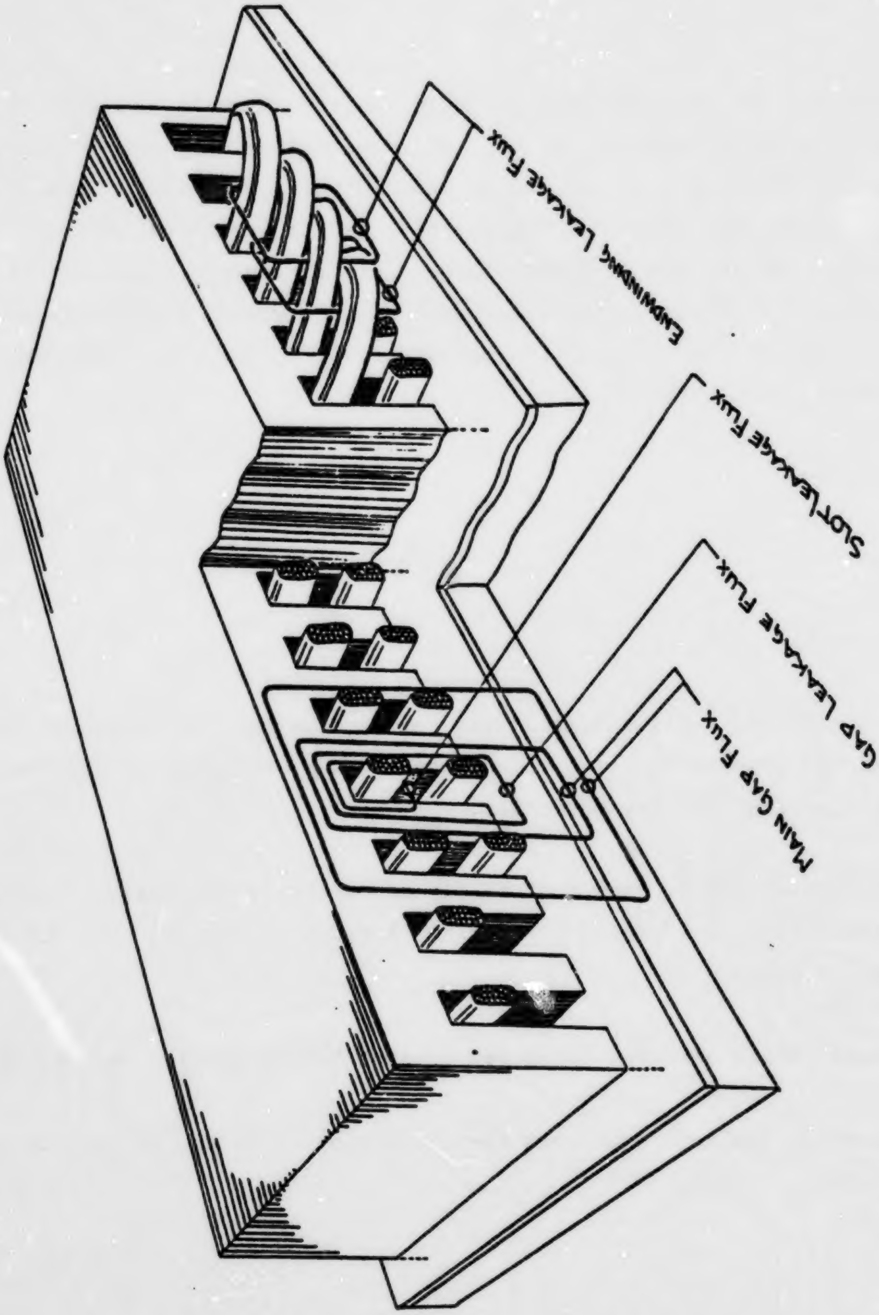
ENDWINDING LEAKAGE FLUX
SLOT LEAKAGE FLUX
GAP LEAKAGE FLUX
MAIN GAP FLUX

DEFINITION OF FLUX PATHS

FIGURE: A1-4

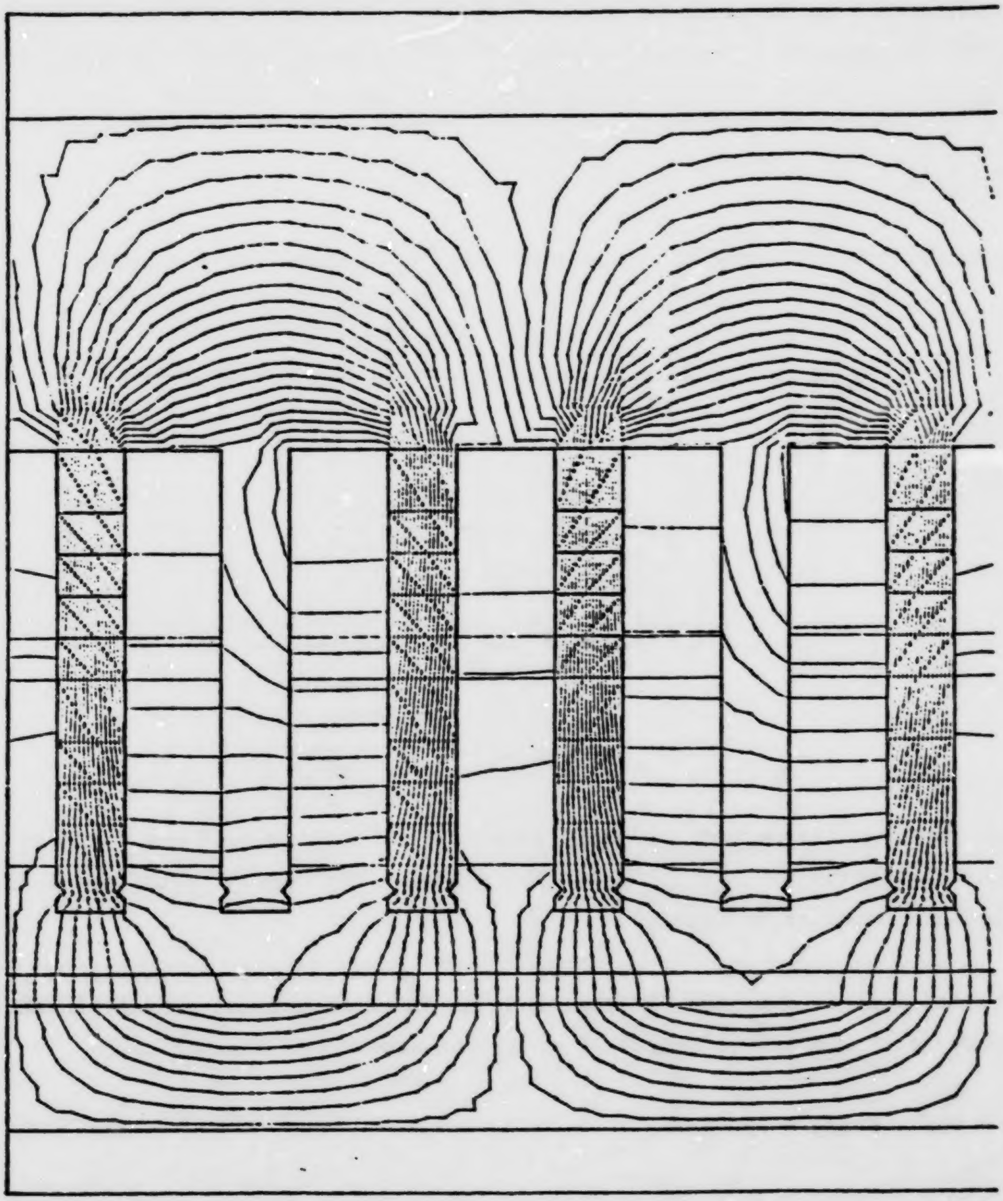

FIGURE A1 -5 FINITE ELEMENT MODEL OF BASELINE LIM

Assumption 1 is justifiable because the LIMs as tested have relatively little endwinding area compared to the core width. The second assumption seems reasonable with reference to Figure A1 -5 which shows the flux lines to be approximately evenly spaced over about 75% of the slot depth, and minimal fringing.

Analysis

Consider the following figure showing part of a three-phase winding.

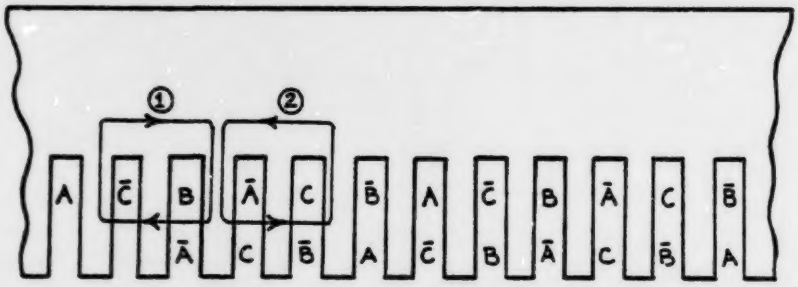

Figure A1 -6: SLOT LEAKAGE

The vertical offset of the coils results in a component of mmf which tends to drive flux horizontally, i.e., across the slots. Two typical paths are indicated in the figure. Consider now path 1.

The mmf generated by the "A" coil and the "$\bar{C}$" coil acts on a "gap" in this case equal to two slot widths. A general formulation would give the mmf as;

$$F = Nbi + Nbi/2 = 3/2\ Nbi$$

and the non-ferrous path length as;

$$\ell_p = 2/3\ \tau_p \frac{W_s}{\tau_s}$$

The magnetic field intensity in the slots is

$$H = \frac{F}{\ell_p} = \frac{3}{2}\,\frac{Nbi}{\ell_p}$$

The magnetic energy in the slots is

$$E = \frac{1}{2}\,\mu_o \int_{vol} H^2\,dv$$

$$= \frac{1}{2}\,\mu_o\,\ell_p\,Wh_s\,\left(\frac{3}{2}\right)^2\,\frac{(Nb)^2 i^2}{\ell_p^2}$$

$$= \frac{9}{8}\,\frac{\mu_o Wh_s (Nb)^2 i^2}{\ell_p} = \frac{27}{16}\,\mu_o\,\frac{Wh_s (Nb)^2 i^2 \tau_s}{\tau_p W_s}$$

Over the length of the machine this energy is repeated L_p/ℓ_p times where L_p is the total magnetic path length

$$L_p = 2P\,\tau_p\,\frac{W_s}{\tau_s}$$

$$\frac{L_p}{\ell_p} = 3\,P$$

Hence the total energy due to slot leakage fields is

$$(3P)\,\frac{27}{16}\,\mu_o Wh_s (Nb)^2\,\frac{i^2 \tau_s}{\tau_p W_s}$$

The leakage inductance can be derived from the energy by using

$$L = \frac{4}{3} \frac{E}{i^2}$$

$$L = \frac{27}{4} \frac{P\mu_0 W h_s (Nb)^2}{\tau_p} \left(\frac{\tau_s}{W_s} \right)$$

Examples

1. **Baseline LIM**

$P = 3,\ W = .177,\ h_s = .04,\ Nb = 33,\ \tau_s = .019,\ W_s = .011,\ \tau_p = .057$

$L_1 = 6.54 \times 10^{-3}$ H

2. **"3/3" LIM**

same as baseline, but Nb = 30, therefore

$L_1 = 5.40 \times 10^{-3}$ H

3. **"4/6" LIM**

here, Nb = 32, $\tau_p = .114$, therefore

$L_1 = 3.1 \times 10^{-3}$ H

Comparison with Experimental Results

Figure A1 -7 shows the primary leakage inductance as a function of entrefer for the three LIM primaries tested. A number of observations relating to the comparison between the theoretical and experimental curves may be made:

1) The theoretical formulation for L_1 is independent of entrefer, but test results indicate a slight increase in L_1 with widening gap.

2) The theoretical curve matches the "4/6" LIM data more closely than the "2/3" and "3/3" data, which it underestimates.

3) The discrepancy between theory and test is greatest for the "3/3" motor.

All of the above observations may be qualitatively explained by the absence of a "gap leakage" term in the theoretical formulation. Gap leakage is due to that proportion of flux which enters the gap region but fails to traverse the complete gap. Intuitively it would seem to be related to the ratio of pole-pitch to entrefer: As the pole-to-pole distance becomes closer to the distance across the gap, the tendency for flux to "leak" from pole to pole is increased. For a given pole-pitch the amount of gap leakage ought to increase with increasing entrefer. These tendencies are supported by the experimental observations.

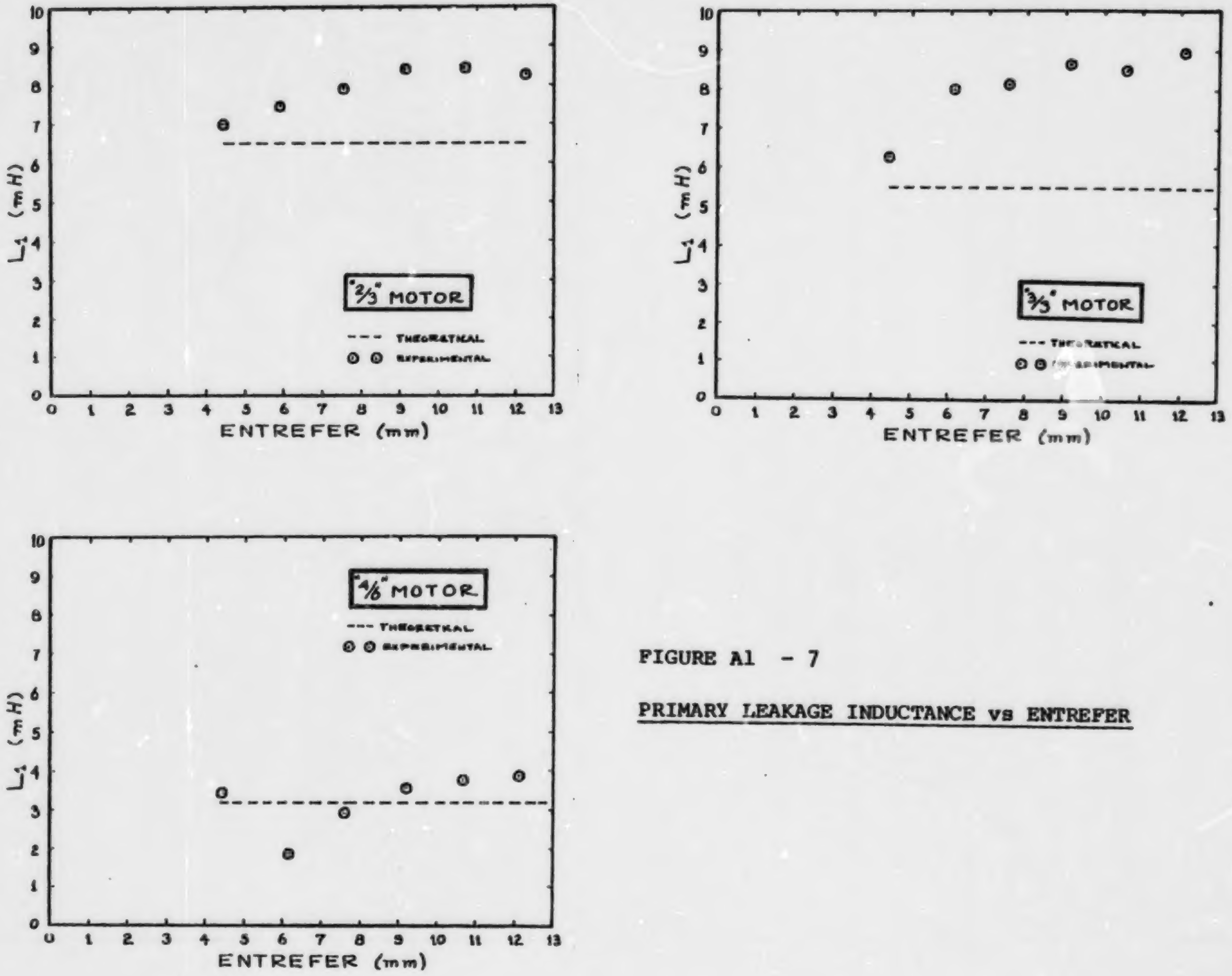

FIGURE A1 - 7

PRIMARY LEAKAGE INDUCTANCE vs ENTREFER

UTDC

UTDC Research & Development Ltd.

Project 60 Hz LIM	**Title** 60 Hz LIM Technology Final Report Appendix 1	**Report No** 453-570-001		
		Date 85.03.29	**Issue** 1	**Page** 24 of 24
		By W.J.B.	**Appd** HHB	

UTDC Research & Development Ltd.

Report No 453-570-001					
Project 60 Hz LIM	**Title** 60 Hz LIM Technology Final Report Appendix 2	**Date** 85.03.29	**Issue** 1	**Page** 1 of 8	
		By W.J.B.		**Appd** HHB	

APPENDIX 2

DERIVATION OF THE EQUIVALENT CIRCUIT PARAMETERS FROM EXPERIMENT

UTDC

UTDC Research & Development Ltd.

Report No 453-570-001			
Date 85.03.29	**Issue** 1	**Page** 2 of 8	
Project 60 Hz LIM	**Title** 60 Hz LIM Technology Final Report Appendix 2	**By** W.J.B.	**Appd** HHB

DETERMINATION OF R_1, L_1, L_m AND R_m FROM TEST DATA

Background

The removal of the conducting sheet or "top-cap" from a LIM configuration corresponds to a removal of the secondary branch from the equivalent circuit. That is:

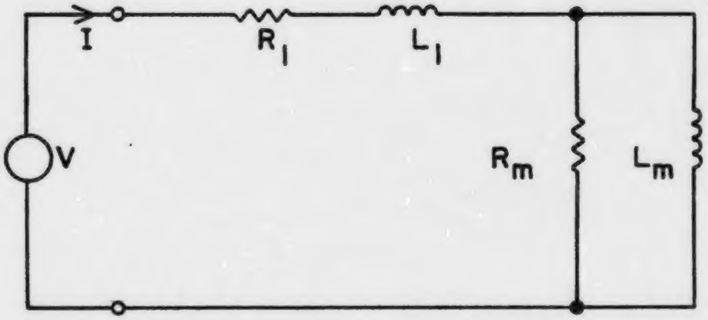

Figure A2 -1: Equivalent Circuit Model - Secondary Branch Removed

The term R_m accounts for hysterisis and eddy current losses in the iron structure and is not directly measurable. Under DC conditions it is effectively infinite and not a part of the circuit. A DC resistance measurement is taken to determine R_1, then R_m and the sum of L_1 and L_m are determined by AC terminal measurements. Finally, a flux density measurment is used to isolate L_m.

Analysis

1) Given V, I, and R_1 determine the sum $L_1 + L_m$. (V, I are complex numbers)

$$\frac{V}{I} = R_1 + jX_1 + \frac{R_m jX_m}{R_m + jX_m} \qquad \text{where } X_m = \omega L_m, \quad X_1 = \omega L_1$$

$$\frac{V}{I} = R_1 + \frac{R_m X_m^2}{R_m^2 + X_m^2} + j\left(X_1 + \frac{R_m^2 X_m}{R_m^2 + X_m^2}\right)$$

Now if $R_m >> X_m$, $\frac{V}{I} = R_1 + \frac{X_m^2}{R_m} + j(X_1 + X_m)$

Hence $$L_1 + L_m = \frac{1}{\omega}\,\mathrm{Im}(V/I)$$

2) Given the integral of the square of the gap flux density, $\int B^2(X)$, and the entrefer, g, and LIM width, W, calculate L_m.

The energy due to the gap field is:

$$E_g = \frac{1}{2}\int_{vol} \frac{B^2(x)}{\mu_o}\,dV$$

If we assume a uniform field in the vertical and lateral directions:

$$E_g = \frac{1}{2\mu_o}\,gW \int_o^{\ell} B^2(x)dx$$

Again, assuming that R_m is large compared to X_m, virtually all the current in the windings is considered to flow through L_m. If the iron structures are considered "infinitely permeable" then the gap energy, E_g, may be equated with the inductive energy given by:

$$E_L = \frac{3}{4} I_{peak}^2 L_m$$

Now

$$L_m = \frac{4}{3} \frac{E_L}{I_{peak}^2} = \frac{4}{3} \frac{E_g}{I_{peak}^2}$$

$$L_m = \frac{2}{3\mu_o I_{peak}^2} gW \int_o^{\ell} B^2(x)dx$$

3) Given V, I, R_1, L_m determine R_m

In part 1. it was shown that

$$\frac{V}{I} = R_1 + \frac{X_m^2}{R_m} + j(X_1 + X_m)$$

hence, $R_1 + \frac{X_m^2}{R_m} = \text{Re}(V/I)$

rearranging $$R_m = \frac{X_m^2}{\text{Re}(V/I) - R_1}$$

Examination of Assumptions

1) Iron Loss Component, R_m

The component R_m accounts for two types of losses which occur within the iron structures and do not contribute to thrust. These are (i) Hysterisis losses, and (ii) Eddy-Current losses. The amount of power dissipated on a local basis relates to the flux densities in the various parts of the iron structures. While the total flux is expected to remain similar in the "No Top-Cap" and "Installed Top-Cap" tests, the local flux densities will not, and so the value calculated under the "No Top-Cap" test may differ when the top-cap is replaced.

2) Magnetizing Inductance, L_m

As calculated, the component L_m incorporates all of the flux crossing the gap. Strictly speaking it should only relate to the fundamental component of the gap flux density wave. Its calculated value therefore may be slightly greater than it should be.

The direct use of the stack width, W, and tooth to secondary-iron clearance, g, in the calculation of L_m may introduce errors due to the non-uniform nature of the field in the tooth-tip and lateral-edge regions. Both of these field distortions would contribute to a slight increase in the "effective" distances for W and g and therefore cause the calculated value of L_m to increase.

The value of L_1 is determined by subtracting L_m from the total measured primary inductance. Therefore, errors made in the calculation of L_m are reflected in L_1 also. The double-nature of this error acts to magnify the error on the calculation of thrust from the equivalent circuit under voltage-driven conditions.

UTDC Research & Development Ltd.

Project 60 Hz LIM	**Title** 60 Hz LIM Technology Final Report Appendix 2	**Report No** 453-570-001		
		Date 85.03.29	**Issue** 1	**Page** 7 of 8
		By W.J.B.	**Appd** HHB	

DETERMINATION OF L_2 AND L_2 FROM TEST DATA

Once the parameters R_1, L_1, R_m and L_m have been determined, the top-cap is replaced. Terminal measurements are again made.

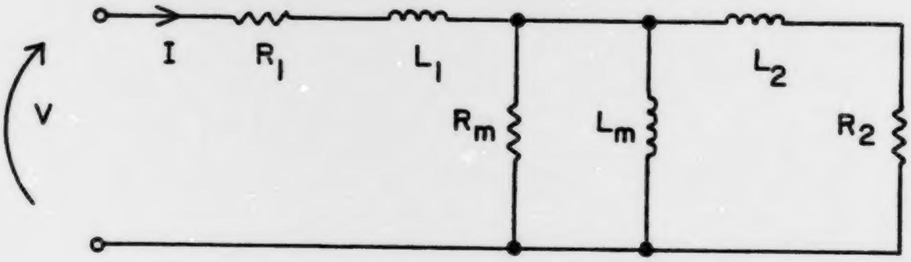

define $\quad Z_1 = R_1 + j\omega L_1$

$$Z_2 = R_2 + j\omega L_2$$

$$Z_m = \frac{R_m jX_m}{R_m + jX_m}$$

$$\frac{V}{I} = Z_1 + \frac{Z_m Z_2}{Z_m + Z_2} = \frac{Z_1 Z_m + Z_m Z_2 + Z_2 Z_1}{Z_m + Z_2}$$

$$(Z_m + Z_2)\, V/I = Z_1 Z_m + Z_m Z_2 + Z_2 Z_1$$

$$Z_2(V/I - Z_m - Z_1) = Z_1 Z_m - Z_m V/I$$

$$\boxed{\begin{aligned} Z_2 &= \frac{Z_1 Z_m - Z_m V/I}{V/I - Z_m - Z_1} \\ R_2 &= \mathrm{Re}(Z_2) \\ L_2 &= \mathrm{Im}(Z_2) \end{aligned}}$$

UTDC Research & Development Ltd.

Report No 453-570-001				
Date 85.03.29	**Issue** 1	**Page** 1 of 29		
Project 60 Hz LIM	**Title** 60 Hz LIM Technology Final Report Appendix 3	**By** W.J.B.	**Appd** HHB	

APPENDIX 3

STATIC PERFORMANCE

SUMMARY-BASED CONFIGURATIONS

UTDC Research & Development Ltd.

Project 60 Hz LIM	**Title** 60 Hz LIM Technology Final Report Appendix 3	**Report No** 453-570-001		
		Date 85.03.29	**Issue** 1	**Page** 2 of 29
		By W.J.B.		**Appd** HHB

i

```
                    60 Hz. PROGRAM -- STATIC TEST SERIES
                    ====================================

     TEST IDENTIFICATION -- RUN A (WITHOUT TOP-CAP): 05-JUL-8415:51:52
                             RUN B (WITH TOP-CAP)   : 05-JUL-8415:58:45

     TEST CONFIGURATION :  AIRGAP (MM)........... 10.76
                           TOP-CAP THICKNESS (MM)  5.00
                           CORE WIDTH (M)........  0.177
                           COIL PITCH (M)........  0.038
                           POLE PITCH (M)........  0.057
                           NO. OF POLES .........  6.0
                           TURNS PER COIL ....... 33.0
                           SLOT PITCH (MM)....... 19.00
                           LIM LENGTH (M)........ 0.394

   RESULTS FROM FSAP (FOURIER SPECTRUM ANALYSIS PROGRAM)
  -------------------------------------------------------
           WITHOUT TOP-CAP
          -----------------                          WITH TOP-CAP
  CHAN      DC   FREQ    MAG     ANG                -------------
                                               DC   FREQ    MAG     ANG

   1       0.0   0.0    0.0     0.0           0.0   0.0    0.0     0.0
   2       1.7  60.5   29.6    44.8           1.8  60.5   38.3   -29.8
   3       0.5  60.5   28.7   -76.5           0.2  60.6   38.2  -143.0
   4       0.8  60.5   29.6   166.1           0.9  60.6   41.0    96.4
   5       1.1  60.5  161.0   -37.3           0.3  60.6  162.0   -93.5
   6       0.2  60.5  163.6    82.7           0.8  60.6  165.7    25.7
   7       1.2  60.5  166.0  -157.6           1.3  60.6  165.0   144.2
   8       3.1   0.1    6.2  -171.0         228.9   8.1  448.0     9.2
  EQUIVALENT CIRCUIT RESULTS
  --------------------------

 R1 : 0.577               R2 :  1.462           RM :  29.389
 L1 : 0.000537            L2 : 0.000456         LM : 0.006006


  PERFORMANCE RESULTS
 --------------------
    PARAMETER                                 DERIVED FROM     DERIVED FROM
    ---------                                 MEASUREMENT      EQUIV. CIRCUIT
                                              -----------      --------------
 POSITIVE SEQUENCE - VOLTAGE (VOLTS)...........116.1<   0.0    116.1<   0.0
                   - CURRENT (AMPS)............ 27.7< -69.1     27.7< -69.1
 INPUT VA (VA)................................   9640.6           9640.6
 INPUT POWER (W).............................. 3440.4           3440.4
 SECONDARY POWER (W).......................... 1885.6           2012.7
 COPPER LOSSES (W)............................ 1326.2           1326.2
 IRON LOSSES (W)..............................  228.6            101.5
 POWER FACTOR.................................    0.357            0.357
 THRUST (N)...................................  220.9            291.7
```

UTDC Research & Development Ltd.		Report No 453-570-001		
		Date 85.03.29	Issue 1	Page 3 of 29
Project 60 Hz LIM	Title 60 Hz LIM Technology Final Report Appendix 3	By W.J.B.		Appd HHB

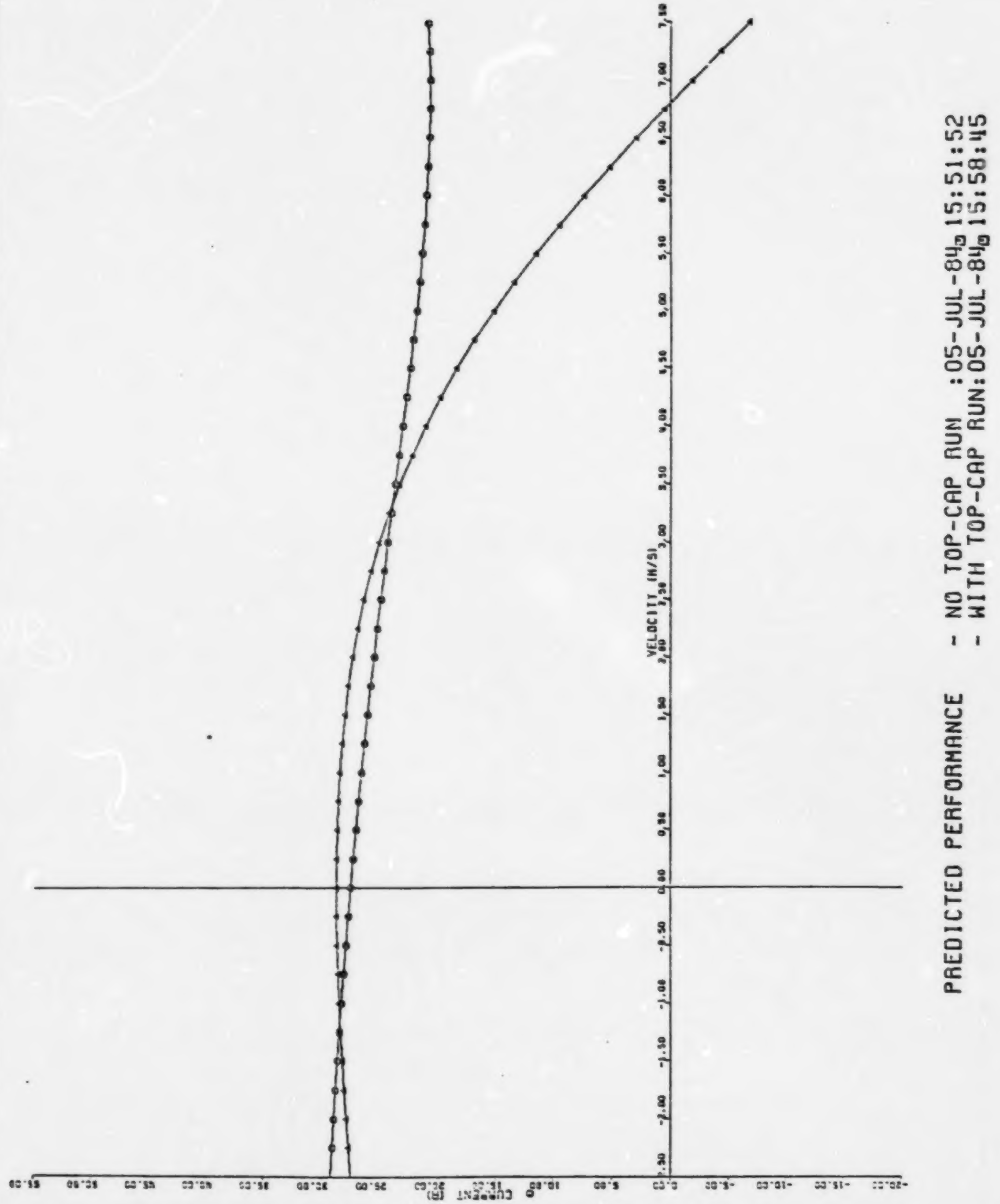

UTDC Research & Development Ltd.		Report No 453-570-001		
		Date 85.03.29	**Issue** 1	**Page** 4 of 29
Project 60 Hz LIM	**Title** 60 Hz LIM Technology Final Report Appendix 3	**By** W.J.B.	**Appd** HHB	

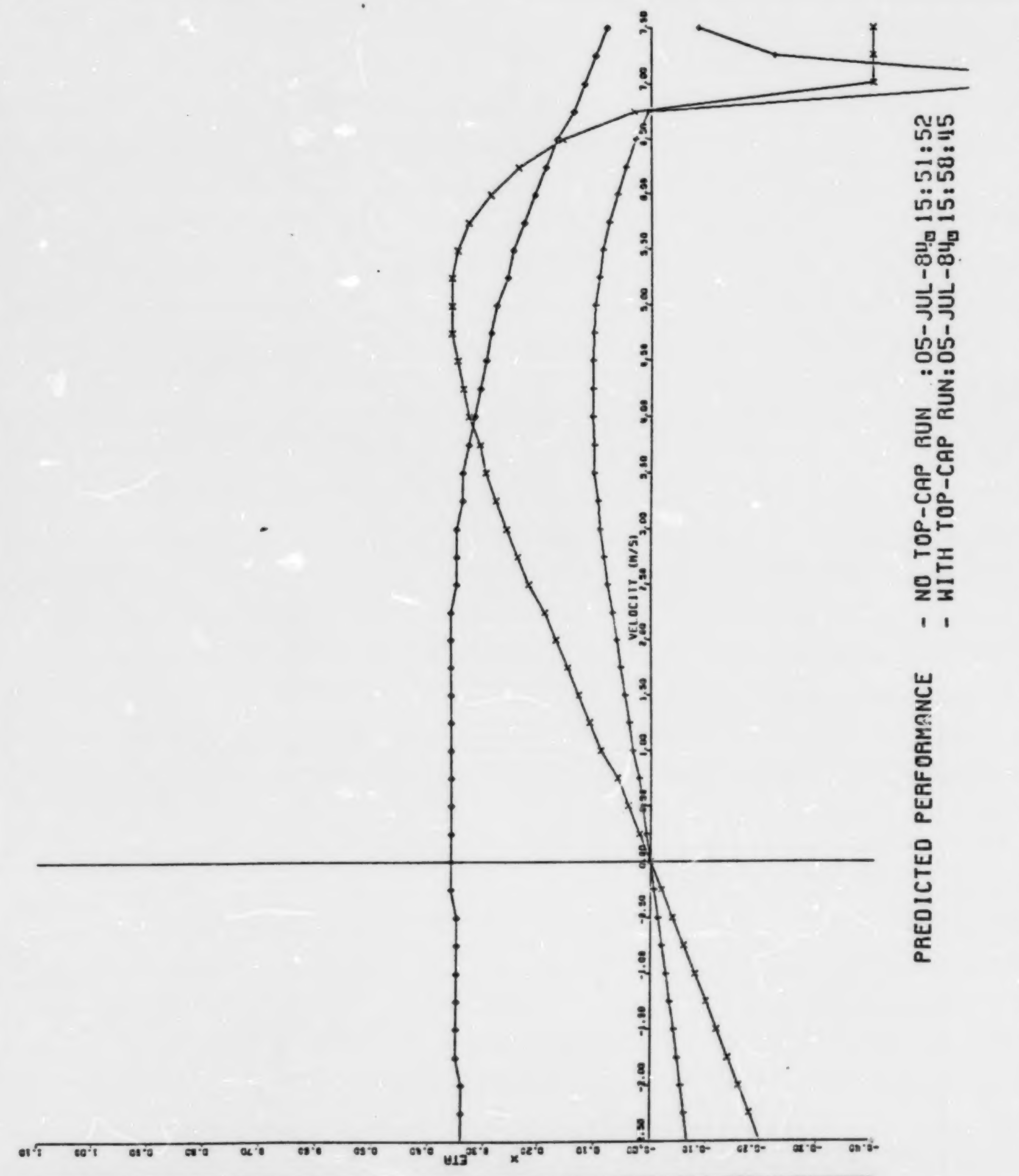

UTDC Research & Development Ltd.

Project 60 Hz LIM	**Title** 60 Hz LIM Technology Final Report Appendix 3	**Report No** 453-570-001		
		Date 85.03.29	**Issue** 1	**Page** 5 of 29
		By W.J.B.	**Appd** HHB	

```
                60 Hz. PROGRAM -- STATIC TEST SERIES
                ====================================

     TEST IDENTIFICATION -- RUN A (WITHOUT TOP-CAP): 05-JUL-8416:05:37
                            RUN B (WITH TOP-CAP)    : 05-JUL-8416:11:10

     TEST CONFIGURATION :  AIRGAP (MM)...........  9.22
                           TOP-CAP THICKNESS (MM)  3.00
                           CORE WIDTH (M)........  0.177
                           COIL PITCH (M)........  0.038
                           POLE PITCH (M)........  0.057
                           NO. OF POLES .........  6.0
                           TURNS PER COIL ....... 33.0
                           SLOT PITCH (MM)....... 19.00
                           LIM LENGTH (M)........  0.394

     RESULTS FROM FSAP (FOURIER SPECTRUM ANALYSIS PROGRAM)
   ---------------------------------------------------------
              WITHOUT TOP-CAP                              WITH TOP-CAP
             -----------------                            --------------
  CHAN        DC   FREQ    MAG     ANG            DC   FREQ     MAG      ANG

    1        0.0    0.0    0.0     0.0           0.0    0.0     0.0      0.0
    2        1.7   60.5   28.5    39.1           1.5   60.5    35.6   -151.1
    3        0.4   60.5   27.7   -82.5           0.3   60.5    35.5     90.1
    4        0.8   60.5   28.4   160.2           1.2   60.5    37.5    -30.0
    5        1.1   60.5  163.0   -43.5           0.8   60.5   159.0    142.0
    6        0.1   60.5  165.2    76.6           0.0   60.5   164.1    -99.2
    7        1.4   60.5  167.8  -163.6           0.5   60.5   163.0     20.3
    8        0.3    0.2    0.7    17.3         252.6    0.1   503.1      9.2

     EQUIVALENT CIRCUIT RESULTS
    ----------------------------

   R1 : 0.575               R2 :  2.050            RM :  36.166
   L1 : 0.008296            L2 : 0.001140          LM : 0.007000


     PERFORMANCE RESULTS
    ----------------------                            DERIVED FROM    DERIVED FROM
       PARAMETER                                      MEASUREMENT     EQUIV. CIRCUIT
       ---------                                      -----------     --------------
   POSITIVE SEQUENCE - VOLTAGE (VOLTS)...........114.6<    0.0   114.6<    0.0
                     - CURRENT (AMPS)............ 25.6< 291.4    25.6< -68.6
   INPUT VA (VA)................................    8803.7          8803.7
   INPUT POWER (W).............................. 3206.6           3206.6
   SECONDARY POWER (W).......................... 1841.0           1958.7
   COPPER LOSSES (W)............................ 1131.9           1131.9
   IRON LOSSES (W)..............................  233.7            116.0
   POWER FACTOR.................................    0.364            0.364
   THRUST (N)...................................  252.6            283.9
```

UTDC UTDC Research & Development Ltd.		**Report No** 453-570-001		
		Date 85.03.29	**Issue** 1	**Page** 6 of 29
Project 60 Hz LIM	**Title** 60 Hz LIM Technology Final Report Appendix 3	**By** W.J.B.		**Appd** HHB

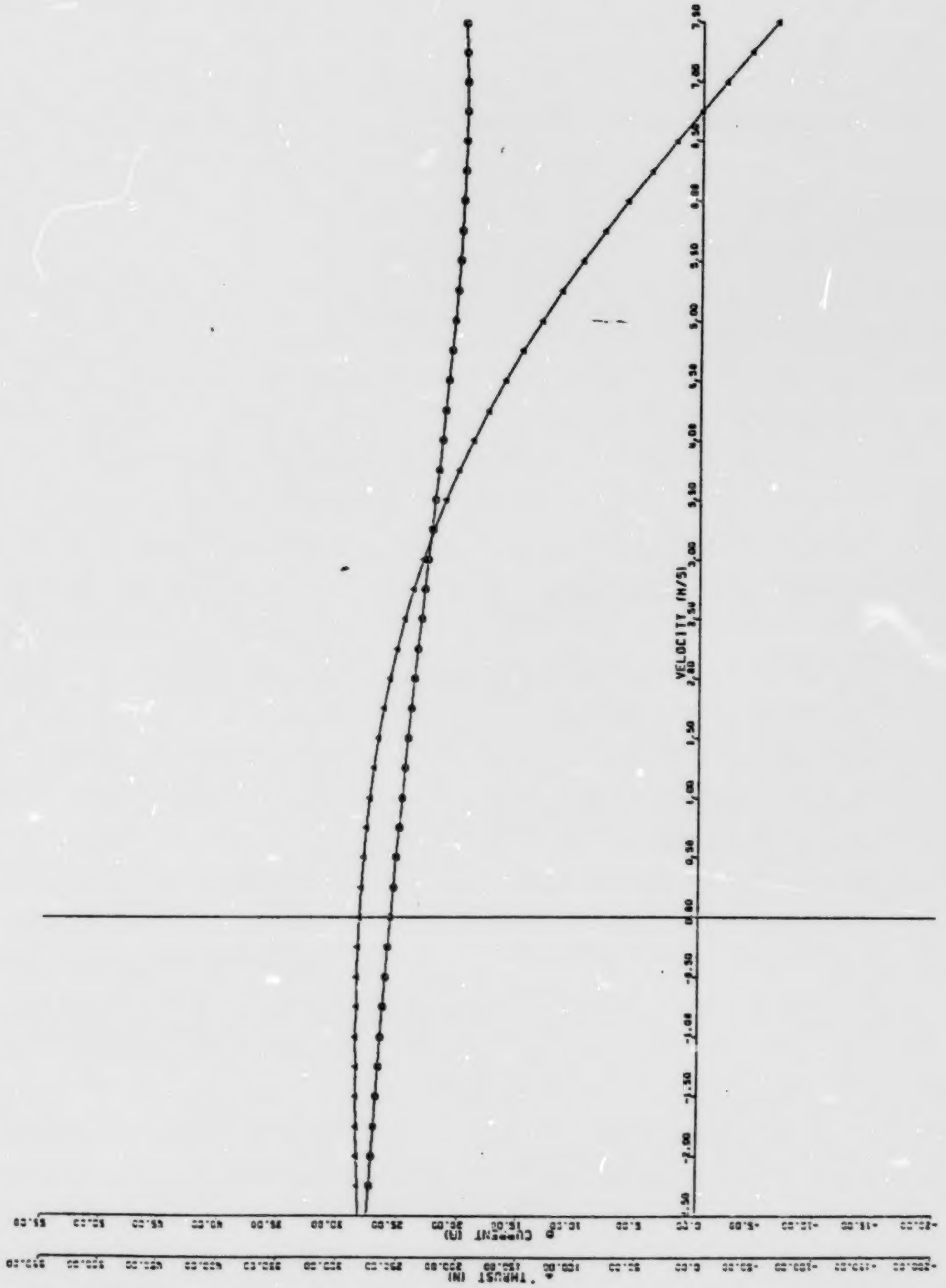

PREDICTED PERFORMANCE
- NO TOP-CAP RUN :05-JUL-84 16:05:37
- WITH TOP-CAP RUN:05-JUL-84 16:11:10

UTDC Research & Development Ltd.

Report No 453-570-001	**Date** 85.03.29	**Issue** 1	**Page** 7 of 29
Project 60 Hz LIM	**Title** 60 Hz LIM Technology Final Report Appendix 3	**By** W.J.B.	**Appd** HHB

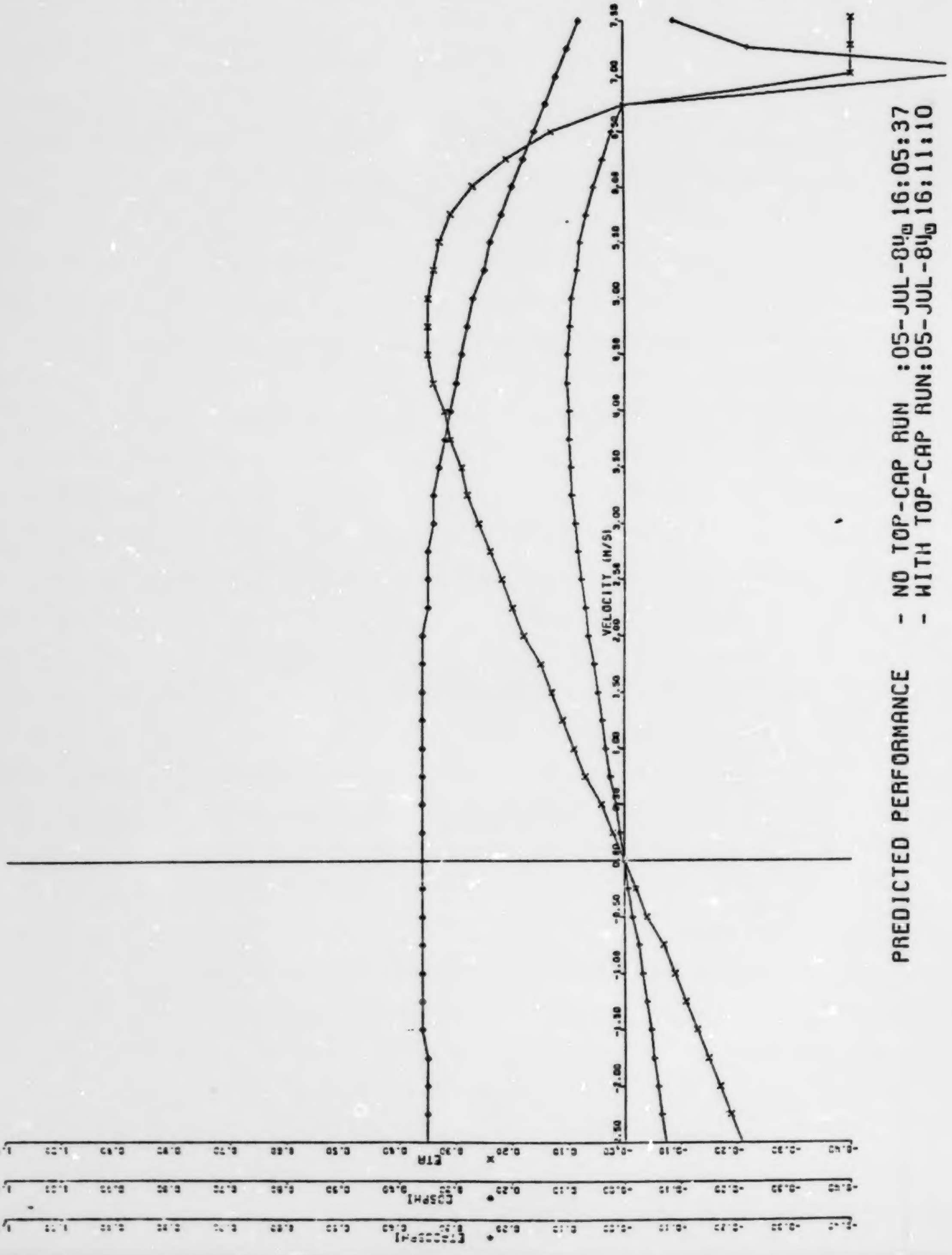

PREDICTED PERFORMANCE - NO TOP-CAP RUN :05-JUL-84 16:05:37
- WITH TOP-CAP RUN:05-JUL-84 16:11:10

UTDC Research & Development Ltd.

Project 60 Hz LIM	**Title** 60 Hz LIM Technology Final Report Appendix 3	**Report No** 453-570-001	
		Date 85.03.29	**Issue** 1
		Page 8 of 29	
		By W.J.B.	**Appd** HHB

```
                60 Hz. PROGRAM -- STATIC TEST SERIES
                ====================================

      TEST IDENTIFICATION -- RUN A (WITHOUT TOP-CAP): 05-JUL-8416:19:11
                              RUN B (WITH TOP-CAP)   : 05-JUL-8416:22:35

      TEST CONFIGURATION :  AIRGAP (MM)..........  7.70
                            TOP-CAP THICKNESS (MM)  1.00
                            CORE WIDTH (M)........ 0.177
                            COIL PITCH (M)........ 0.038
                            POLE PITCH (M)........ 0.057
                            NO. OF POLES ......... 6.0
                            TURNS PER COIL ....... 33.0
                            SLOT PITCH (MM)....... 19.00
                            LIM LENGTH (M)........ 0.394

      RESULTS FROM FSAP (FOURIER SPECTRUM ANALYSIS PROGRAM)
      -----------------------------------------------------
              WITHOUT TOP-CAP                              WITH TOP-CAP
              ---------------                             -------------
    CHAN      DC   FREQ    MAG     ANG             DC   FREQ    MAG     ANG

     1        0.0   0.0     0.0      0.0            0.0   0.0     0.0      0.0
     2        1.7  60.5    26.4     34.3            1.6  60.5    28.4     61.3
     3        0.4  60.5    25.7    -87.5            0.5  60.5    28.2    -58.6
     4        0.8  60.5    26.2    155.3            0.8  60.5    29.4    182.2
     5        1.0  60.5   161.6    -48.8            1.2  60.5   160.5     -8.2
     6        0.0  60.5   163.2     71.5            0.6  60.5   163.6    110.3
     7        1.4  60.5   165.9   -168.8            0.9  60.5   164.6   -129.7
     8        0.1   0.2     0.2   -157.3          183.4   0.1   365.3      9.2

      EQUIVALENT CIRCUIT RESULTS
      --------------------------

    R1 : 0.575              R2 :  6.237              RM :  46.723
    L1 : 0.007964           L2 : 0.001505            LM : 0.008369

      PERFORMANCE RESULTS
      -------------------
        PARAMETER                                       DERIVED FROM   DERIVED FROM
        ---------                                       MEASUREMENT    EQUIV. CIRCUIT
                                                        -----------    --------------
    POSITIVE SEQUENCE - VOLTAGE (VOLTS)............115.2<    0.0   115.2<    0.0
                      - CURRENT (AMPS)............ 20.3< -70.9    20.3< -70.9
    INPUT VA (VA).................................   7008.9          7008.9
    INPUT POWER (W)............................... 2292.7          2292.7
    SECONDARY POWER (W)........................... 1361.1          1395.2
    COPPER LOSSES (W)............................. 709.7           709.7
    IRON LOSSES (W)............................... 221.9           187.8
    POWER FACTOR..................................   0.327           0.327
    THRUST (N).................................... 183.4           202.2
    SURFACE CURRENT DENSITY (AMPS/MM)............. 70.460          70.460
```

UTDC Research & Development Ltd.		Report No 453-570-001	
		Date 85.03.29	Issue 1
Project 60 Hz LIM	Title 60 Hz LIM Technology Final Report Appendix 3	By W.J.B.	Appd HHB

Page 9 of 29

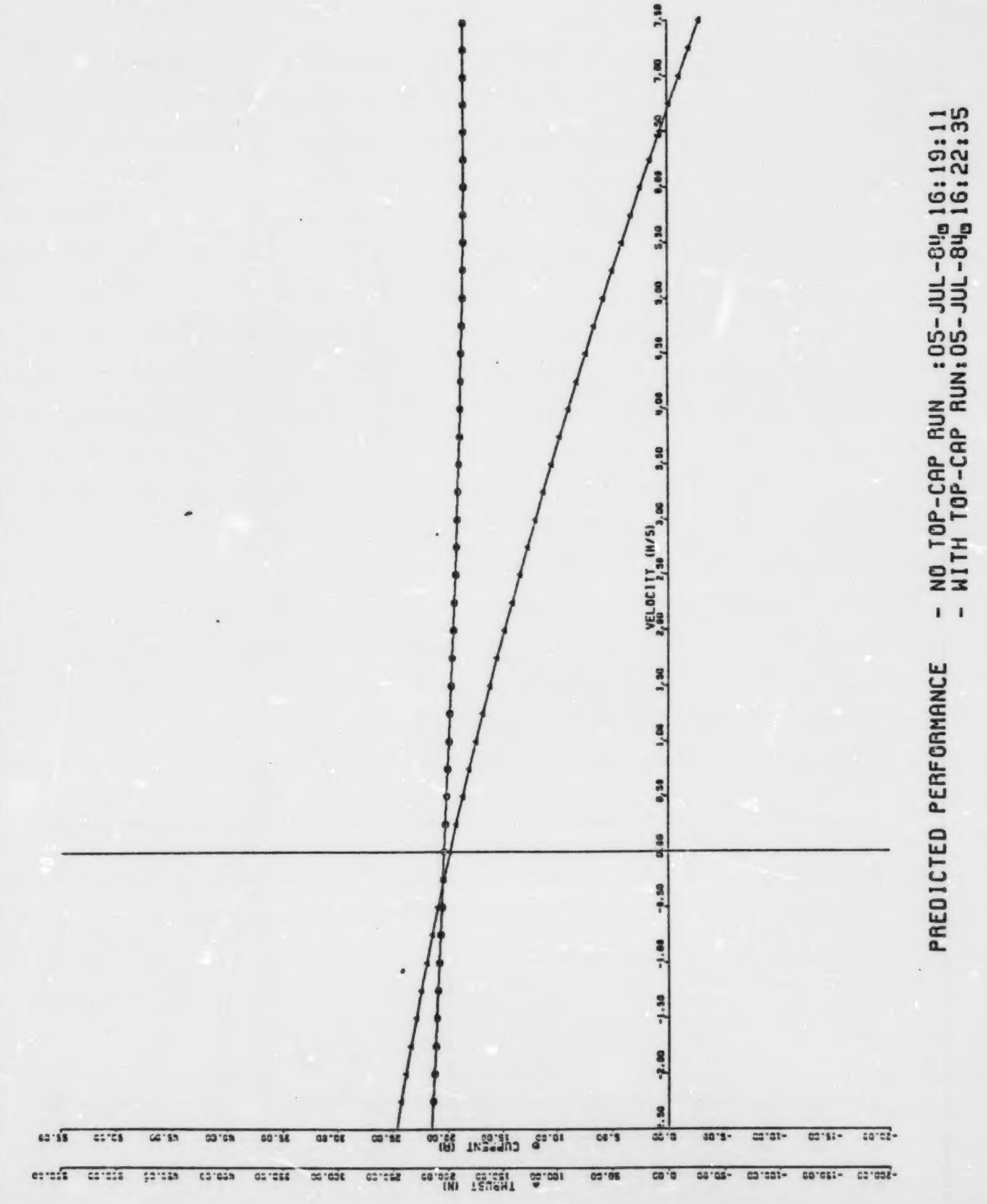

UTDC Research & Development Ltd.

Report No 453-570-001					
Project 60 Hz LIM	**Title** 60 Hz LIM Technology Final Report Appendix 3	**Date** 85.03.29	**Issue** 1	**Page** 10 of 29	
		By W.J.B.	**Appd** HHB		

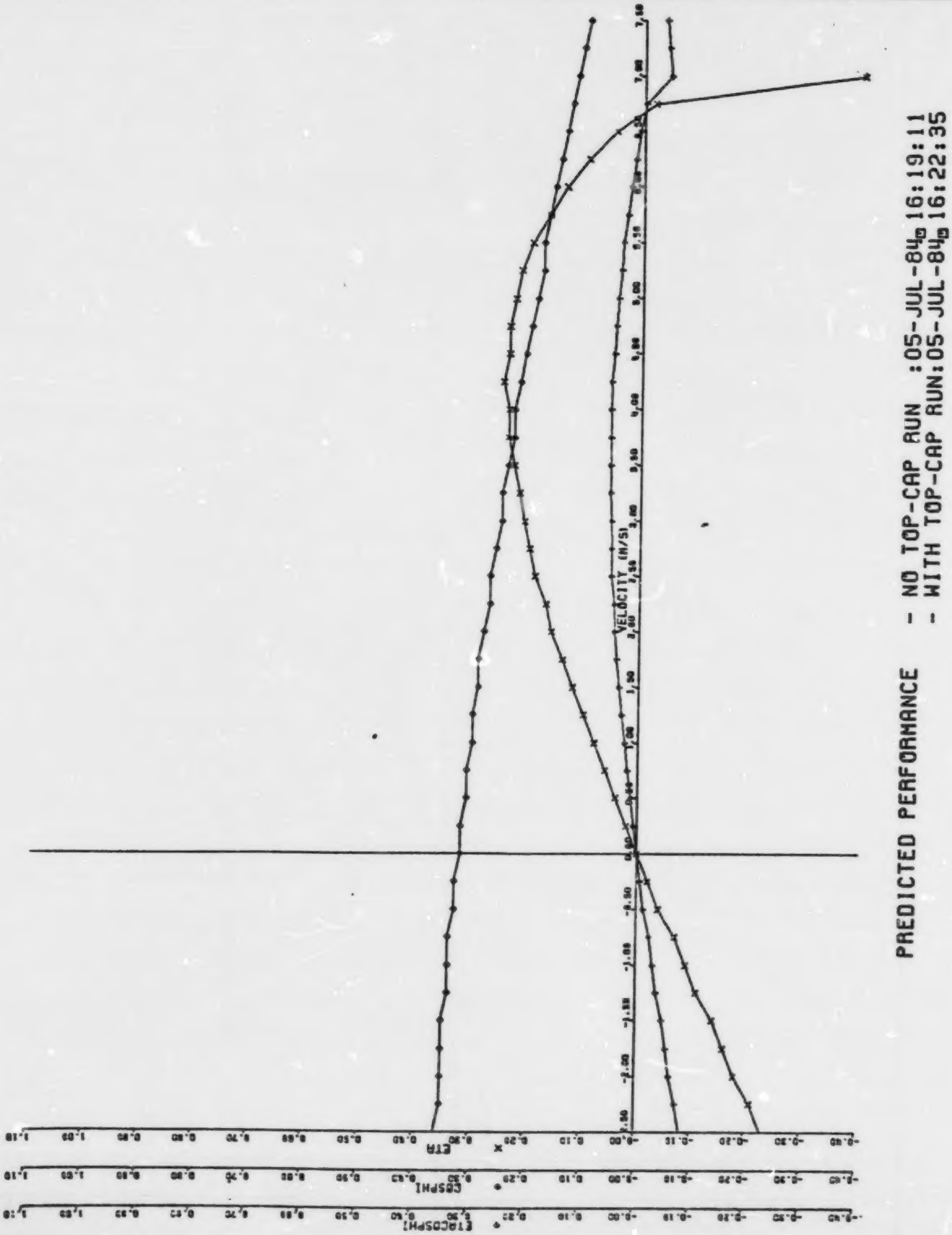

UTDC

UTDC Research & Development Ltd.

Report No	453-570-001			
Date	85.03.29	**Issue**	1	**Page** 11 of 29
Project	60 Hz LIM	**Title**	60 Hz LIM Technology Final Report Appendix 3	
By	W.J.B.	**Appd**	HHB	

```
                    60 Hz. PROGRAM -- STATIC TEST SERIES
                    ====================================

 TEST IDENTIFICATION -- RUN A (WITHOUT TOP-CAP): 27-JUN-8414:31:17
                        RUN B (WITH TOP-CAP)   : 27-JUN-8414:43:00

 TEST CONFIGURATION :  AIRGAP (MM)........... 10.76
                       TOP-CAP THICKNESS (MM)  5.00
                       CORE WIDTH (M)........  0.177
                       COIL PITCH (M)........  0.057
                       POLE PITCH (M)........  0.057
                       NO. OF POLES .........  6.0
                       TURNS PER COIL ....... 30.0
                       SLOT PITCH (MM)....... 19.00
                       LIM LENGTH (M)........ 0.394

 RESULTS FROM FSAP (FOURIER SPECTRUM ANALYSIS PROGRAM)
------------------------------------------------------------
          WITHOUT TOP-CAP                          WITH TOP-CAP
          ---------------                         ------------
CHAN      DC   FREQ    MAG     ANG            DC   FREQ    MAG     ANG

 1        0.0   0.0    0.0     0.0            0.0   0.0    0.0     0.0
 2        1.4  60.5   26.5   165.4            1.4  60.5   37.5  -169.4
 3        0.5  60.5   26.1   -70.4            0.6  60.5   36.6   -48.3
 4        1.1  60.5   25.1    45.2            1.0  60.5   37.2    68.3
 5        0.1  60.5  160.2    85.7            0.6  60.5  157.9   121.5
 6        0.9  60.5  151.4  -155.8            0.3  60.5  161.7  -118.1
 7        0.6  60.5  159.5   -36.0            0.6  60.5  163.6     0.8
 8        9.4   0.1   18.7     9.2          237.1   0.1  472.2     9.2

 EQUIVALENT CIRCUIT RESULTS
 ---------------------------

R1 : 0.545                R2 :  1.722            RM :  28.123
L1 : 0.000443             L2 : 0.001123          LM : 0.007682

 PERFORMANCE RESULTS
 --------------------
   PARAMETER                                     DERIVED FROM    DERIVED FROM
   ---------                                     MEASUREMENT   EQUIV. CIRCUIT
                                                 -----------   --------------
POSITIVE SEQUENCE - VOLTAGE (VOLTS).............113.9<   0.0  113.9<   0.0
                  - CURRENT (AMPS)............. 26.2< 291.2   26.2< -68.8
INPUT VA (VA)..................................  8957.4          8957.4
INPUT POWER (W)................................ 3237.6          3237.6
SECONDARY POWER (W)............................ 1808.8          1985.2
COPPER LOSSES (W).............................. 1123.4          1123.4
IRON LOSSES (W)................................  305.4           129.0
POWER FACTOR...................................    0.361           0.361
THRUST (N).....................................  237.1           287.7
```

UTDC Research & Development Ltd.

Project 60 Hz LIM	**Title** 60 Hz LIM Technology Final Report Appendix 3	**Report No** 453-570-001		
		Date 85.03.29	**Issue** 1	**Page** 12 of 29
		By W.J.B.	**Appd** HHB	

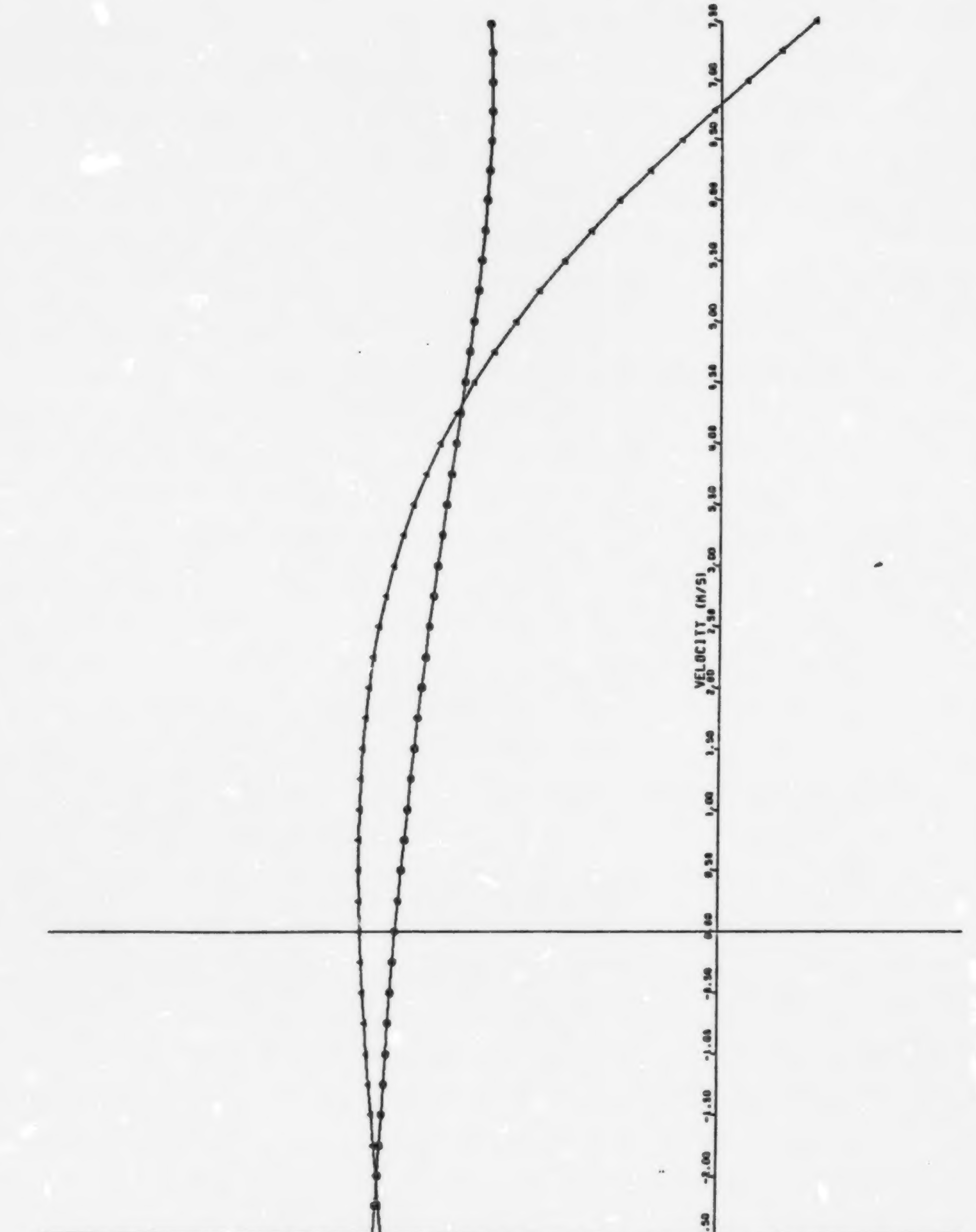

PREDICTED PERFORMANCE
- NO TOP-CAP RUN :27-JUN-84 14:31:17
- WITH TOP-CAP RUN:27-JUN-84 14:43:00

UTDC

UTDC Research & Development Ltd.

Project 60 Hz LIM	**Title** 60 Hz LIM Technology Final Report Appendix 3	**Report No** 453-570-001	
		Date 85.03.29	**Issue** 1
		Page 13 of 29	
		By W.J.B.	**Appd** HHB

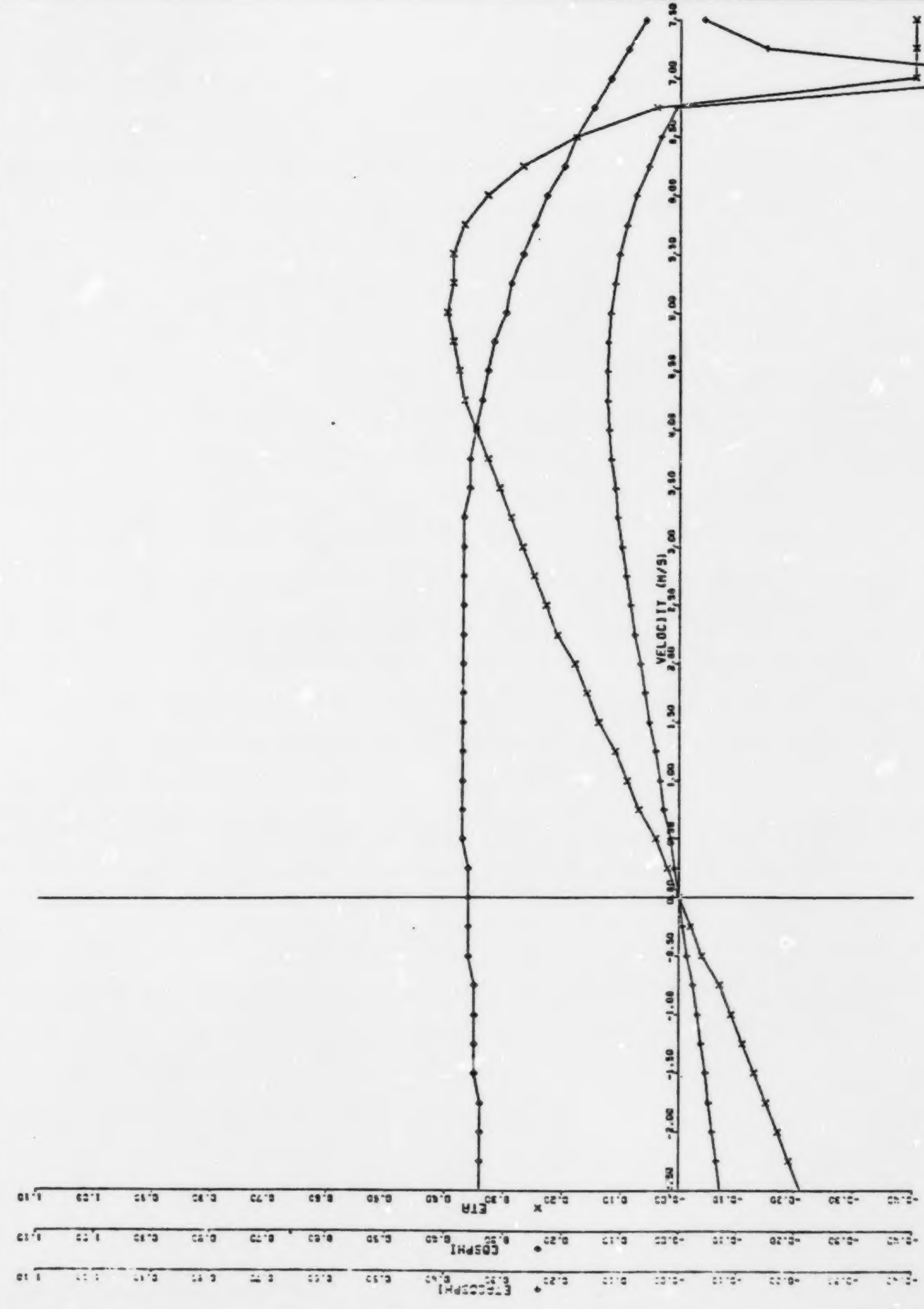

PREDICTED PERFORMANCE - NO TOP-CAP RUN :27-JUN-84 14:31:17
- WITH TOP-CAP RUN:27-JUN-84 14:43:00

```
                    60 Hz. PROGRAM -- STATIC TEST SERIES
                    ====================================

    TEST IDENTIFICATION -- RUN A (WITHOUT TOP-CAP): 26-JUN-8411:06:01
                           RUN B (WITH TOP-CAP)   : 26-JUN-8411:15:01

    TEST CONFIGURATION :  AIRGAP (MM)..........  9.22
                          TOP-CAP THICKNESS (MM)  3.00
                          CORE WIDTH (M).......  0.177
                          COIL PITCH (M).......  0.057
                          POLE PITCH (M).......  0.057
                          NO. OF POLES ........  6.0
                          TURNS PER COIL ...... 30.0
                          SLOT PITCH (MM)...... 19.00
                          LIM LENGTH (M)....... 0.394

   RESULTS FROM FSAP (FOURIER SPECTRUM ANALYSIS PROGRAM)
  -----------------------------------------------------

          WITHOUT TOP-CAP                         WITH TOP-CAP
          ---------------                         ------------
CHAN      DC  FREQ   MAG    ANG              DC  FREQ    MAG    ANG

  1      0.0   0.0   0.0     0.0            0.0   0.0    0.0    0.0
  2      1.5  60.5  26.0  -158.8            1.7  60.5   35.4   47.9
  3      0.6  60.5  25.7   -34.4            0.2  60.5   34.5  169.7
  4      0.9  60.5  24.6    81.1            1.1  60.5   34.7  -74.1
  5      0.6  60.5 163.5   120.9            1.2  60.5  159.3  -18.8
  6      0.4  60.5 166.3  -120.7            0.5  60.5  163.1  101.0
  7      0.7  60.5 162.8     0.0            1.1  60.5  165.7 -139.5
  8      0.3   0.1   0.6  -170.0          268.7   0.1  535.2    9.2

   EQUIVALENT CIRCUIT RESULTS
  ---------------------------

 R1 : 0.545              R2 :  2.142            RM :  33.129
 L1 : 0.000699           L2 : 0.000652          LM : 0.008120


   PERFORMANCE RESULTS
  --------------------
                                                DERIVED FROM   DERIVED FROM
     PARAMETER                                  MEASUREMENT    EQUIV. CIRCUIT
     ---------                                  -----------    --------------
 POSITIVE SEQUENCE - VOLTAGE (VOLTS)...........115.1<   0.0    115.1<   0.0
                   - CURRENT (AMPS)............ 24.7< -66.9     24.7< -66.9
 INPUT VA (VA).................................   8512.8          8512.8
 INPUT POWER (W)............................... 3333.8          3333.8
 SECONDARY POWER (W)........................... 2059.2          2195.3
 COPPER LOSSES (W).............................  994.6           994.6
 IRON LOSSES (W)...............................  280.0           143.9
 POWER FACTOR..................................    0.392           0.392
 THRUST (N)....................................  268.7           318.2
```

UTDC Research & Development Ltd.		Report No 453-570-001		
Project 60 Hz LIM	**Title** 60 Hz LIM Technology Final Report Appendix 3	**Date** 85.03.29	**Issue** 1	**Page** 15 of 29
		By W.J.B.	**Appd** HHB	

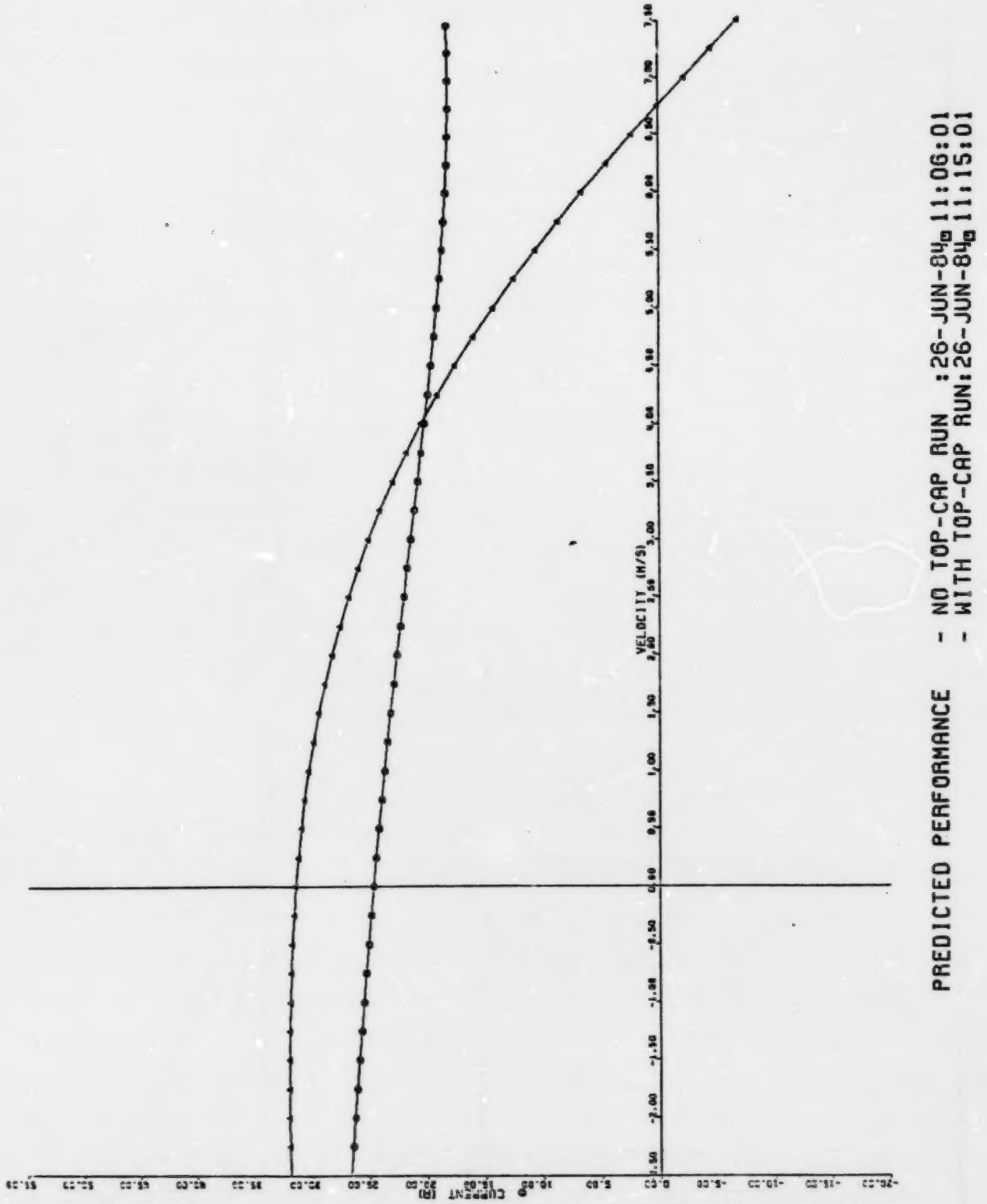

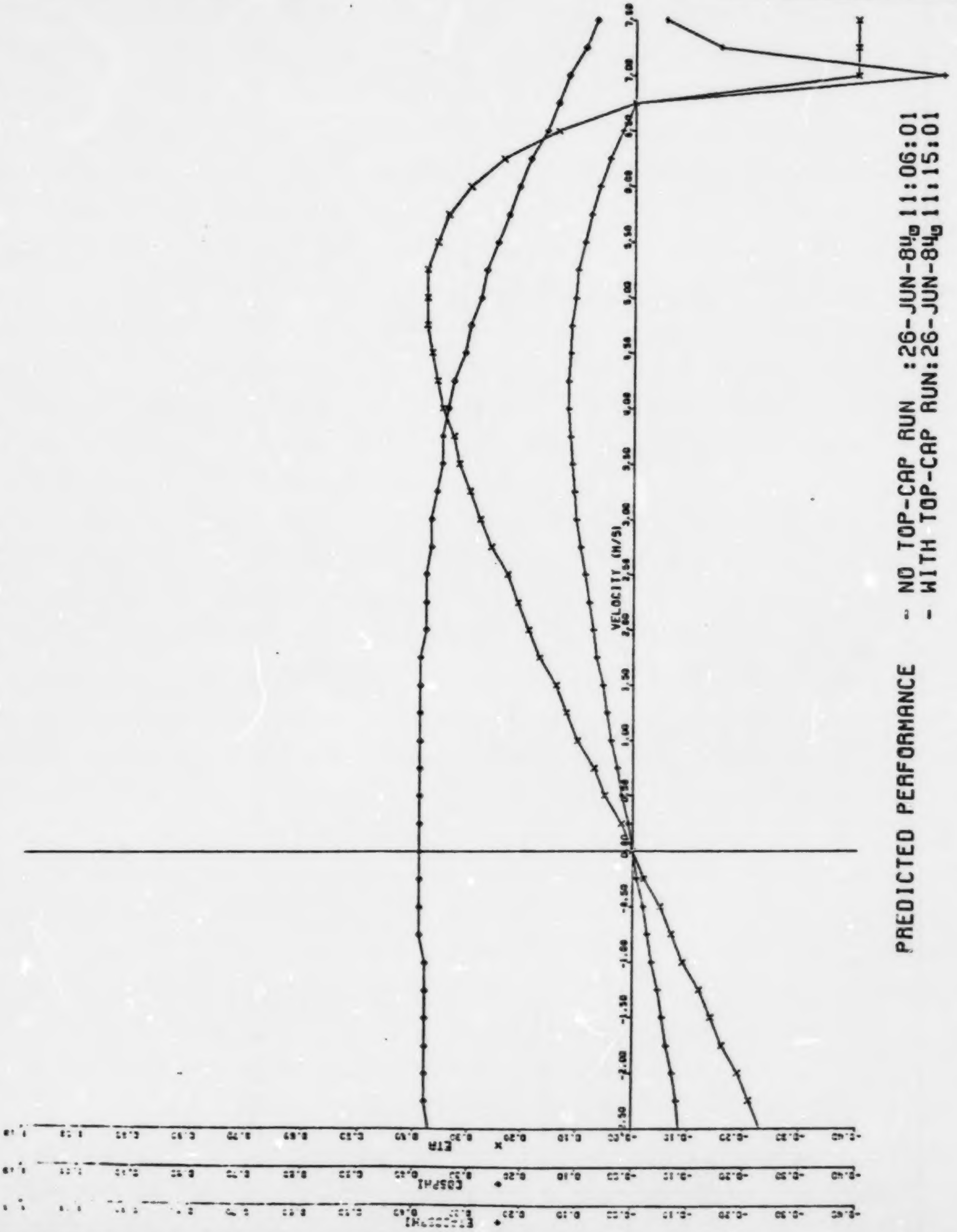
PREDICTED PERFORMANCE
- NO TOP-CAP RUN :26-JUN-84 11:06:01
- WITH TOP-CAP RUN:26-JUN-84 11:15:01
VELOCITY (M/S)
7.50
7.00
6.50
6.00
5.50
5.00
4.50
4.00
3.50
3.00
2.50
2.00
1.50
1.00
0.50
0.00
-0.50
-1.00
-1.50
-2.00
-2.50
× ETA
+ COSPHI
+ ETACOSPHI

UTDC Research & Development Ltd.

Project 60 Hz LIM	**Title** 60 Hz LIM Technology Final Report Appendix 3	**Report No** 453-570-001		
		Date 85.03.29	**Issue** 1	**Page** 17 of 29
		By W.J.B.	**Appd** HHB	

```
                    60 Hz. PROGRAM -- STATIC TEST SERIES
                    ====================================

     TEST IDENTIFICATION -- RUN A (WITHOUT TOP-CAP): 26-JUN-0414:18:29
                            RUN B (WITH TOP-CAP)   : 26-JUN-0414:49:00

     TEST CONFIGURATION :   AIRGAP (MM)..........  7.70
                            TOP-CAP THICKNESS (MM) 1.00
                            CORE WIDTH (M)........ 0.177
                            COIL PITCH (M)........ 0.057
                            POLE PITCH (M)........ 0.057
                            NO. OF POLES ......... 6.0
                            TURNS PER COIL ....... 30.0
                            SLOT PITCH (MM)....... 19.00
                            LIM LENGTH (M)........ 0.394

    RESULTS FROM FSAP (FOURIER SPECTRUM ANALYSIS PROGRAM)
    -----------------------------------------------------
            WITHOUT TOP-CAP
            ---------------                             WITH TOP-CAP
                                                        ------------
  CHAN      DC   FREQ    MAG     ANG              DC   FREQ    MAG     ANG

   1       0.0   0.0     0.0     0.0              0.0   0.0     0.0     0.0
   2       1.5  60.5    24.0   114.7              1.8  60.5    26.0   -22.1
   3       0.4  60.5    23.9  -119.9              0.3  60.5    26.3   100.1
   4       1.1  60.5    22.5    -4.6              0.9  60.5    26.2  -143.5
   5       0.0  60.5   164.2    35.5              0.4  60.5   161.4   -90.3
   6       1.1  60.5   164.6   152.9              0.7  60.5   164.1    29.4
   7       0.1  60.5   163.8   -86.5              1.4  60.5   164.6   148.2
   8       6.9   0.1    13.7     9.3            193.9   0.1   306.3     9.2
    EQUIVALENT CIRCUIT RESULTS
    --------------------------

  R1 : 0.557               R2 :  6.949            RM :  46.640
  L1 : 0.000065            L2 : 0.001487          LM : 0.010204

    PERFORMANCE RESULTS
    -------------------
      PARAMETER                                    DERIVED FROM     DERIVED FROM
      ---------                                    MEASUREMENT      EQUIV. CIRCUIT
                                                   -----------      --------------
  POSITIVE SEQUENCE - VOLTAGE (VOLTS)............115.5<   0.0     115.5<   0.0
                    - CURRENT (AMPS)............ 18.7< -69.1      18.7< -69.1
  INPUT VA (VA).................................   6478.6            6478.6
  INPUT POWER (W)............................... 2314.7            2314.7
  SECONDARY POWER (W)........................... 1464.7            1505.1
  COPPER LOSSES (W).............................  584.0             584.0
  IRON LOSSES (W)...............................  266.0             225.7
  POWER FACTOR..................................    0.357             0.357
  THRUST (N)....................................  193.9             218.2
```

UTDC Research & Development Ltd.

Report No 453-570-001			
Date 85.03.29	**Issue** 1	**Page** 18 of 29	
Project 60 Hz LIM	**Title** 60 Hz LIM Technology Final Report Appendix 3	**By** W.J.B.	**Appd** HHB

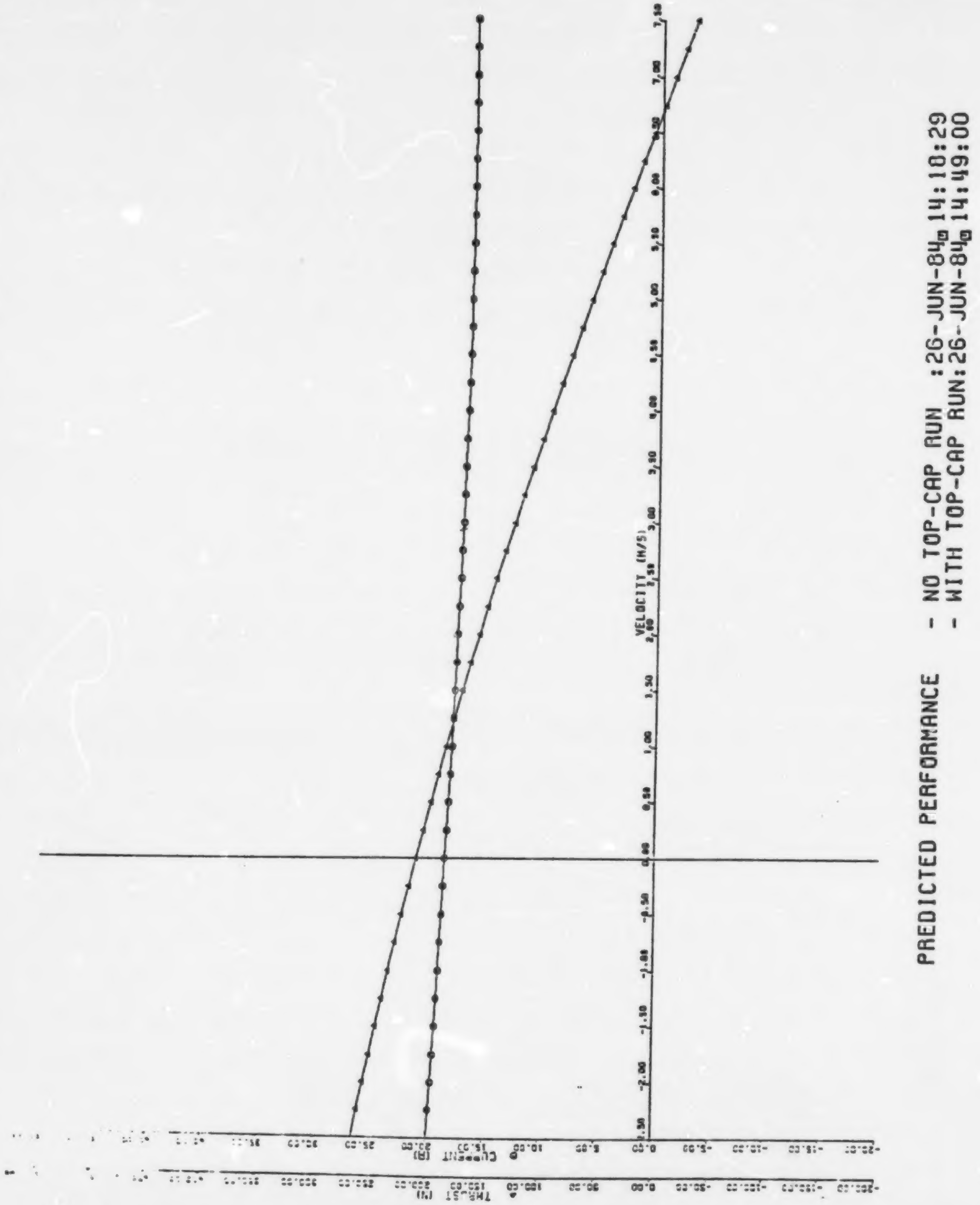

UTDC Research & Development Ltd.

Project 60 Hz LIM	**Title** 60 Hz LIM Technology Final Report Appendix 3	**Report No** 453-570-001		
		Date 85.03.29	**Issue** 1	**Page** 19 of 29
		By W.J.B.	**Appd** WJB	

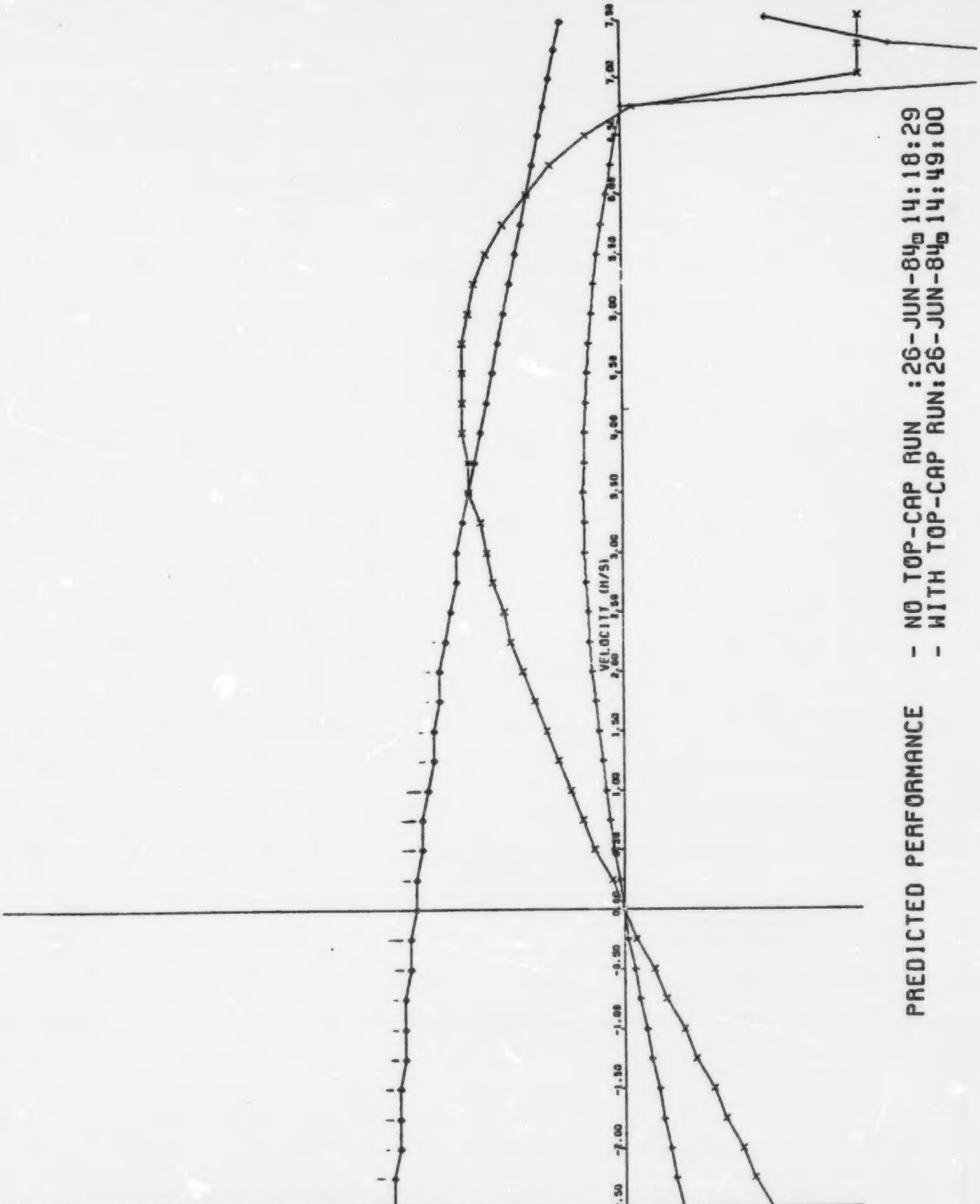

```
                    60 Hz. PROGRAM -- STATIC TEST SERIES
                    ====================================

TEST IDENTIFICATION -- RUN A (WITHOUT TOP-CAP): 25-JUL-8414:14:05
                       RUN B (WITH TOP-CAP)   : 25-JUL-8414:21:54

TEST CONFIGURATION :  AIRGAP (MM)........... 10.76
                      TOP-CAP THICKNESS (MM)  4.00
                      CORE WIDTH (M)........  0.177
                      COIL PITCH (M)........  0.076
                      POLE PITCH (M)........  0.114
                      NO. OF POLES .........  6.0
                      TURNS PER COIL ....... 16.0
                      SLOT PITCH (MM)....... 19.00
                      LIM LENGTH (M)........ 0.708

RESULTS FROM FSAP (FOURIER SPECTRUM ANALYSIS PROGRAM)
------------------------------------------------------------
          WITHOUT TOP-CAP                          WITH TOP-CAP
          ---------------                          ------------
CHAN      DC   FREQ    MAG     ANG            DC   FREQ    MAG     ANG

 1        0.0   0.0    0.0     0.0           0.0   0.0    0.0     0.0
 2        1.5  60.5   25.4  -137.1           2.0  60.5   66.1   -53.5
 3        0.3  60.5   25.1   102.9           0.0  60.5   61.9  -173.4
 4        1.2  60.5   26.3   -15.9           1.0  60.5   66.9    70.4
 5        0.8  60.5  158.0   139.0           0.1  60.5  157.5  -118.3
 6        0.0  60.5  160.0  -100.2           0.9  60.5  153.6     2.1
 7        0.6  60.5  164.6    18.9           1.2  60.5  160.7   122.3
 8        7.4   0.1   14.8  -170.8         241.9   0.1  481.6     9.1

EQUIVALENT CIRCUIT RESULTS
--------------------------

R1 : 0.339               R2 :  0.093          RM :  78.399
L1 : 0.003752            L2 : 0.002137        LM : 0.012717

PERFORMANCE RESULTS
--------------------
                                                DERIVED FROM    DERIVED FROM
   PARAMETER                                    MEASUREMENT     EQUIV. CIRCUIT
   ---------                                    -----------     --------------
POSITIVE SEQUENCE - VOLTAGE (VOLTS)...........111.2<   0.0    111.2<   0.0
                  - CURRENT (AMPS)............ 45.9< -65.9     45.9< -65.9
INPUT VA (VA)................................  15318.6          15318.6
INPUT POWER (W).............................. 6260.0           6260.0
SECONDARY POWER (W).......................... 3762.9           3973.1
COPPER LOSSES (W)............................ 2204.1           2204.1
IRON LOSSES (W)..............................  293.0             82.7
POWER FACTOR.................................   0.409            0.409
THRUST (N)...................................  241.9            287.9
SURFACE CURRENT DENSITY (AMPS/MM)............ 77.331           77.331
```

UTDC Research & Development Ltd.

Report No 453-570-001			
Date 85.03.29	**Issue** 1	**Page** 21 of 29	
Project 60 Hz LIM	**Title** 60 Hz LIM Technology Final Report Appendix 3	**By** W.J.B.	**Appd** HHB

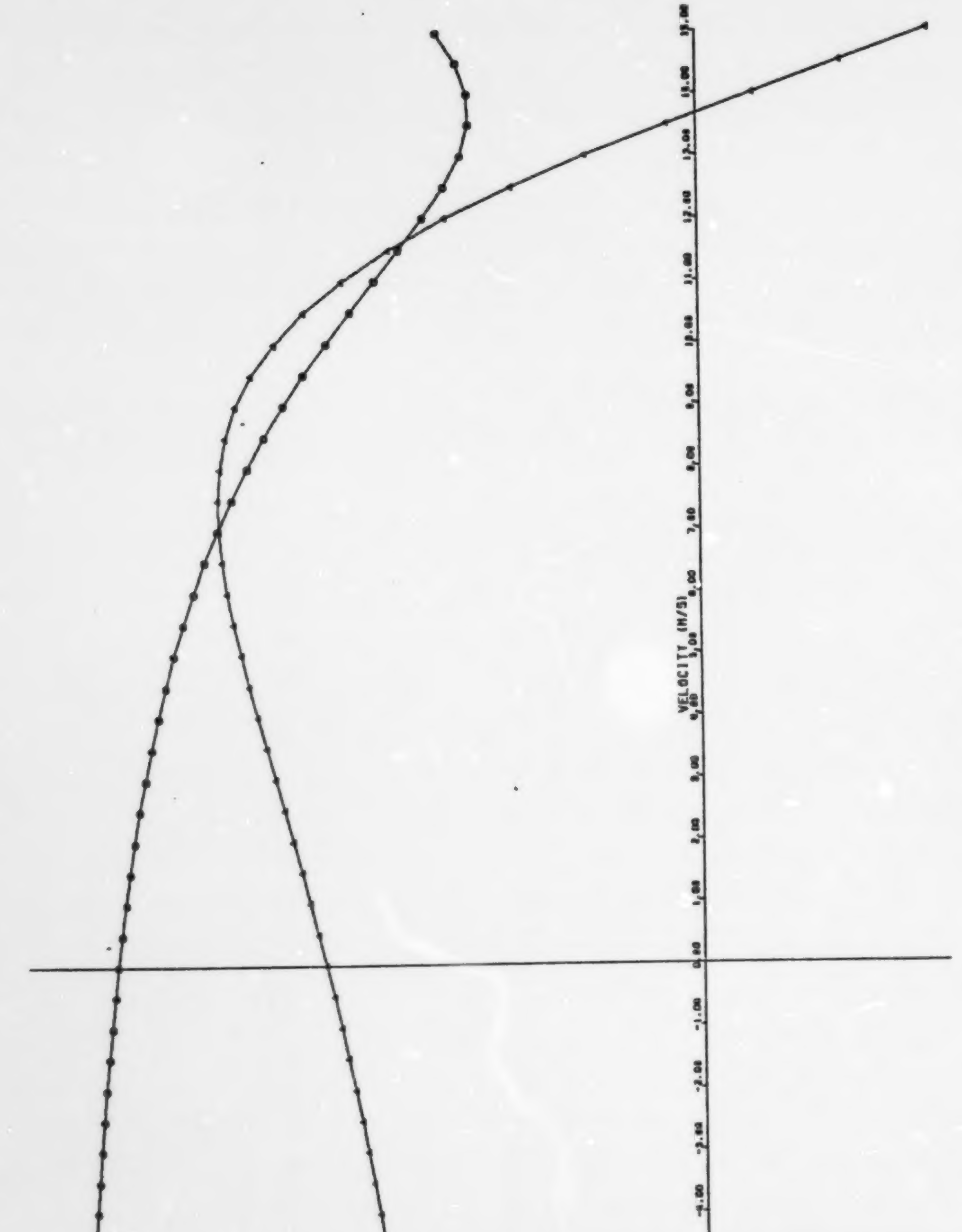

PREDICTED PERFORMANCE - NO TOP-CAP RUN :25-JUL-84 14:14:05
- WITH TOP-CAP RUN:25-JUL-84 14:21:54

UTDC Research & Development Ltd.

Project	Title	Report No		
60 Hz LIM	60 Hz LIM Technology Final Report Appendix 3	453-570-001		
		Date 85.03.29	**Issue** 1	**Page** 22 of 29
		By W.J.B.	**Appd** WJB	

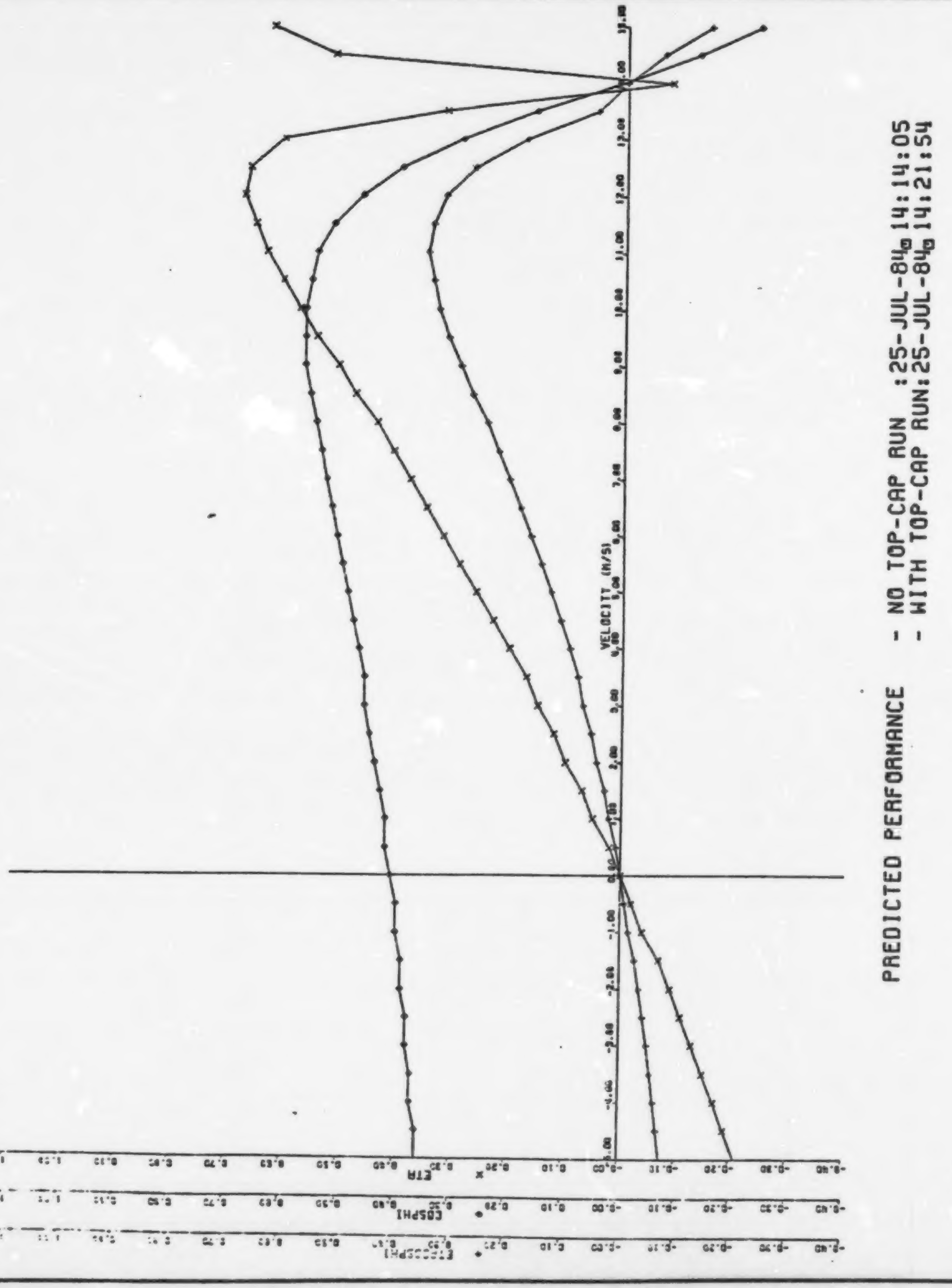

PREDICTED PERFORMANCE - NO TOP-CAP RUN :25-JUL-84 14:14:05
- WITH TOP-CAP RUN:25-JUL-84 14:21:54

```
                    60 Hz. PROGRAM -- STATIC TEST SERIES
                    ====================================

        IDENTIFICATION -- RUN A (WITHOUT TOP-CAP): 25-JUL-8414:30:23
                          RUN B (WITH TOP-CAP)   : 25-JUL-8414:39:20

      CONFIGURATION :  AIRGAP (MM)...........  9.22
                       TOP-CAP THICKNESS (MM)  3.20
                       CORE WIDTH (M)........  0.177
                       COIL PITCH (M)........  0.076
                       POLE PITCH (M)........  0.114
                       NO. OF POLES .........  6.0
                       TURNS PER COIL ....... 16.0
                       SLOT PITCH (MM)....... 19.00
                       LIM LENGTH (M)........ 0.780

   RESULTS FROM FSAP (FOURIER SPECTRUM ANALYSIS PROGRAM)
  -----------------------------------------------------
          WITHOUT TOP-CAP                       WITH TOP-CAP
          ---------------                       ------------
 CHAN     DC   FREQ   MAG    ANG              DC   FREQ   MAG    ANG

   1      0.0   0.0    0.0    0.0            0.0   0.0    0.0     0.0
   2      1.6  60.5   23.2   70.0            1.5  60.5   61.6    85.9
   3      0.5  60.5   22.8  -41.3            0.7  60.5   57.3   -34.4
   4      0.9  60.5   24.0 -160.1            0.7  60.5   61.7  -150.0
   5      1.1  60.5  157.0   -5.4            0.9  60.5  155.6    26.1
   6      0.8  60.5  160.2  115.0            1.0  60.5  152.1   146.0
   7      0.8  60.5  165.4 -125.8            0.2  60.5  160.1   -93.6
   8      0.2   0.2    0.3   13.1          307.6   0.1  612.6     9.2

   EQUIVALENT CIRCUIT RESULTS
  ---------------------------

 R1 : 0.350              R2 :  1.277           RM :  90.587
 L1 : 0.003467           L2 : 0.002410         LM : 0.014601


   PERFORMANCE RESULTS
  ---------------------                            DERIVED FROM    DERIVED FROM
     PARAMETER                                     MEASUREMENT     EQUIV. CIRCUIT
     ---------                                     -----------     --------------
 POSITIVE SEQUENCE - VOLTAGE (VOLTS)...........110.3<   0.0    110.3<   0.0
                   - CURRENT (AMPS)............ 42.6< -61.0     42.6< -61.0
 INPUT VA (VA)................................. 14074.4          14074.4
 INPUT POWER (W)............................... 6817.6           6817.6
 SECONDARY POWER (W)........................... 4641.1           4816.0
 COPPER LOSSES (W)............................. 1898.6           1898.6
 IRON LOSSES (W)...............................  270.0            103.1
 POWER FACTOR..................................   0.484            0.484
 THRUST (N)....................................  307.6            349.0
 SURFACE CURRENT DENSITY (AMPS/MM)............. 71.660            71.660
```

UTDC

UTDC Research & Development Ltd.

Project 60 Hz LIM	**Title** 60 Hz LIM Technology Final Report Appendix 3	**Report No** 453-570-001		
		Date 85.03.29	**Issue** 1	**Page** 24 of 29
		By W.J.B.	**Appd** HHB	

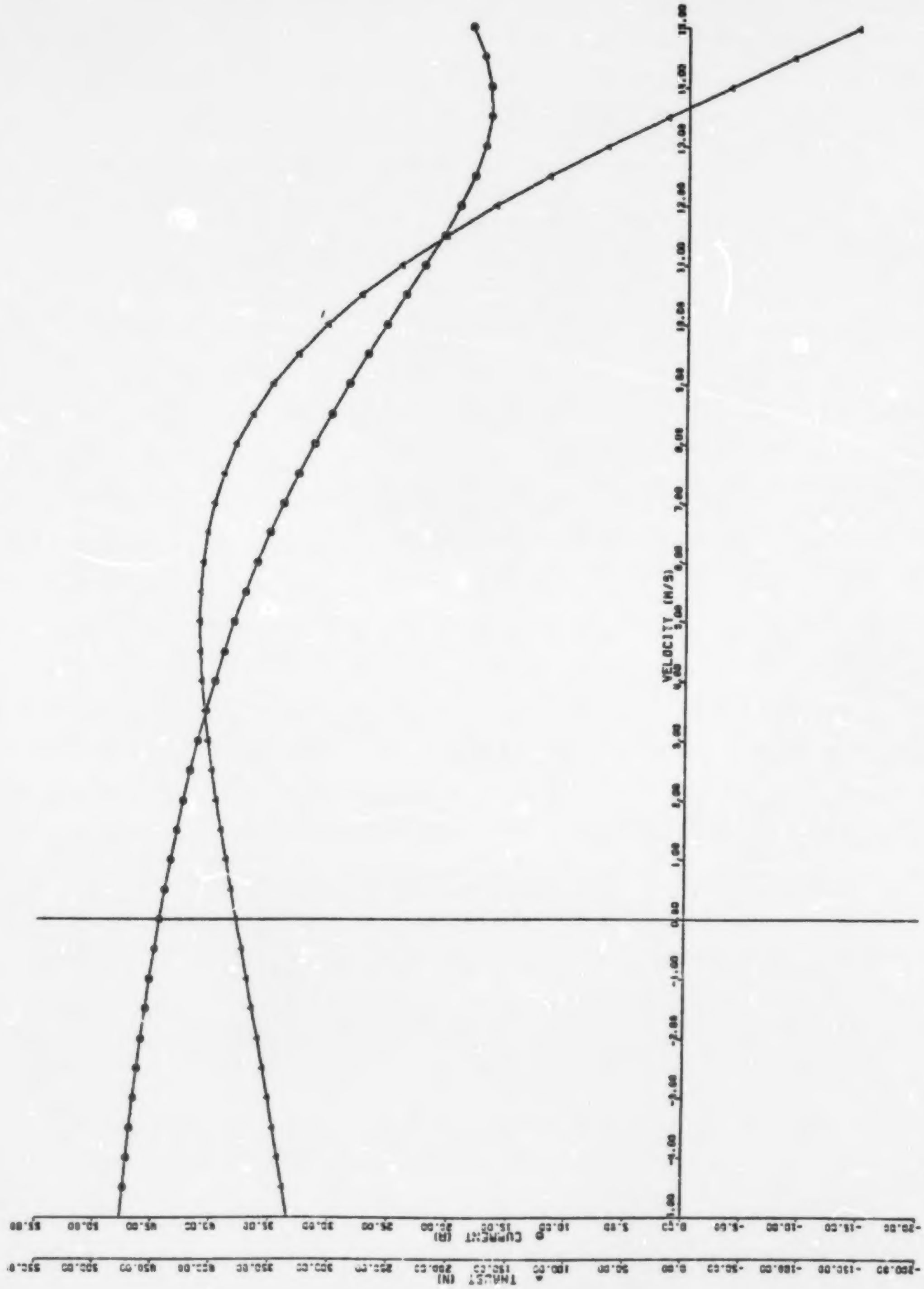

PREDICTED PERFORMANCE - NO TOP-CAP RUN :25-JUL-84□ 14:30:23
- WITH TOP-CAP RUN:25-JUL-84□ 14:39:20

UTDC Research & Development Ltd.		Report No 453-570-001		
		Date 85.03.29	Issue 1	Page 25 of 29
Project 60 Hz LIM	Title 60 Hz LIM Technology Final Report Appendix 3	By W.J.B.		Appd HHB

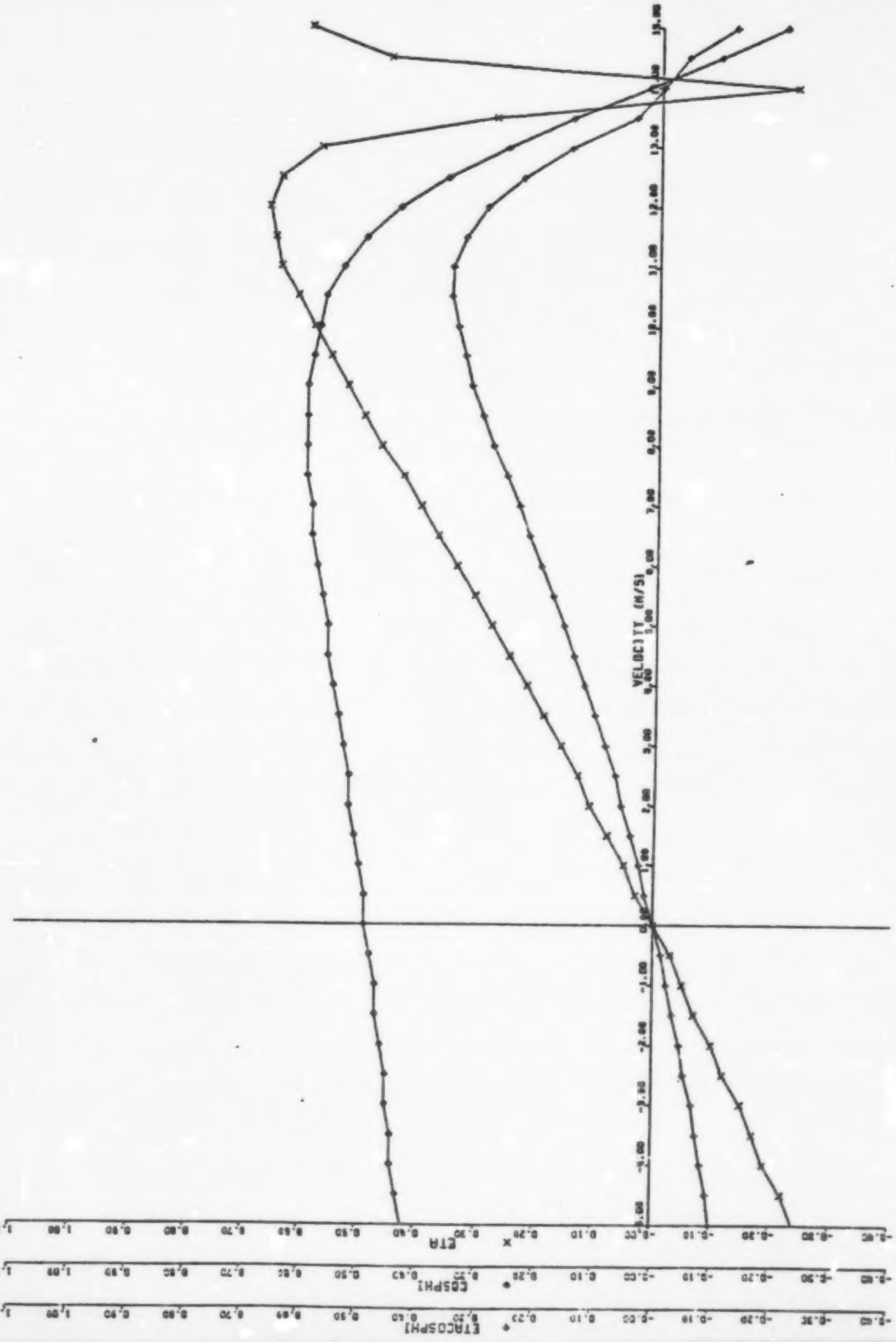

PREDICTED PERFORMANCE - NO TOP-CAP RUN :25-JUL-84 14:30:23
- WITH TOP-CAP RUN:25-JUL-84 14:39:20

```
                    60 Hz. PROGRAM -- STATIC TEST SERIES
                    ====================================

      TEST IDENTIFICATION -- RUN A (WITHOUT TOP-CAP): 25-JUL-8414:47:54
                             RUN B (WITH TOP-CAP)   : 25-JUL-8414:51:10

      TEST CONFIGURATION :  AIRGAP (MM)............  7.70
                            TOP-CAP THICKNESS (MM)  1.00
                            CORE WIDTH (M).........  0.177
                            COIL PITCH (M).........  0.076
                            POLE PITCH (M).........  0.114
                            NO. OF POLES ..........  6.0
                            TURNS PER COIL ....... 16.0
                            SLOT PITCH (MM)....... 19.00
                            LIM LENGTH (M)........ 0.788

      RESULTS FROM FSAP (FOURIER SPECTRUM ANALYSIS PROGRAM)
     ------------------------------------------------------
               WITHOUT TOP-CAP                          WITH TOP-CAP
              -----------------                        --------------
   CHAN       DC   FREQ   MAG    ANG             DC   FREQ    MAG     ANG

    1        0.0   0.0    0.0     0.0            0.0   0.0    0.0     0.0
    2        1.6  60.5   20.6    62.2            1.4  60.5   39.0   137.9
    3        0.5  60.5   20.3   -57.5            0.6  60.5   36.9    18.4
    4        0.9  60.5   21.3   183.6            1.0  60.5   39.9   -98.5
    5        1.1  60.5  157.4   -21.7            0.1  60.5  157.5    87.9
    6        0.4  60.5  160.2    98.7            0.8  60.5  154.3  -151.3
    7        1.0  60.5  164.9  -142.0            0.6  60.5  160.4   -31.5
    8        1.9   0.1    3.9  -172.4          313.8   0.1  624.9     9.3

      EQUIVALENT CIRCUIT RESULTS
     ---------------------------

   R1 : 0.350               R2 :  3.919           RM : 107.936
   L1 : 0.002889            L2 : 0.003286         LM : 0.017391

      PERFORMANCE RESULTS
     ---------------------                              DERIVED FROM    DERIVED FROM
        PARAMETER                                       MEASUREMENT    EQUIV. CIRCUIT
        ---------                                       -----------    --------------
   POSITIVE SEQUENCE - VOLTAGE (VOLTS)...........111.3<   0.0   111.3<   0.0
                     - CURRENT (AMPS)............ 27.3< -51.0    27.3< -51.0
   INPUT VA (VA).................................   9112.1          9112.1
   INPUT POWER (W)............................... 5734.6          5734.6
   SECONDARY POWER (W)........................... 4690.7          4762.1
   COPPER LOSSES (W).............................  782.0           782.0
   IRON LOSSES (W)...............................  261.9           190.5
   POWER FACTOR..................................   0.629           0.629
   THRUST (N)....................................  313.0           345.1
   SURFACE CURRENT DENSITY (AMPS/MM)............. 45.962          45.962
```

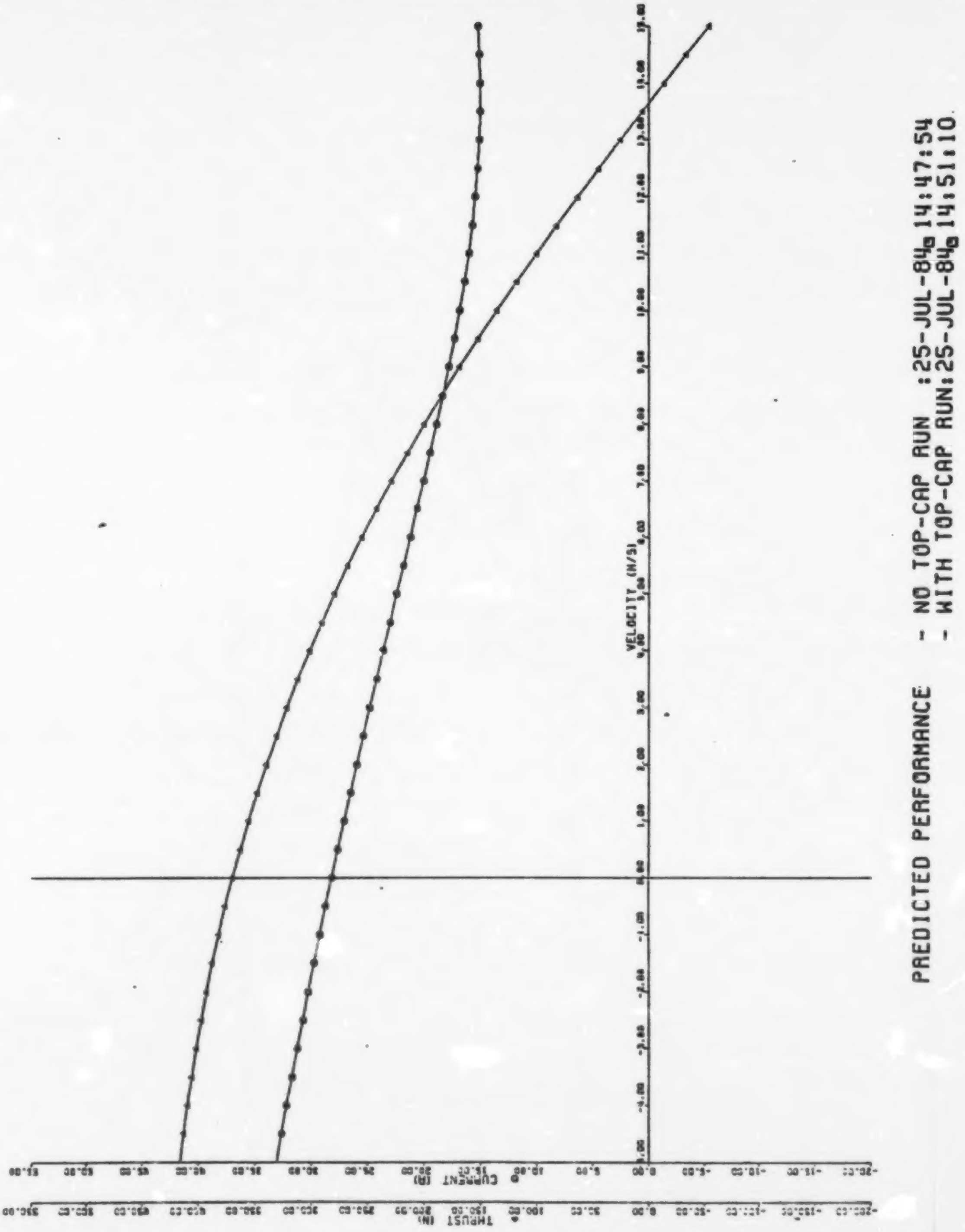
PREDICTED PERFORMANCE - NO TOP-CAP RUN :25-JUL-84 14:47:54
- WITH TOP-CAP RUN:25-JUL-84 14:51:10
VELOCITY (M/S)
-5.00
-4.00
-3.00
-2.00
-1.00
0.00
1.00
2.00
3.00
4.00
5.00
6.00
7.00
8.00
9.00
10.00
11.00
12.00
13.00
14.00
15.00
● CURRENT (A)
-20.00
-15.00
-10.00
-5.00
0.00
5.00
10.00
15.00
20.00
25.00
30.00
35.00
40.00
45.00
50.00
55.00
◆ THRUST (N)
-200.00
-150.00
-100.00
-50.00
0.00
50.00
100.00
150.00
200.00
250.00
300.00
350.00
400.00
450.00
500.00
550.00

UTDC Research & Development Ltd.

Project 60 Hz LIM	**Title** 60 Hz LIM Technology Final Report Appendix 3	**Report No** 453-570-001		
		Date 85.03.29	**Issue** 1	**Page** 28 of 29
		By W.J.B.	**Appd** IHHB	

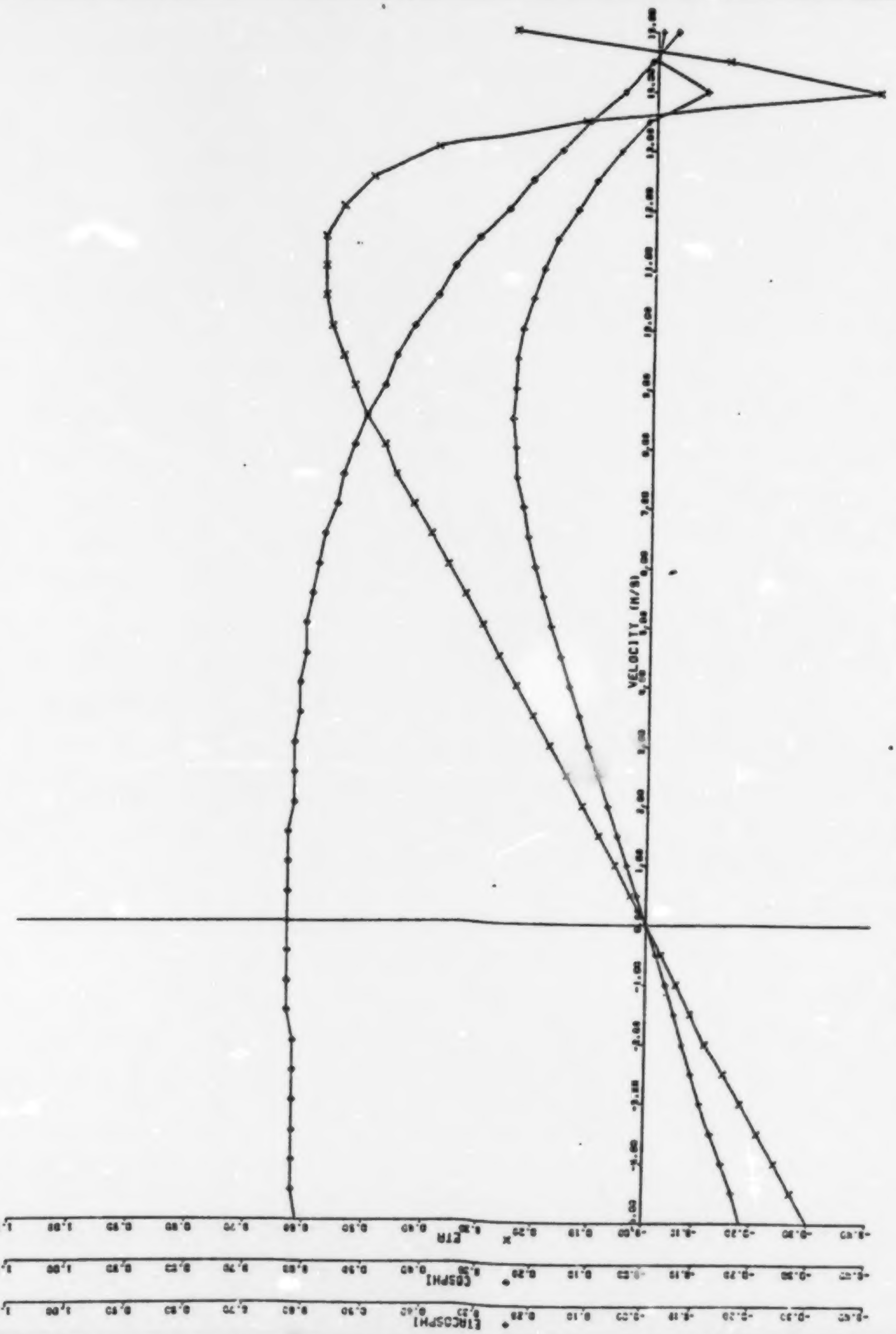

PREDICTED PERFORMANCE - NO TOP-CAP RUN :25-JUL-84 14:47:54
- WITH TOP-CAP RUN:25-JUL-84 14:51:10

UTDC Research & Development Ltd.

Project 60 Hz LIM	**Title** 60 Hz LIM Technology Final Report Appendix 3	**Report No** 453-570-001			
		Date 85.03.29	**Issue** 1	**Page** 29 of 29	
		By W.J.B.	**Appd** HHB		

UTDC Research & Development Ltd.

Report No 453-570-001				
Date 85.03.29	**Issue** 1	**Page** 1 of 17		
Project 60 Hz LIM	**Title** 60 Hz LIM Technology Final Report Appendix 4	**By** W.J.B.	**Appd** HHB	

APPENDIX 4

LIM-BASED CONTROL SYSTEM MODEL

1.0 INTRODUCTION

Typical motion control problems in which LIMs are employed as actuators include speed regulation, speed profile following, and stop-positioning. The design of suitable control systems is made simpler if a system model and computer solution technique are available. Presented here is a fairly complete model of a LIM-based motion-control system. The techniques used in formulating the model and solving the resulting equations are very powerful and may be used to create even more sophisticated systems than the ones considered here.

2.0 BACKGROUND

The so-called "Classical Control Theory" restricts itself to systems in which the physical behaviour can be described by linear, non-time-varying equations. Often, especially in stability analysis, it is valid to "linearize" the system equations for a restricted operating range so that classical techniques can be employed.

If it is required to predict the time response of a system over a large operating range, classical analysis is seldom useful. Most practical systems exhibit behaviour which, mathematically speaking, is both "non-linear" and "time varying". LIM-based motion control systems are no exception: Load and drag variations, the LIM thrust characteristic, and the nature of practical sensing systems are non-linear effects which must be included in the system model.

A useful approach to formulating and solving models of non-linear systems is to adopt the state-variable representation in conjunction with a time-step integration solution method. In this scheme, a system is described with matrices and vectors. The matrix coefficients are based on system properties such as vehicle mass, gain constants, time constants, thrust-speed relationships, etc. The vectors represent: i) the system states (response variables); and ii) the system inputs (forcing variables).

2.1 SOLVING NON-LINEAR EQUATIONS

A system which has been expressed in the State-Variable form is really a set of linear first-order differential equations. These may be solved numerically over small time increments to determine how the system behaves over time.

A typical form of "non-linearity" which can occur in a system is that some system property is not constant, but varies with one or more of the system states.

An example of this type of non-linearity is the function which relates LIM thrust to the applied voltage. The function is both voltage and speed dependent, and the dependencies are not the same for motoring and braking modes.

In this example the non-linear nature is handled by updating the associated system matrix coefficient at every time step to reflect the changes that have occurred in the speed and voltage states.

The form of non-linearity described in the preceeding example is due to the physical nature of the LIM, and results in state-dependent system properties. Another form of non-linearity may be the result of a logic process which is designed into the system. For example, in sensing vehicle speed, a microprocessor-based technique is often employed: The elapsed time between detections occurring at a fixed known distance is used to initiate a digital speed calculation. The resulting "speed", which will possibly be used as a feedback quantity in the control system, is not linearly related to the actual instantaneous speed.

If we desire to do so, it may be possible to arrive at some kind of non-linear, speed dependent function which relates sensed speed to actual speed. The value of this function at any given time instant would be reflected in the system matrix coefficients just as in the previous example.

A better way to handle non-linearities imposed by a logic process is to "imitate" that process in the computer while the time-step numerical solution of the equations is proceeding. This approach is known as simulation and can be used to model many effects which are not easily handled using analytical functions.

Our control system model, then, will consist of a set of first-order, non-linear differential equations which are solved by a time-step integration method. Superimposed on the time-step solution process, we may wish to introduce one or more logic processes which simulate the behaviour of real system elements or processes. The following sections develop such a model as an example of the approach.

3.0 ASSUMED CONFIGURATION

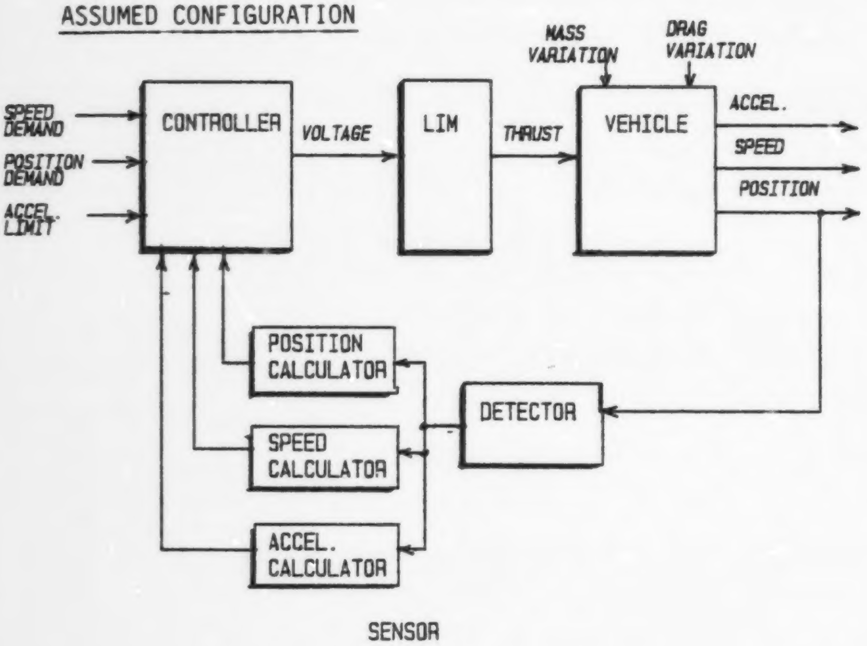
MASS VARIATION
DRAG VARIATION
SPEED DEMAND
POSITION DEMAND
ACCEL. LIMIT
CONTROLLER
VOLTAGE
LIM
THRUST
VEHICLE
ACCEL.
SPEED
POSITION
POSITION CALCULATOR
SPEED CALCULATOR
ACCEL. CALCULATOR
DETECTOR
SENSOR

FIGURE A5-1

3.1 LIM TRANSFER FUNCTION

3.1.1 Steady State Characteristics (Ref. Fig. A5.2)

A LIM will exhibit some characteristic thrust vs. speed relationship for a given voltage. As the voltage is changed, every point on the characteristic curve will change as the square of the voltage (assuming no magnetic saturation). If the voltage phase sequence is reversed, the thrust versus speed curve changes form, but the "voltage squared" relationship still holds. We can describe the voltage/speed/thrust relationship by two equations:

$$F = V^2 (a_0 + a_1 v + a2v2 + a3v3) \text{ (motoring)}$$

UTDC Research & Development Ltd.

Report No 453-570-001			
Project 60 Hz LIM	**Title** 60 Hz LIM Technology Final Report Appendix 4	**Date** 85.03.29	**Issue** 1
		Page 6 of 17	
		By W.J.B.	**Appd** HHB

a) LIM FUNCTIONAL DIAGRAM:

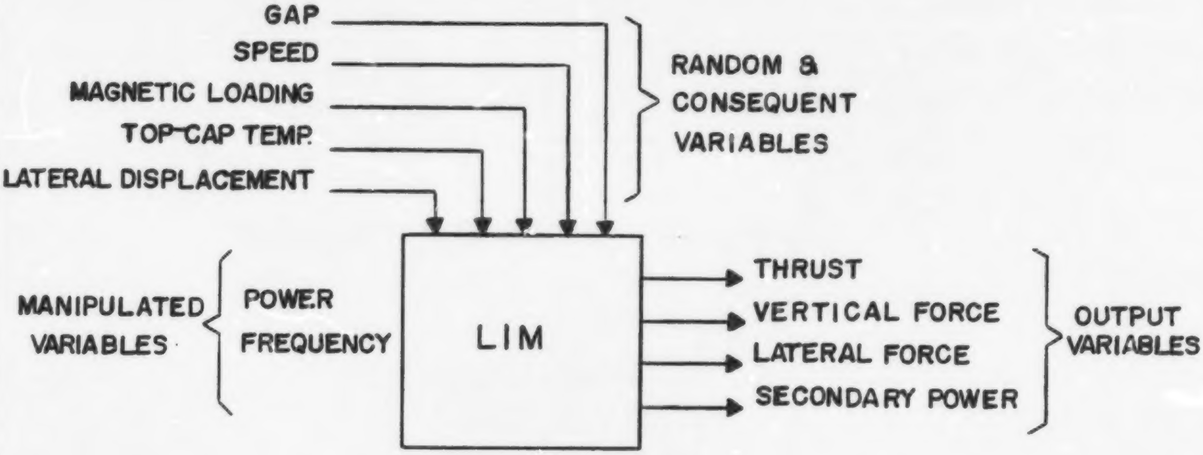
GAP
SPEED
MAGNETIC LOADING
TOP-CAP TEMP.
LATERAL DISPLACEMENT
RANDOM & CONSEQUENT VARIABLES
MANIPULATED VARIABLES
POWER
FREQUENCY
LIM
THRUST
VERTICAL FORCE
LATERAL FORCE
SECONDARY POWER
OUTPUT VARIABLES

b) SIMPLIFIED FUNCTIONAL DIAGRAM:

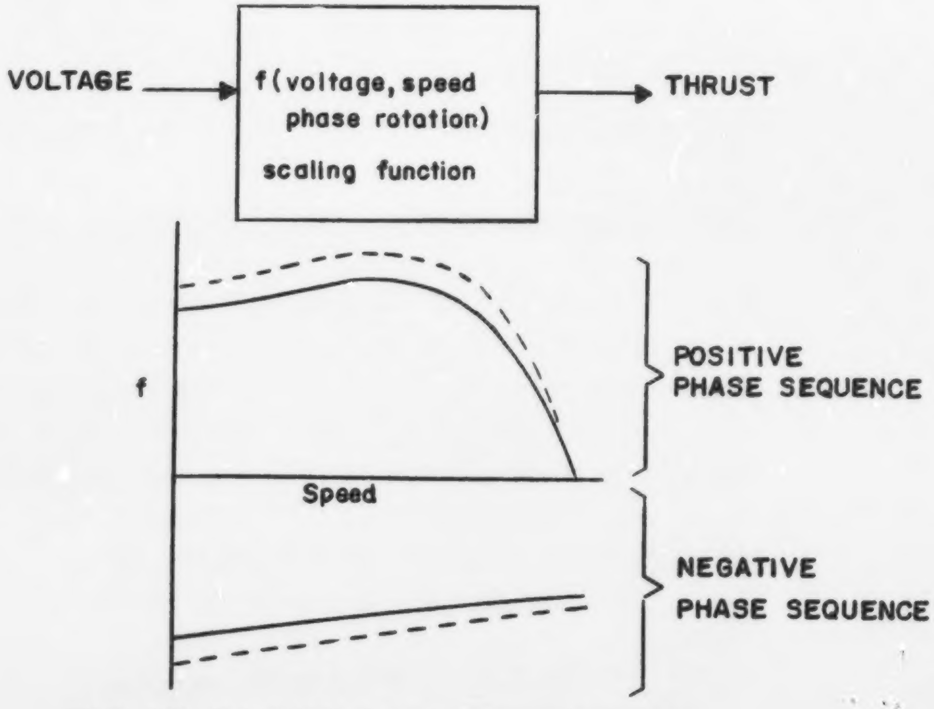
VOLTAGE
f (voltage, speed phase rotation)
scaling function
THRUST
f
Speed
POSITIVE PHASE SEQUENCE
NEGATIVE PHASE SEQUENCE

FIG. A5-2: LIM CHARACTERISTICS

$$F = -V^2 (a_0 + b_1 v + b_2 v^2) \qquad \text{(braking)}$$

Where F = thrust
V = voltage
v = speed
a, b = Polynomial coefficients

The polynomial relationships are an approximate representation of the thrust curve but are suitable in most cases. More sophisticated curve-fitting functions could be employed if required.

3.1.2 Transient Characteristics

Though in many applications LIM thrust may be considered to respond instantaneously to applied voltage, the physical system does exhibit a characteristic delay. We assume this is to be first-order with time constant .

The overall transfer function, written in terms of the Laplace operator, s, becomes:

$$V \longrightarrow \boxed{\frac{f_{LM}}{1 + s\tau_L}} \longrightarrow F \qquad \text{(motoring)}$$

$$V \longrightarrow \boxed{\frac{f_{LB}}{1 + s\tau_L}} \longrightarrow F \qquad \text{(braking)}$$

Where $f_{LM} = V(a_0 + a_1 v + \ldots)$

$f_{LB} = V(a_0 + b_1 v + \ldots)$

3.1.3 Controller Transfer Function

Typically, induction motor voltage controllers are designed to supply an output voltage (3-phase) proportional to a dc input signal. The polarity of the input signal determines the phase sequence (A, B, C or A, C, B) of the 3-phase output, so that a positive control signal would result in motoring action and a negative control signal would result in braking action.

In general we should assume the voltage controller has a transient characteristic, and so we introduce a voltage controller time constant .

We may wish to add a proportional-integral stage to the basic voltage controller. We assume adjustable gain factors k_p and k_i for the "proportional" and "integral" functions respectively. Control inputs and feedback inputs are compared with difference amplifiers. The completed transfer function is:

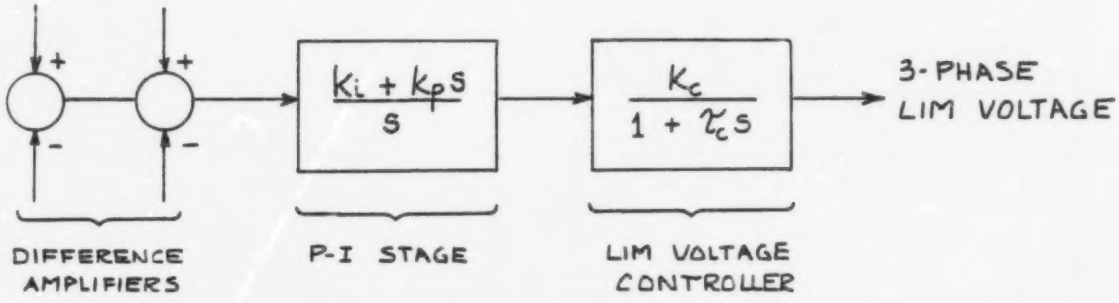

3.1.4 Vehicle Transfer Function

A very simple vehicle model, with longitudinal freedom only, is sufficient for most analyses. We assume that the LIM force acts to accelerate the vehicle mass, m, and to overcome the drag, d. Note that d need not be constant, and in the complete model formulation could be made dependent on velocity according to any desired relationship.

The transfer function is:

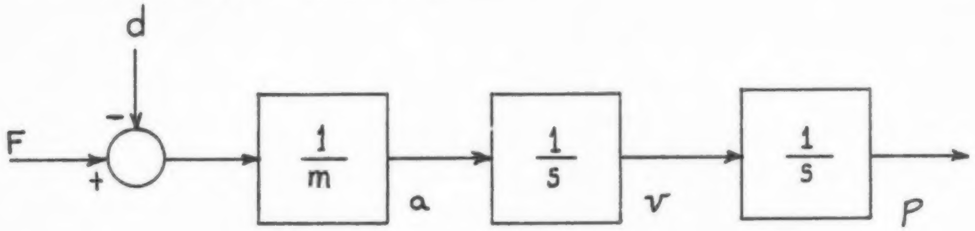

F = LIM thrust
d = drag
m = mass
a = acceleration
v = velocity
p = position

3.1.5 Overall System Block Diagram

See Figure A5-4.

3.1.6 Signal Flow Graph

See Figure A5-5.

3.1.7 System State Equations

See Figure A5-6.

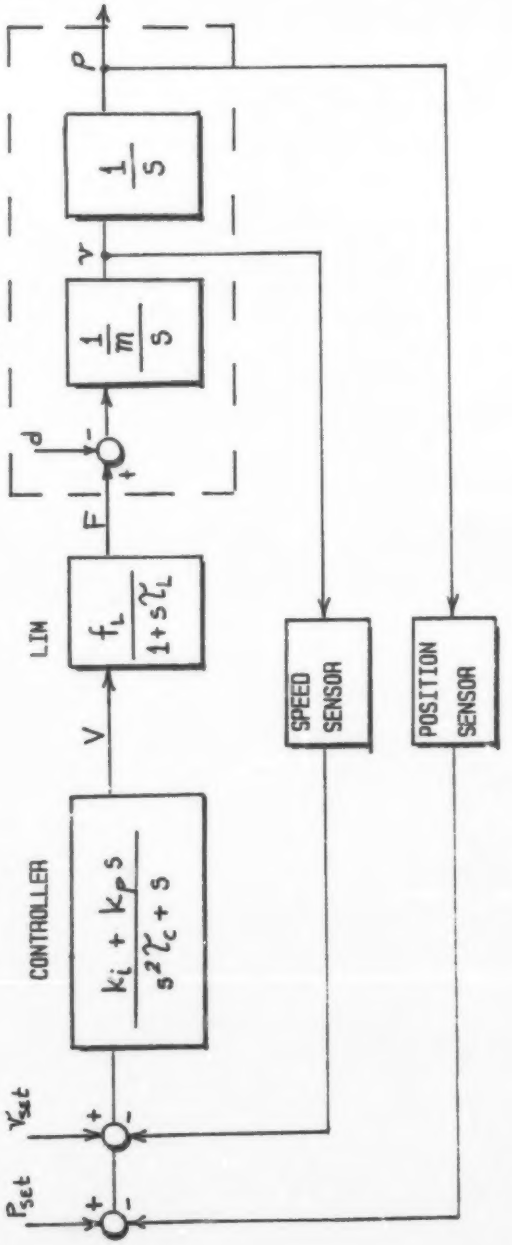
VEHICLE
P
$\frac{1}{s}$
v
$\frac{\frac{1}{m}}{s}$
d
$-$
$+$
F
LIM
$\frac{f_L}{1+s\tau_L}$
V
CONTROLLER
$\frac{k_i + k_p s}{s^2\tau_c + s}$
SPEED SENSOR
POSITION SENSOR
v_{set}
P_{set}
$+$
$-$

A5-4 OVERALL SYSTEM BLOCK DIAGRAM

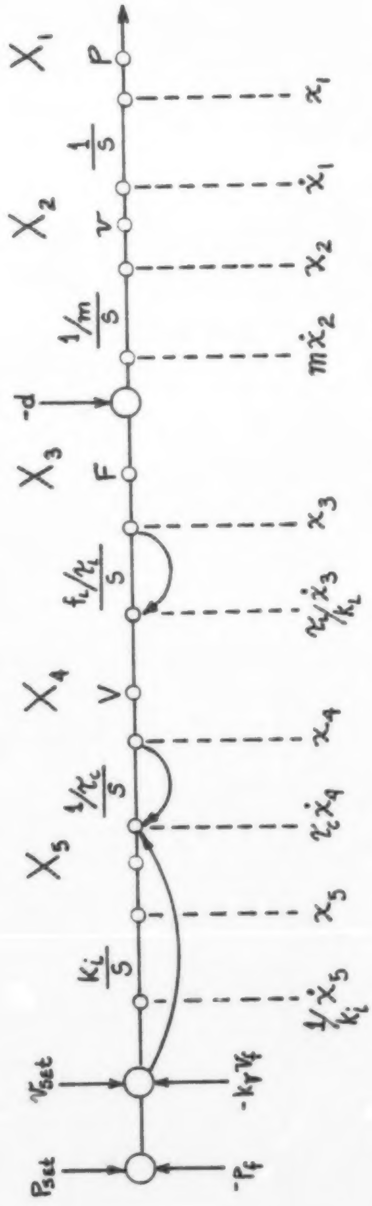
X_1
P
x_1
$\frac{1}{s}$
$\dot{x}_1$
X_2
v
x_2
$\frac{1/m}{s}$
$m\dot{x}_2$
$-d$
X_3
F
x_3
$\frac{f_L/\tau_L}{s}$
$\tau_L\dot{x}_3/k_L$
X_4
V
x_4
$\frac{1/\tau_c}{s}$
$\tau_c\dot{x}_4$
X_5
x_5
$\frac{k_i}{s}$
$\frac{1}{k_i}\dot{x}_5$
v_{set}
$-k_v v_f$
P_{set}
$-P_f$

A5-5 SIGNAL FLOW GRAPH

$$\dot{x}_1 = x_2$$

$$\dot{x}_2 = \frac{1}{m}(x_3 - d)$$

$$\dot{x}_3 = \frac{f_L}{\tau_L}\left(x_4 - x_3/f_L\right)$$

$$\dot{x}_4 = \frac{1}{\tau_c}\left(-x_4 + k_p\left(v_{set} + p_{set} - p_f - k_v v_f\right) + x_5\right)$$

$$\dot{x}_5 = k_i\left(v_{set} + p_{set} - p_f - k_v v_f\right)$$

$$\begin{Bmatrix} \dot{x}_1 \\ \dot{x}_2 \\ \dot{x}_3 \\ \dot{x}_4 \\ \dot{x}_5 \end{Bmatrix} = \begin{bmatrix} 0 & 1 & 0 & 0 & 0 \\ 0 & 0 & 1/m & 0 & 0 \\ 0 & 0 & -1/\tau_L & f_L/\tau_L & 0 \\ 0 & 0 & 0 & -1/\tau_c & 1/\tau_c \\ 0 & 0 & 0 & 0 & 0 \end{bmatrix} \begin{Bmatrix} x_1 \\ x_2 \\ x_3 \\ x_4 \\ x_5 \end{Bmatrix} + \begin{bmatrix} 0 & 0 & 0 & 0 & 0 \\ 0 & 0 & 0 & 0 & -1/m \\ 0 & 0 & 0 & 0 & 0 \\ k_p/\tau_c & k_p/\tau_c & -k_p/\tau_c & -k_p/\tau_c & 0 \\ k_i & k_i & -k_i & -k_i & 0 \end{bmatrix} \begin{Bmatrix} p_{set} \\ v_{set} \\ p_f \\ k_v v_f \\ d \end{Bmatrix}$$

UTDC Research & Development Ltd.

Report No 453-570-001			
Date 85.03.29	**Issue** 1	**Page** 13 of 17	
Project 60 Hz LIM	**Title** 60 Hz LIM Technology Final Report Appendix 4	**By** W.J.B.	**Appd**

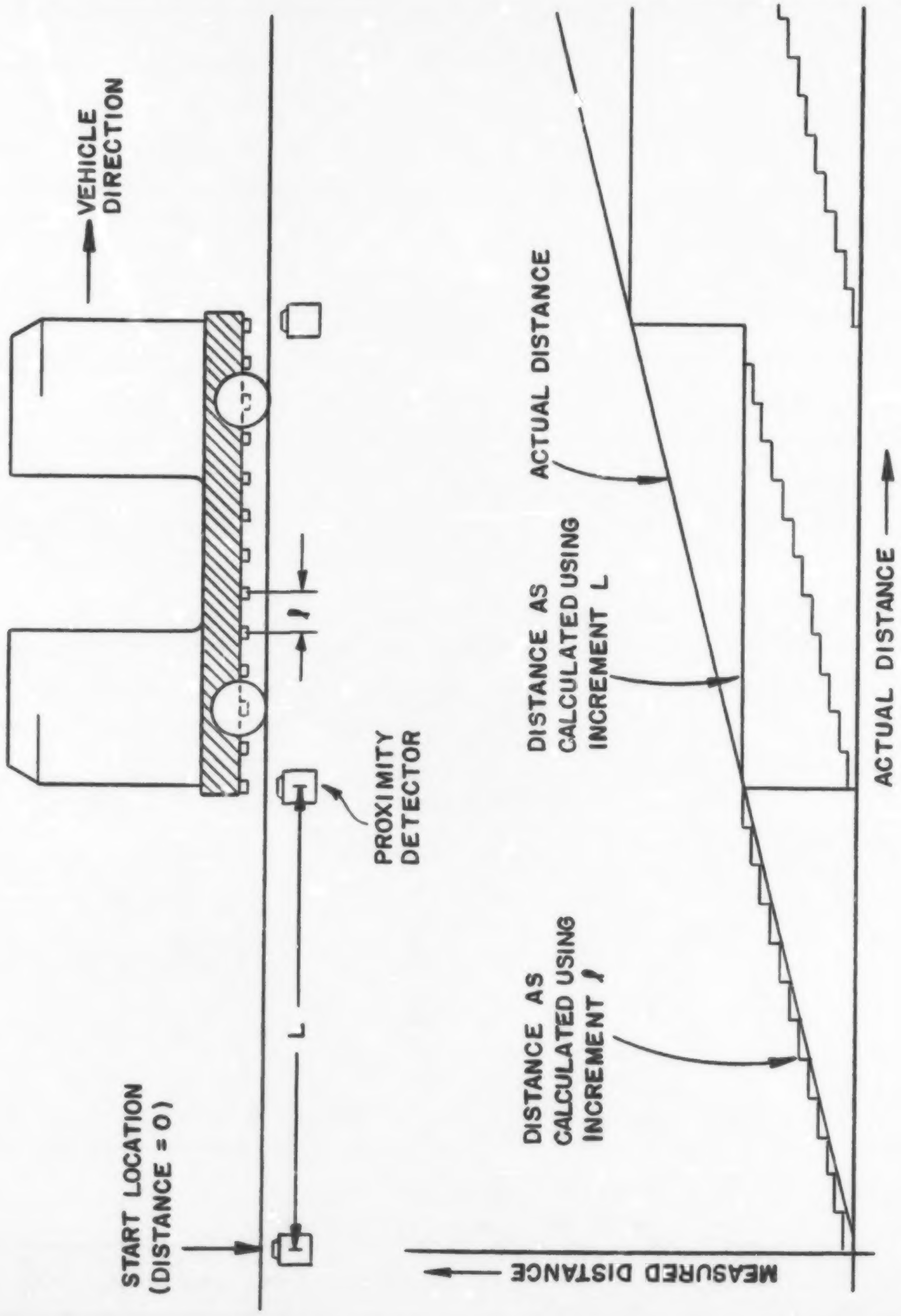
VEHICLE DIRECTION
ACTUAL DISTANCE
l
PROXIMITY DETECTOR
DISTANCE AS CALCULATED USING INCREMENT L
ACTUAL DISTANCE
L
DISTANCE AS CALCULATED USING INCREMENT l
START LOCATION (DISTANCE = 0)
MEASURED DISTANCE

FIG. A5-7: DISTANCE SENSING ARRANGEMENT

3.1.8 Position Calculator

LIM-in-track propulsion systems usually propel passive vehicles. This implies that the sensing system is track-based. A practical form of track-based sensing involves non-contact "proximity detectors", which respond to the presence of a vehicle. These detectors are placed in the track at known distance intervals and therefore may form the basis of a vehicle position-sensing system (Figure A5-7).

A single proximity detector may be used to resolve vehicle position in relatively fine increments if the vehicle is subdivided along its own length in "detectable units" (Figure A5-7). The length of these units will have some lower limit which depends on either 1) the resolution limits of the proximity detector, or 2) the combination of vehicle speed and detector transient response.

Consider a position sensing system which is initiated at the moment a vehicle passes a preset point on the track. Distance is calculated by summing the number of unit detections made by the proximity detector over time. We can consider either type of detectable unit shown in the figure; the principle is the same. Intuitively, we may suppose that both units could be used in practice. The coarse units providing information about the general location of the vehicle on the track, the fine units providing the basic "position feedback" required for precise stop-positioning control.

Our system model may include position feedback of this nature by employing a simple simulation routine which runs concurrently with the time-step solution procedure.

3.1.9 Speed Calculator

Given the type of proximity detection system introduced in the previous section, it is possible to calculate vehicle speed as well as position. Various means exist for converting a pulse-train signal into a speed-analog. A simple "averaging" filter works as a crude converter, provided pulse-width is short relative to the period. Other means include frequency to voltage conversion and true speed calculation. The latter is readily implemented with microprocessor logic and is best suited to low-speed sensing.

To calculate speed, the processor requires the time between two subsequent detections. The calculation may actually involve a mathematical inversion of the number representing this time, followed by a multiplication by a number representing the known distance of the "detectable unit". It is also possible to eliminate any real "calculation" by employing a "look-up table" technique. Here the inversion/multiplication procedure is replaced by a time-dependent function which is stored in digitized form in a memory. Any given time measurement will be associated with a memory location; the content of that location is a number representing speed.

Regardless of the technique employed in the actual system, we will consider for the purposes of system modelling that the speed calculator outputs a new speed value at every subsequent detection. In practice this "update" is not instantaneous, as it takes some amount of time for the microprocessor to execute the required steps, but this time is likely to be quite short relative to the time between detections.

The algorithm employed in the model is shown in flowchart form in Figure A5-8. It is assumed that the size of time step used in the solution routine is much smaller than the time between subsequent detections in the physical system.

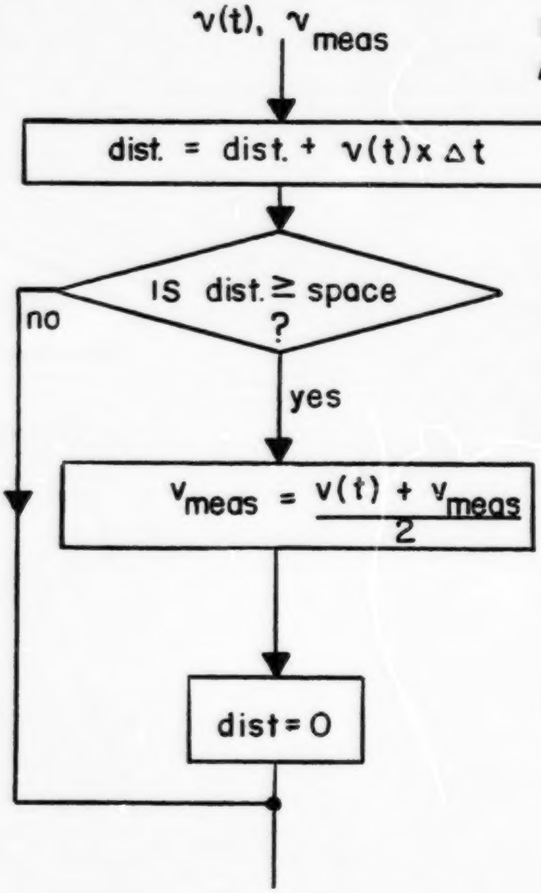
$v(t)$, v_{meas}
dist. = dist. + $v(t) \times \Delta t$
IS dist. ≥ space ?
no
yes
$v_{meas} = \frac{v(t) + v_{meas}}{2}$
dist = 0

INPUT CURRENT VALUES OF SPEED AND CALCULATED SPEED

INCREASE DISTANCE COUNTER FOR THIS TIME STEP

CHECK DISTANCE COUNTER: HAS THE SPACE BETWEEN DETECTION MARKERS BEEN EXCEEDED IN THIS TIME-STEP?

IF YES:

1) SET A NEW CALCULATED SPEED AS THE AVERAGE OF PREVIOUS CALCULATED SPEED AND CURRENT ACTUAL SPEED
2) RESET DISTANCE COUNTER

IF NO:

COMPLETE THE REMAINDER OF THE LOOP AND INCREMENT TO THE NEXT TIME STEP

FIG. A4-8: CONTROL SYSTEM MODEL ALGORITHM

APPENDIX 5

LIM THERMAL MODEL

1.0 INTRODUCTION

The thermal behaviour of a LIM is most easily conceptualized by adopting a "Thermal equivalent circuit" approach, which is a lumped-parameter, electrical analogue of the physical system. The quantities of interest and their corresponding electrical quantities are listed below:

Thermal Quantity	Symbol	Units	Electrical Quantity	Symbol	Units
Heat Flow	$\dot{q}$	joules/ sec	Current	i	amperes (coulomb/ sec)
Thermal Capaciture	C_T	joules/ K	Capacitance	C	Farads (coulomb/ volt)
Thermal Resistance	R_T	K.sec/ joule	Resistance	R	Ohms (V.sec/ coul
Temperature Difference	ΔT	K	Potential Difference (Voltage)	v	Volts
Heat	q	joules	Charge	q	Coulombs

$C_T = cm$ where c = specific heat of material (joule/kg.K) (1)

m = mass of material (kg)

$R_T = \frac{1}{kAW}$ where k = thermal conductivity (joule/sec.m^3.K) (2)

A = area perpendicular to heat flow (m^2)

W = length of heat flux path (m)

2.0 THE HEAT SOURCE

In the LIM primary, heat is generated mostly by currents flowing in the windings. (A smaller proportion is generated by eddy current and hysterisis losses in the iron core, but these will be neglected here.)

If we consider a cross-sectional slice of the LIM core as shown in the figure below, we can calculate the power loss per unit of conductor length, P.

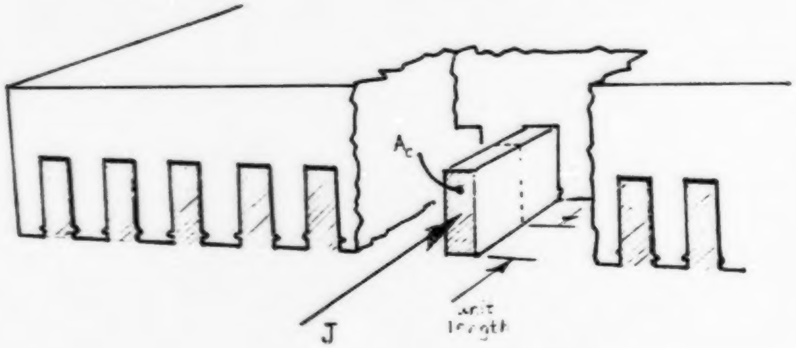

$P = J^2 A_c \rho$ (3) where J = current density (A/m^2)

A_c = conductor area perpendicular to current flow (m^2)

ρ = resistivity of conductor material (ohm.m)

The power dissipated per length of conductor is equivalent to the heat flow in the conductor (conservation of energy).

$\dot{q} = J^2 A_c \rho$ (4) (joules/sec.m)

3.0 THERMAL CAPACITANCE

Consider the LIM to be made up of repeatable units:

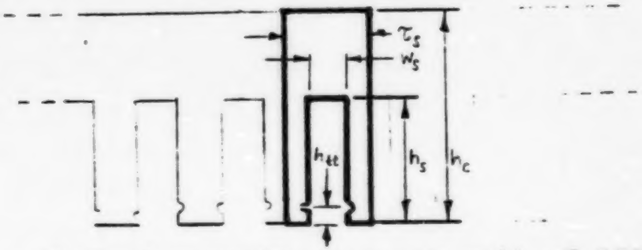

The thermal capacitances per unit of LIM width within the stack region can be lumped into two parameters, C_{cu} and C_{fe} which are determined by the specific heats and masses of the copper and iron, respectively. We need consider only the masses contained in the above defined repeatable unit.

The iron Thermal Capacitance per unit LIM with is

$C_{fe} = c_{fe} (\tau_s h_c - w_s h_s) d_{fe}$ (5) where c_{fe} = specific heat of elec. steel

d_{fe} = density of elec. steel

The copper Thermal Capacitance per unit LIM width is

$C_{cu} = c_{cu} w_s (h_s - h_{tt}) k_{fill} d_{cu}$ (6) where c_{cu} = specific heat of copper

k_{fill} = winding fill factor

d_{cu} = density of copper

4.0 THERMAL RESISTANCE

Heat which is generated in the motor winding flows through various paths to the surrounding air. The heat flow is 3 dimensional, and so an electrical circuit analog (which is 1 dimensional) has limited descriptive capability. Still, we can identify certain basic heat flow paths and attempt to assign an effective thermal resistance to them. A simplifying assumption we will make is that the copper and steel provide zero thermal resistance. The thermal resistances are considered to be associated with the following interfaces:

1) Copper/Insulation/Iron, $R_{cu/fe}$
2) Copper/Insulation/Air, $R_{cu/air}$
3) Iron/Air, $R_{fe/air}$

The Equivalent Thermal Network is thus shown as:

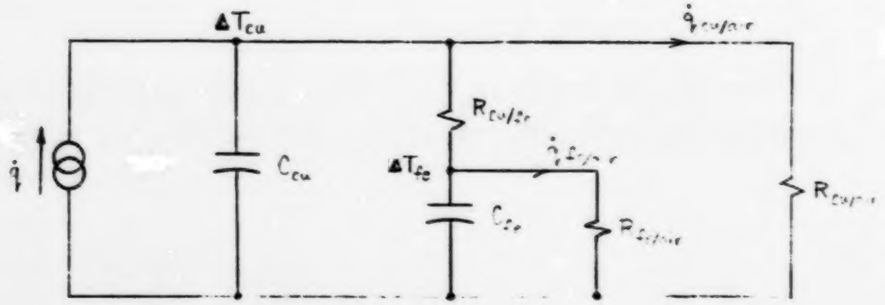

5.0 SOLUTION OF THE THERMAL MODEL

Given values for the various lumped thermal capacitances and resistances, the thermal circuit may be used to determine the transient and steady-state values of temperature difference and heat flow. A useful solution approach is the time-step integration method, implemented by computer program. This method allows, by relatively straightforward extension, a means to alter the values of the circuit elements in response to changing temperature differences, thus modelling more realistically the behaviour which occurs is thermal systems.

For the circuit shown, the following vector equation must be satisfied:

$$\begin{bmatrix} \Delta\dot{T}_{cu} \\ \Delta\dot{T}_{fe} \end{bmatrix} = \begin{bmatrix} -\left(\frac{1}{C_{cu}R_{cu/fe}} + \frac{1}{C_{cu}R_{cu/air}}\right) & \left(\frac{1}{C_{cu}R_{cu/fe}}\right) \\ \left(\frac{1}{C_{fe}R_{cu/fe}}\right) & -\left(\frac{1}{C_{fe}R_{cu/fe}} + \frac{1}{C_{fe}R_{fe/air}}\right) \end{bmatrix} \begin{bmatrix} \Delta T_{cu} \\ \Delta T_{fe} \end{bmatrix} + \begin{bmatrix} \frac{1}{C_{cu}} \\ 0 \end{bmatrix} \left[\dot{q} \right]$$

6.0 EXAMPLE

Consider a LIM primary which is used in a LIM-in-track system. In such systems the LIM tends to be "on" for a very small amount of time compared to the total cycle time. Typical design practice with motors of any kind is to calculate the "duty cycle" or the ratio of "on time" to "cycle time" and calculate the "effective" motor current density as:

$$J_{eff} = J_{max} \times D^{0.5} \qquad (7)$$

where J_{eff} = effective current density
J_{max} = current density while motor is "on"
D = duty cycle

The implicit assumption in the use of "effective" current density is that the time constant associated with the copper thermal circuit is so large that behaviour is the same for intermittent energy input as it is for continuous energy input, so long as the average energy rate is the same. Figure A5-1 illustrates the point that these cases can be quite different, especially for very high input, short duration conditions. This type of condition, which is a characteristic of LIM-in-track systems especially, is "hidden" in most traditional forms of thermal analysis, which are essentially steady-state methods. A further development of the approach introduced here seems warranted.

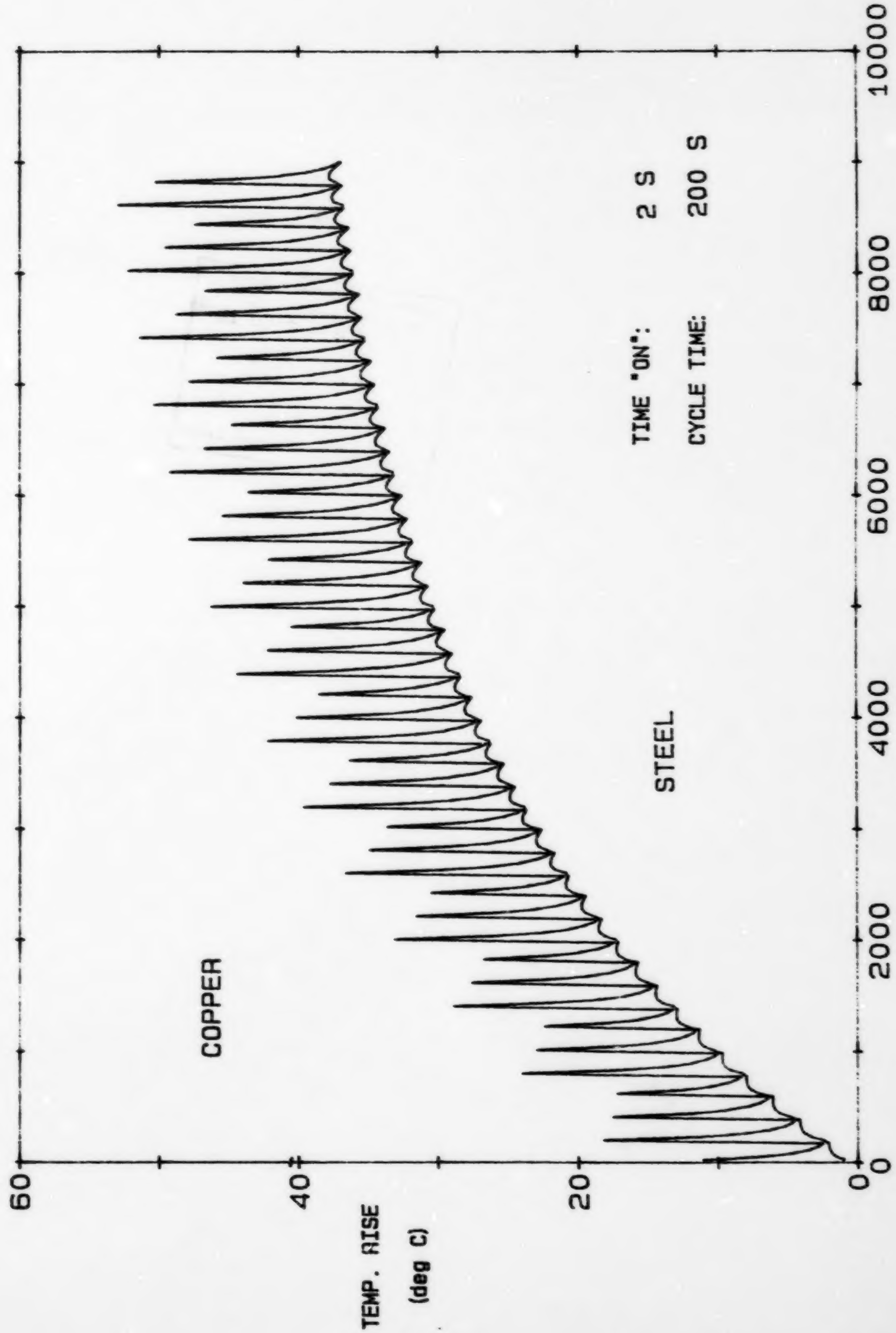

FIG. A5-1 LIM THERMAL MODEL RESULTS